NASA Contractor Report 177563

Advanced Recovery Systems Wind Tunnel Test Report

R. H. Geiger and W. K. Wailes

Pioneer Aerospace Corporation
Melbourne, Florida

Prepared for
Ames Research Center
CONTRACT NAS8-36631
August 1990

NASA
National Aeronautics and
Space Administration

Ames Research Center
Moffett Field, California 94035-1000

TABLE OF CONTENTS

LIST OF TABLES AND FIGURES

LIST OF TABLES AND FIGURES (continued)

LIST OF TERMS AND SYMBOLS

a	Distance between the point at which Fu attaches to the parafoil and the point at which Ru passes through the PACS top plate, ft
A_{REF}	Reference Area(s), sq-ft
b	Span of parafoil, ft
c	Chord of parafoil, ft
C_D, CD	Drag coefficient
C_L, CL	Lift coefficient
C_l, CMX	Rolling moment coefficient
CLDi	Control line load coefficient (i = 1 to 2)
C_M, CMY	Pitching moment coefficient
C_n, CMZ	Yawing moment coefficient
C_Y, CY	Side force coefficient
CTLi	Control line deflection (i = 1 to 2), in.
C.P.	Confluence point
C/4, Q.C.	Quarter chord of parafoil
C.G.	Center of gravity
CX	Distance between Fu and Ru on the parafoil keel, ft
D	Drag, lbf
Fu	Leading edge exposed riser length, ft
FCLDi	Force in control line (i = 1 to 2), lbf
FRISEi	Force in riser (i = 1 to 20), lbf
FTETHi, Ti	Force in lateral tethers (i = 1 to 4), lbf
i, ia	Parafoil rigging angle (angle between line perpendicular to the parafoil keel and a line from the quarter chord to the confluence point), deg
k	Keel length, ft
L_i	Riser line distance from bottom of parafoil to bottom of PACS bottom plate, ft
L_{DF}(i), F, R	Riser line distance from top of PACS top plate to bottom of bottom plate, ft
L/D	Lift to drag ratio
L	Lift, lbf
L_{REF}	Reference Length (c for longitudinal, b for lateral), ft
L.E.	Leading edge riser line
L, LBAR	Distance from PACS pivot point to weight centroid, in.
LR	Length of riser from parafoil to confluence point, ft
LA	Total exposed riser line length, ft
LP	Distance from top of PACS to plate to confluence point, ft
MRP	Moment reference point
PACS	Parafoil attitude control system
q	Dynamic pressure, psf
RISEi	Riser load coeffocient (i = 1 to 20)
Ru	Aft exposed riser length, ft

LIST OF TERMS AND SYMBOLS (CONTINUED)

s	Planform area of parafoil, sq-ft
TETHi	Lateral tether load coefficient (i = 1 to 4)
UVi	Unit vector for each tether (i = 1 to 4)
W_{pacs}	Weight of PACS without struts, lbs.
X_{CP}, XCP	Center of pressure location, in.
x/c	Location of airfoil as a portion of chord, x direction
X, XBAR	X-axis weight centroid of PACS, in.
XX	Distance between Fu and Ru on the PACS top plate, ft
Xf	Distance from PACS hinge to leading edge riser hole, ft
y/c	Location on airfoil as a portion of chord, y direction
Z, ZBAR	Z-axis weight centroid of PACS, in.

GREEK TERMS AND SYMBOLS

α, ALPHA	Angle of attack of the parafoil (measured from keel of parafoil to freestream velocity vector), deg.
α_p, ALPHAP	Angle between the top plate of the PACS and the tunnel floor, deg.
γ	Angle between top plate and the line from the PACS pivot point to the PACS weight centroid deg.
δ_p, DELP	Angle between the top and bottom plate of the PACS, deg.
θ, THETA	Angle between the leading edge/centerline riser and the top plate of the PACS in the spanwise direction, deg.
ϕ, PHI	Angle between the leading edge/centerline riser and the top plate of the PACS in the chordwise direction, deg.

FOREWORD

This document presents the results of wind tunnel testing performed under the Phase 2 option of contract NAS8-36631, Advanced Recovery Systems for Advanced Launch Vehicles. It satisfies the requirements for reporting wind tunnel data under the ARS contract.

1.0 SUMMARY

Pioneer Aerospace Corporation (PAC) conducted parafoil wind tunnel testing in the NASA-AMES 80 X 120 test section of the National Full-scale Aerodynamic Complex, Moffett Field, California (Fig. 1.0-1). The investigation was conducted to determine the aerodynamic characteristics of two (2) scale ram air wings in support of air drop testing and full scale development of Advanced Recovery Systems For The Next Generation Space Transportation System.

Two models were tested during this investigation - The primary test article, a 1/9 Geometric scale model with wing area of 1200 square feet and secondary test article, a 1/36 geometric scale model with wing area of 300 square feet, both of which had an aspect ratio of 3.

The test results show that both models were statically stable about a model reference point at angles of attack from 2 to 10 degrees. The maximum lift-drag ratio varied between 2.9 and 2.4 for increasing wing loading.

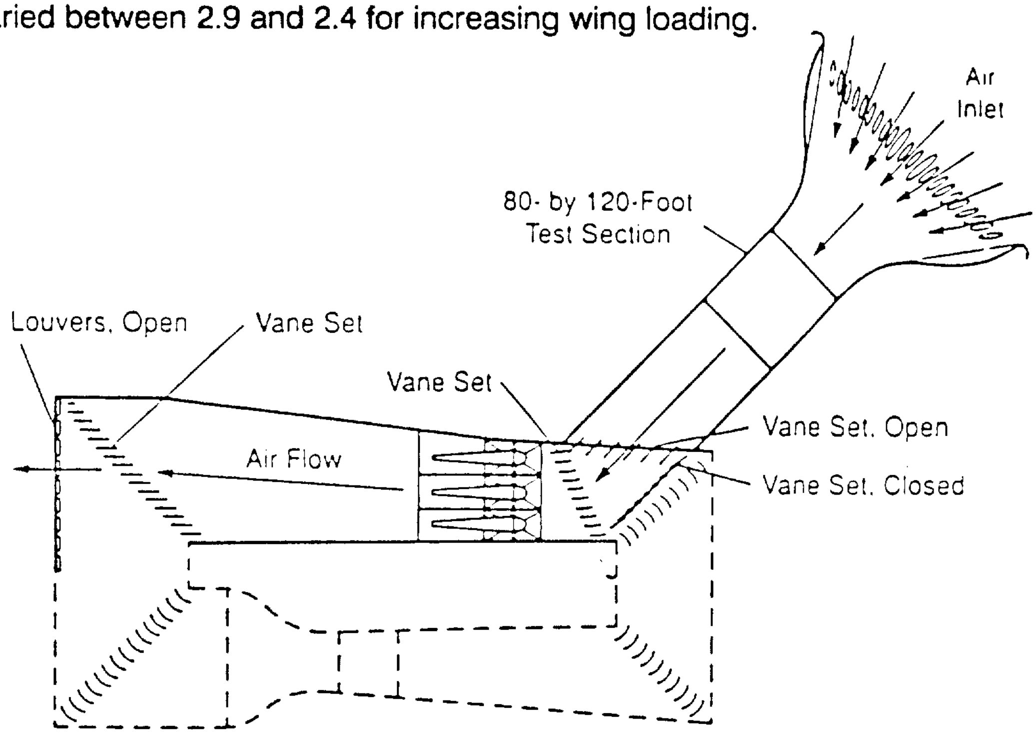

80- by 120-Foot Wind Tunnel Operation

FIGURE 1.0-1, NATIONAL FULL-SCALE AERODYNAMIC COMPLEX

2.0 INTRODUCTION

Pioneer Aerospace Corporation (PAC) was selected by NASA's MSFC to investigate promising concepts for recovering valued assets from the Next Generation Space Transportation System. Reuse of selected STS elements (such as core stages, upper stage propulsion/avionics modules, booster stages, booster P/A modules, and fuel-oxidizer tanks) is critical to a low cost space transportation system. Reuse inherently requires recovery, retrieval and refurbishment. Therefore, development of advanced recovery systems for high cost launch vehicle components, along with the ability to recover at selected sites, to refurbish rapidly, and reuse certain vehicle components is needed to provide an efficient operating system with minimal overall program cost. Through Phase 1 concept identification and preliminary trades analysis tasks, Pioneer identified "best candidate" recovery system concept for a list of prospective recoverable STS elements. ARS Phase 2 will demonstrate the Advanced Recovery Systems ability to precisely and controllably soft land an emulated P/AM which in full scale, would weigh approximately 60,000 pounds. This requires employment of a controllably maneuverable Ram Air Inflated Wing whose size and weight characteristics are well beyond today's state-of-the-art. An orderly program has been planned which includes analytical modeling, scale model tow testing, wind tunnel testing and air drop flight testing. The demonstration culminates in a flight test of a full-scale Ram Air Inflated (Parafoil) prototype system.

2.1 BACKGROUND

Prior to the selection of a Ram Air Inflated Wing for this program, various recovery methods were considered. Among those considered were a Ballistic (L/D = 0) Parachute System and a Low Glide (L/D = 1) Parachute System. For both the Ballistic and the Low Glide systems, a huge data base exists upon which to build, making either of these systems relatively low risk. Along with the low risk factors which these two systems share, the data also show that each system carries a large weight penalty and has very little or no capability to maneuver. Both systems are good, reliable decelerators but have almost no target acquisition capability.

The Ram Air Inflated Wing has many advantages over the more conventional Parachute system such as low weight, high maneuverability and the capability to flare for a soft, stable landing. However the vast majority of the data base for Ram Air Inflated Wings is for small (personnel size) systems. Going beyond the personnel sized canopies (175 to 340 ft^2), some very limited research has been done on Ram Air Inflation Systems up to 3200 ft^2. The canopy size required for this test program must go far beyond any that have been previously studied. The full scale prototype (10,800 ft^2) exceeds the size of 3,200 ft^2 by 338%.

Several wind tunnel investigations were conducted in the 1960's in the University of Notre Dame 2' X 2' test section by John D. Nicolaides[4] and in the NASA Langley 30' X 60' (elliptic) test section by George M. Ware and James L. Hassell, Jr.[5]. These wind tunnel tests were conducted on models at relatively low wing loadings (1-2 PSF) and small size models up to 300 ft^2. Due to the lack of data for ARS size Parafoils a large scale wind tunnel test was conducted to establish a data base of large (1,200 ft^2) Ram Air inflated wings.

2.2 TEST SITES AND DATES

This wind tunnel test program is sponsored by NASA-MSFC with Pioneer Aerospace Corporation being the prime contractor. Lockheed Missiles and Space Company is a sub-contractor whose primary wind tunnel related task is development of the wind tunnel interface, Parafoil Attitude Control System (PACS). The wind tunnel testing was conducted during the month of September 1988 in the 80' X 120' test section of the National Full-Scale Aerodynamics Complex (NFAC) at the National Aeronautics and Space Administration's (NASA) Ames Research Center (ARC), Moffett Field, California.

3.0 OBJECTIVES

The objective of the wind tunnel test was to obtain data in support of air drop flight testing and development of a full-scale Ram Air Inflated prototype Advanced Recovery System.

3.1 BASIC IN-PLANE LONGITUDINAL AERODYNAMICS

The first primary objective was to obtain basic in-plane longitudinal aerodynamics, ie., lift, drag and pitching moment data. These data were obtained over a range of angles of attack from approximately zero to stall (0 to 10 degrees). This range was selected to support the basic gliding flight and rigging requirements of the air drop test program.

3.2 FLARE DATA FOR TRAILING EDGE DEFLECTIONS

The second primary objective was to obtain data to support the flare maneuver. Lift, drag and pitching moment data was collected for various trailing edge deflections and angles of attack. Associated control line loads were also measured for all deflections.

3.3 CONTROL DATA

The last primary objective was to obtain data to support the sizing of the control mechanisms for the drop test. Control line loads as a function of displacement and incremental changes in longitudinal aerodynamics was acquired for various control methods. As a secondary objective associated lateral aerodynamic forces and moment were obtained for different control methods. Figure 3.3-1 shows the different control methods.

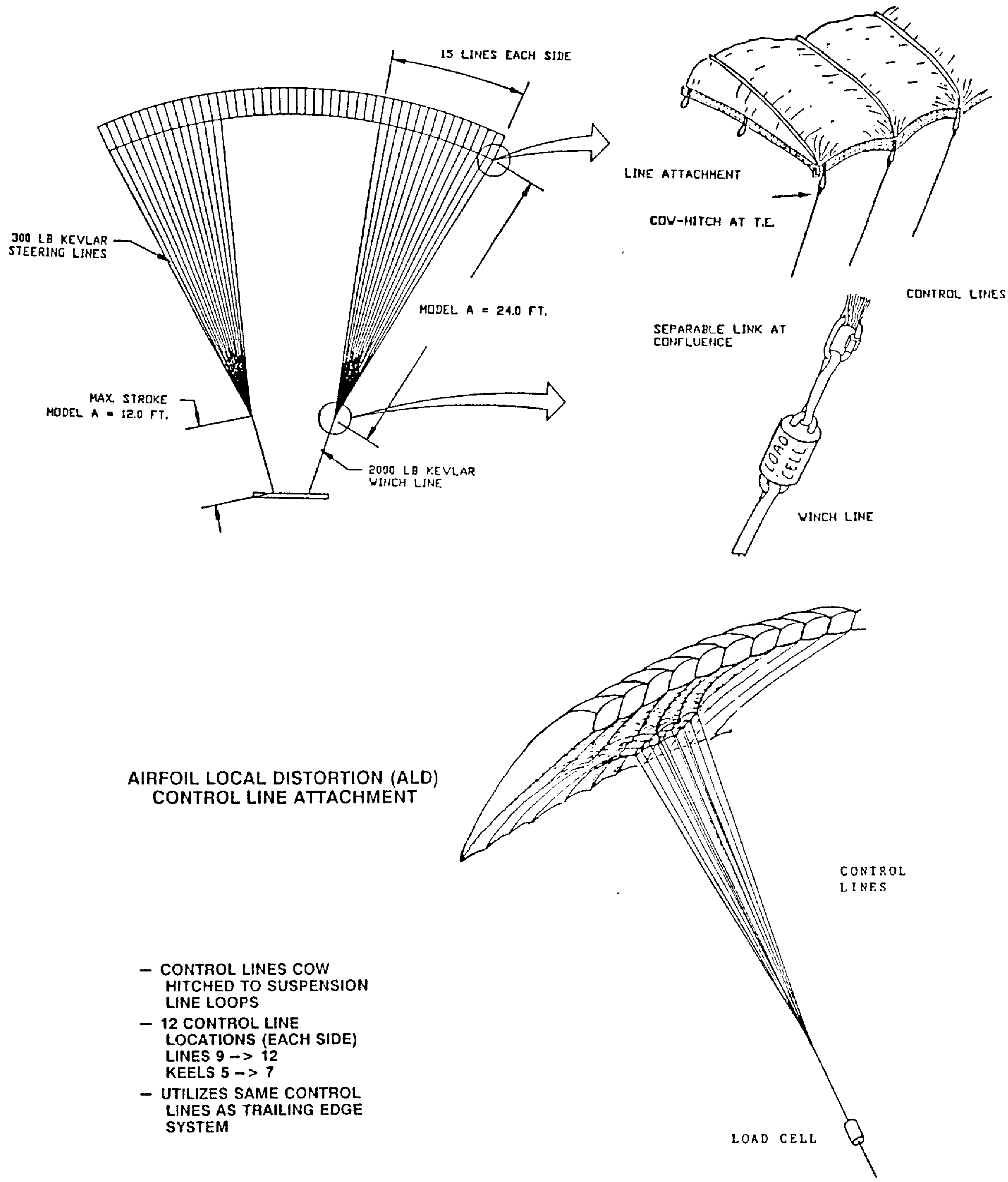

FIGURE 3.3-1, TRAILING EDGE STEERING, L/D MODULATION LINE ARRANGEMENT

3.4 LOAD DISTRIBUTION

The load distribution across the wing is needed for canopy and suspension line design of drop test and eventual full-scale models. The distribution of the load on the parafoil was measured by placing load cells in chordwise and spanwise locations in the suspension lines and data obtained for all configurations.

3.5 SCALE EFFECTS

A review of past programs indicates that there is often a scaling problem associated with flexible wings. Therefore the next objective of the test was to obtain data on scale effects to aid in scaling the data up to full scale. This was accomplished by testing a second model one half the linear scale of the primary model. Testing of the smaller model was limited to selected test conditions. Table 3.5-1 shows an overview of how and when each objective was met.

DATE	RUN #	Q	OBJECTIVE	COMMENTS
8 SEPT.	1	3	TRIM PARAFOIL	FIRST RUN
9 SEPT.	2 3	0 6	CALIBRATION LONGITUDINAL AERO	PACS/INSTRUMENTATION CALIBRATION
12 SEPT.	4	6	LONGITUDINAL AERO	
13 SEPT.	5	6/9	LONGITUDINAL AERO	FINAL TRIMMING OF PARAFOIL
14 SEPT.	6	6	FLARE DATA	
15 SEPT.	7	0	CALIBRATION	
19 SEPT.	8	3	PHOTOGRAPHS	
20 SEPT.	9 10	9 9	LONGITUDINAL & FLARE AERO FLARE DATA	
21 SEPT.	11 12	6 6/9	CONTROL INPUTS CONTROL/FLARE	TRAILING EDGE DEFLECTORS
22 SEPT.	13 14	6 9/12	CONTROL INPUTS CONTROL/LONGITUDINAL DATA	AIRFOIL LOCAL DISTORTION
23 SEPT.	15	6/9/12	PACS AERODYNAMICS	PARAFOIL REMOVED
27 SEPT.	16	3/6	TRIM PARAFOIL	SMALL PARAFOIL
28 SEPT.	17	6	LONGITUDINAL AERO SCALE DATA	

TABLE 3.5-1, WIND TUNNEL TEST OVERVIEW

4.0 TEST FACILITIES AND TECHNIQUES

4.1 TUNNEL DESCRIPTION

A review of past programs indicates that there is often a scaling problem associated with flexible (Parachute/Parafoil) configurations. Therefore, conducting a wind tunnel test with the largest possible scale model was the main goal. This goal was achieved by selecting the largest available wind tunnel for testing. The newly commissioned 80' X 120' test section of the National Full-Scale Aerodynamics Complex at NASA's Ames Research Center was chosen because it is the largest wind tunnel available. The new 80' X 120' leg is basically an open circuit tunnel with a closed throat test section (Figure 4.1-1). The 135,000 horse power fan drive system is enough to attain speeds at more then 115 MPH, more than enough to achieve the relatively high wing loadings required for this test program.

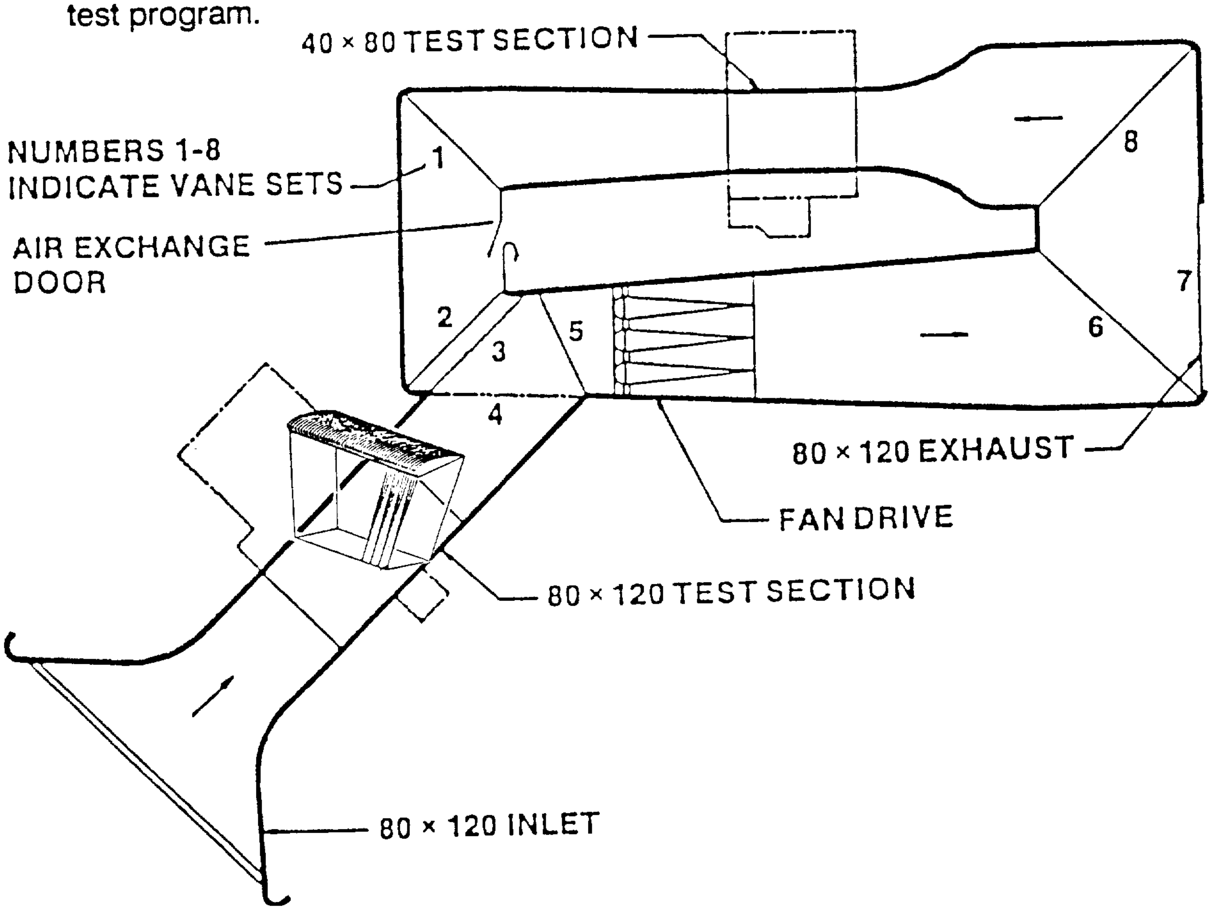

FIGURE 4.1-1, NATIONAL FULL-SCALE AERODYNAMIC COMPLEX

4.2 TEST STAND - PARAFOIL ATTITUDE CONTROL SYSTEM

The Parafoil Attitude Control System (PACS)(Figure 4.2-1) was developed to enable the parafoil to reach its natural trim point and still be able to change the parafoil angle of attack. The PACS includes two carriage struts which attach to the tunnel support/balance system. Each of these struts incorporates a free-floating pivot point which attaches to the top plate of the hinged plate substructure. This point is translated along the top plate by the Xcp actuator mechanism. The hinged plates are driven apart by the L/D actuator. The combination of the Xcp and L/D actuators results in setting the parafoil to the desired attitude. Each plate is divided into removable sections which contain the riser pattern for the parafoil being tested. The suspension lines pass through the top plate and continue through the bottom plate then are attached to the underside of the bottom plate. Two control winches are mounted on the underside of the bottom plate and are used for the various control deflections. Two linear potentiometers monitor the Xcp and L/D actuators. The control winches are monitored by rotary potentiometers while the angle between the leading edge/center suspension line and the top plate (ϕ and θ) is measured by a single joystick potentiometer. An inclinometer was used to measure the top plate angle (αp) with respect to the tunnel floor. A flow deflector was mounted on the tunnel floor just upstream of the PACS to minimize data uncertainty resulting from flow interaction with the PACS. A more detailed description of the PACS is contained in the "Preliminary Analysis of Parafoil Attitude Control (PAC) Model", ARS-WP-09.[6]

ORIGINAL PAGE IS
OF POOR QUALITY

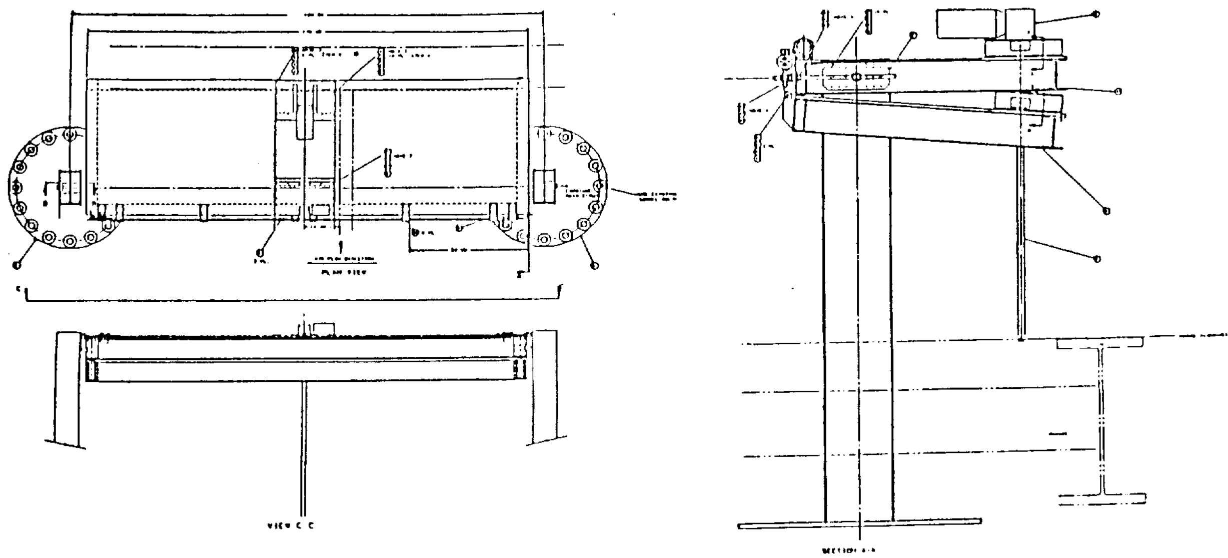

FIGURE 4.2-1, PARAFOIL ATTITUDE CONTROL SYSTEM (PACS)

4.3 TEST MODELS

In keeping with the main objective of this test program, testing the largest possible model, Pioneer designed the largest wing that could effectively be flown in the wind tunnel. The parafoil size was chosen to be as big as possible without interfering with the air flow near the tunnel walls.

The primary test article (Part #7901) was a 1/9 area scale model of the ARS prototype parafoil. The model had a chord of 20 ft and a span of 60 ft, thus having 1,200 ft^2 area. The parafoil consisted of 47 spanwise cells and was constructed with 1.1 oz/yd nylon. This wing had 960 suspension lines attached in 48 spanwise rows and 20 chordwise columns. Each suspension line was 300 lb Kevlar and each three spanwise groups were cascaded down to one attachment point on the PACS making a total of 320 PACS connecting locations. One of the objectives for this model was to collect data for various symmetrical and asymmetrical trailing edge/control deflections to support the flare and control maneuvers. The wing was equipped with 30 movable/removable control lines that were adjusted using the two winches located on the PACS.

Another of the objectives for this test program was to determine what the effects of size (scaling) are. A 1/36 area scale model (1/4 scale of the primary test article) (Part # 7900) was constructed and tested for this propose. The small model had a chord of 10 ft, a span of 30 ft and an area of 300 ft^2. This second parafoil was identical to the first parafoil in geometry, material and construction (48 cells, 1.1 oz/yd nylon/300 lb Kevlar and same airfoil section). This parafoil was not equipped with the various control methods. This model was exclusively used to evaluate the scaling effects on wings of this type.

Both models are shown in Figure 4.3-1. A stress and design analysis is contained in "Advanced Recovery System Parachute/Parafoil Stress and Design Loads Analysis", ARS-WP-10 Rev. A.[7]

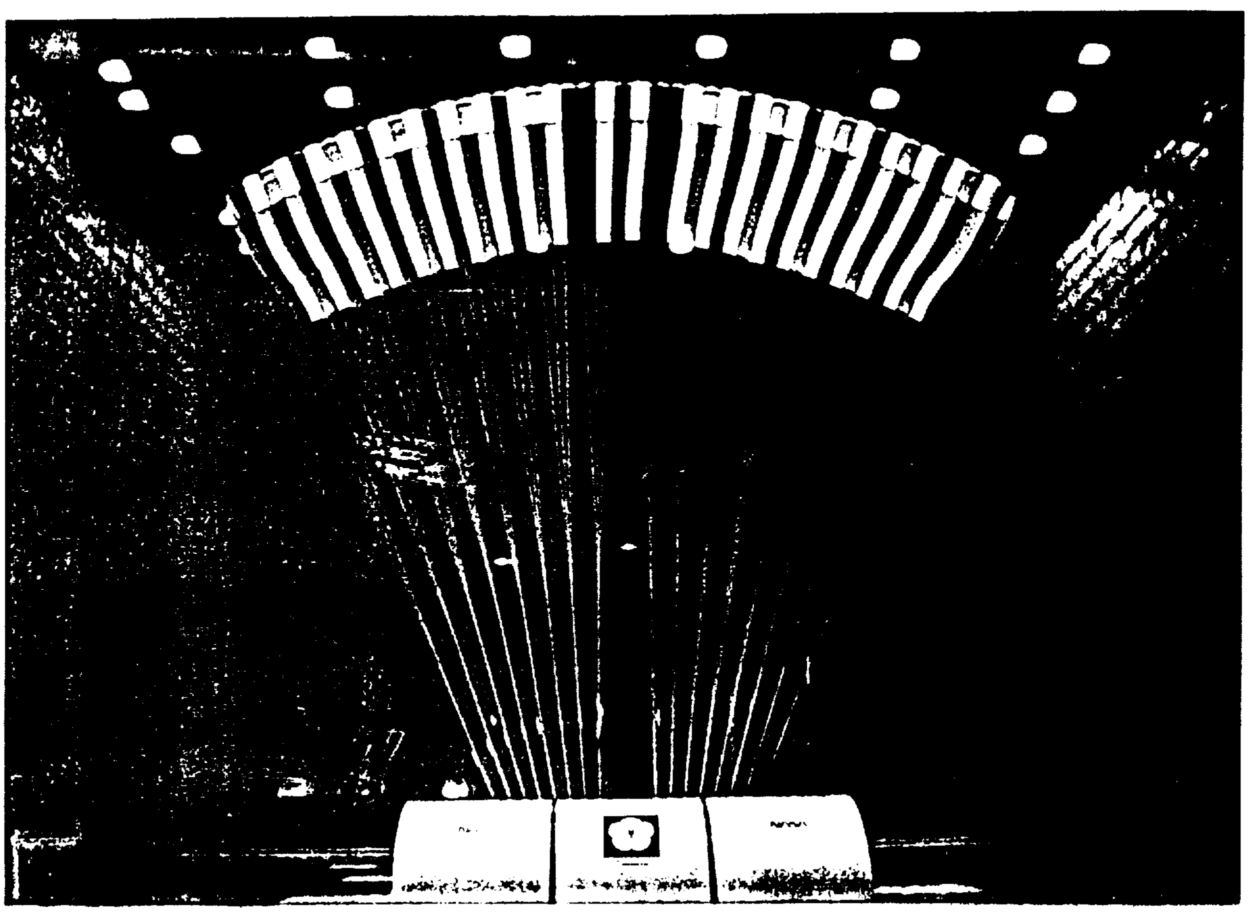

FIGURE 4.3-1, WIND TUNNEL TEST MODEL CONFIGURATION

ORIGINAL PAGE IS OF POOR QUALITY

4.4 TEST TECHNIQUES

Figure 4.4-1 shows the 20' x 60' parafoil during testing. While testing both models were allowed to fly in the wind tunnel by use of a active tether system (Figure 4.4-2). Five ceiling and four side tethers were used to raise the parafoil for initial inflation and to hold the wing to measure lateral loads during asymmetrical control deflections. During most of the testing, once the parafoil reached a stable trim point, all tethered were released to allow the wing to fly unrestrained. A test procedure was adopted during testing that when the parafoil reached stall or any unstable condition the wind tunnel was shut down, the parafoil angle of attack decreased and ceiling tethers tightened. By using this procedure the wing would stabilize quickly and reduce the chance of any damage occurring to the wing.

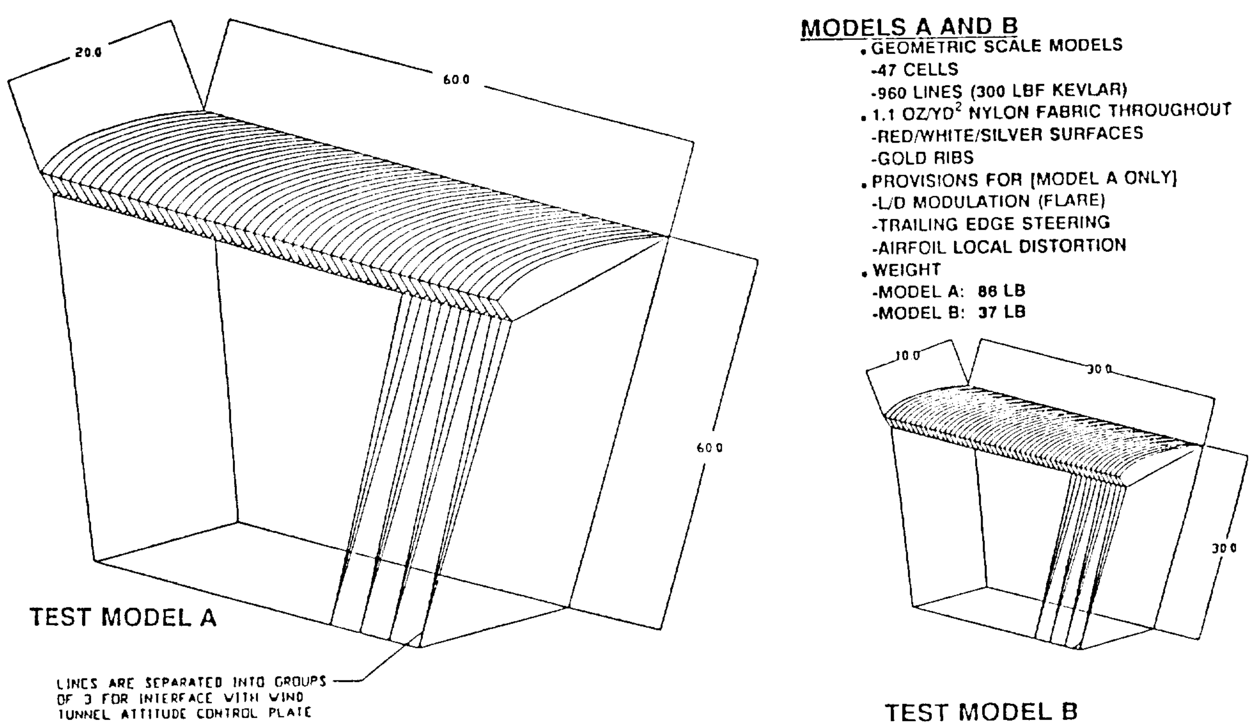

FIGURE 4.4-1, 20' x 60' PARAFOIL

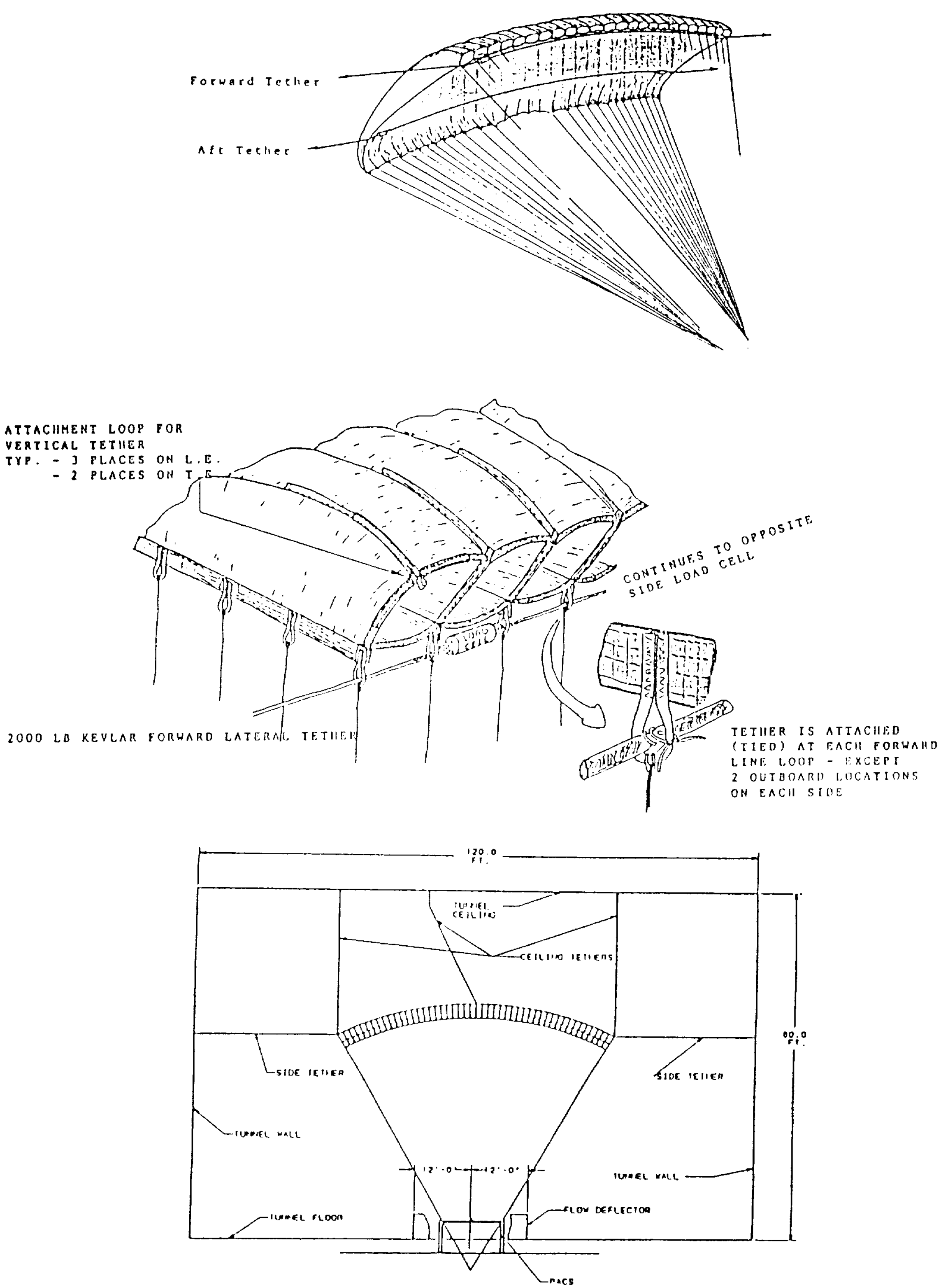

ELEVATION LOOKING SOUTH

FIGURE 4.4-2, LATERAL TETHER LOCATIONS

4.5 DATA ACQUISITION

The PACS served as the interface between the parafoil and the tunnel's balance/data acquisition system. Lift, drag and side forces were transmitted directly through the PACS to the balance and recorded on the systems computer. Rolling and yawing moments were also measured using the tunnel balance system. The PACS was designed to find the center of pressure of the parafoil by finding the point on the plate where the pitching moment was zero. Then using simple force transformations the pitching moment could be calculated.

Twenty load cells were placed in the suspension lines to give spanwise and chordwise load distribution across the wing. The load cells were connected directly to the tunnels data acquisition system. Four additional load cells were placed in the side tethers to measure side forces during the control deflections. Two load cells were also placed in the two (one each side) control lines to measure the force required for control line deflections.

All data was recorded for each data point on the tunnel's computer. The data was then corrected using the tunnels standard corrections and output on hard copies for further use.

Five video cameras were placed at various locations around the wind tunnel to observe and record the testing. One of the five cameras was located on the west wall, adjacent to the parafoil wing tip. This camera was used as an alternate method of measuring the angle of attack of the wing. The other four cameras were used for documentation purposes only.

4.6 PROBLEMS AND CORRECTIVE ACTION

Several problems occurred during testing. This section describes the problems and the corrective action utilized.

PROBLEM: PACS Xcp Retention Pin Failure - The pin used to hold the Xcp thrust bearing in place sheared during testing. The retention pin design was faulty in that it could not withstand the high shear loads during testing.
CORRECTIVE ACTION: The bearing journal was modified to accept a collar that would fit on both sides of the thrust bearing thus retaining the bearing under high loading conditions. Figure 4.6-1 shows the Xcp retention pin failure and modification used to correct the problem.

XCp RETENTION PIN FAILURE

MODIFIED BEARING RETENTION

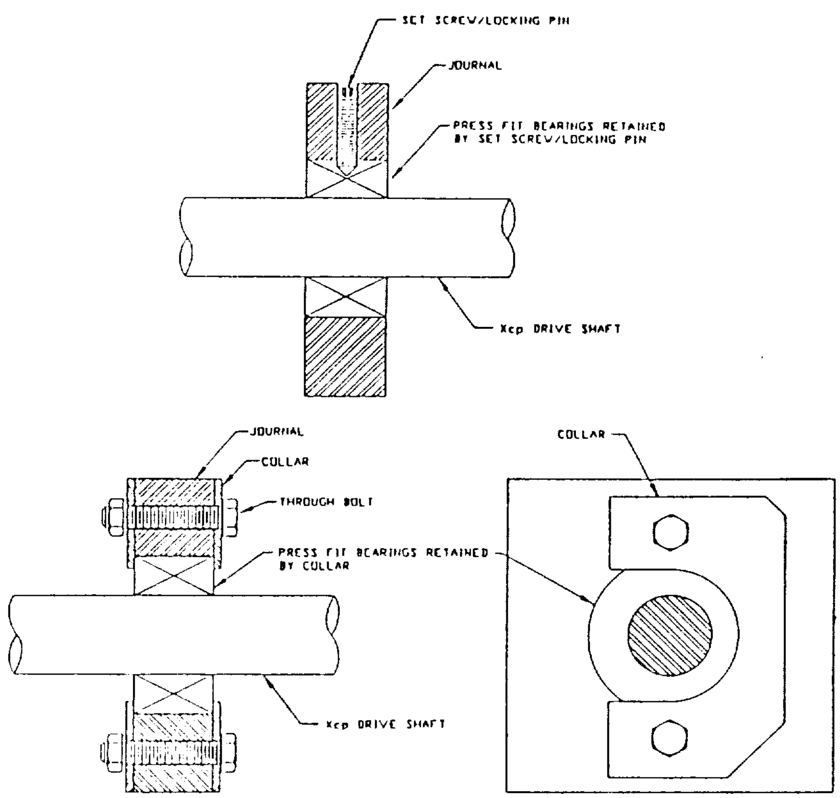

FIGURE 4.6-1, RETENTION PIN MODIFICATION

ORIGINAL PAGE IS OF POOR QUALITY

PROBLEM: Parafoil/Tether Failure - The Parafoil was designed with nine tether attachment locations. The tethers were used to keep the wing from diverging too far once the wing reached an unstable trim point. During testing the tethers encountered loads that were higher than expected. The results were that the parafoil was damaged in the locations where the tethers were located.

CORRECTIVE ACTION: The parafoil was fixed and strengthened at the tether locations using Rip-Stop and Kevlar reinforcing materials. The materials were sewn in place using a sewing machine. All tether locations were reinforced and no more damage occurred during testing. Figure 4.6-2 shows the parafoil/tether damage and correction.

PROBLEM:

PARAFOIL/TETHER DAMAGE

CORRECTIVE ACTION:

PARAFOIL STRENGTHENED AT TETHER LOCATIONS

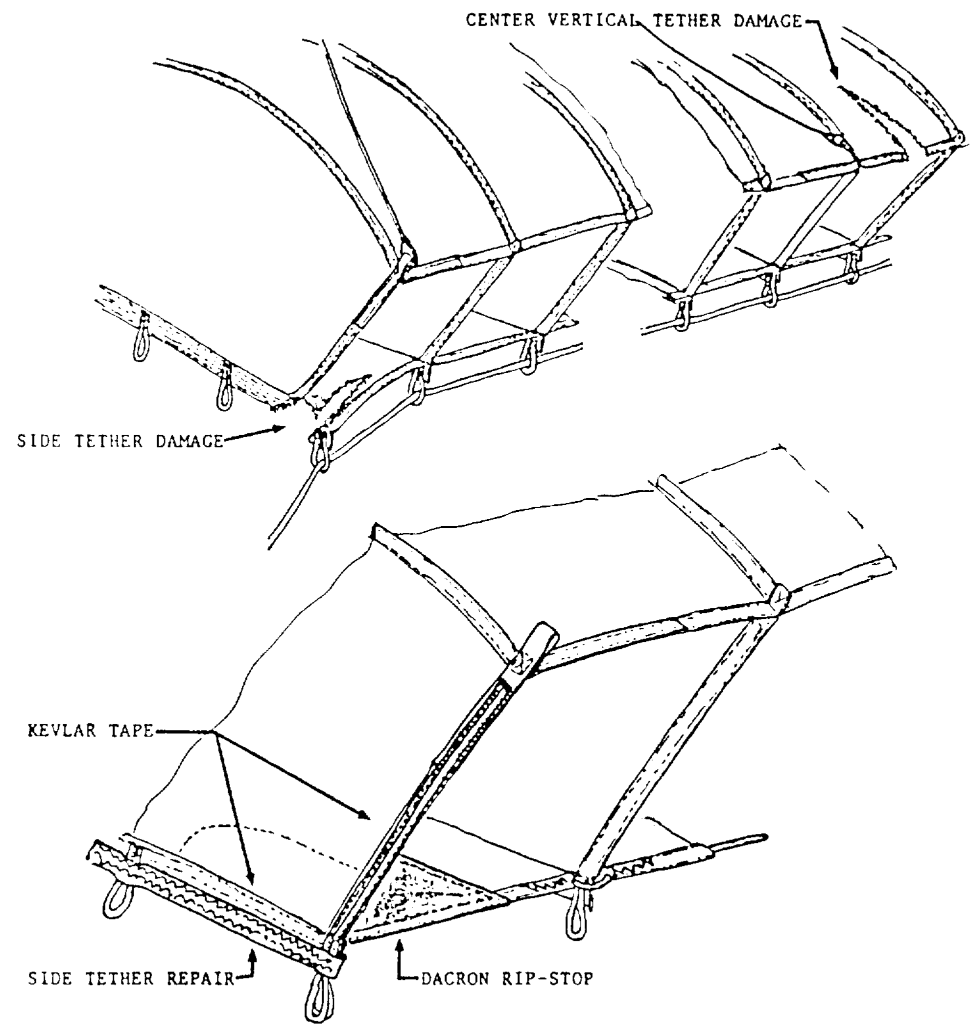

FIGURE 4.6-2, PARAFOIL/ TETHER DAMAGE AND CORRECTION

PROBLEM: Small Parafoil PACS Problem - The 10' x 30' parafoil could not generate enough lift to balance the PACS due to the short range of the PACS Xcp drive system.
CORRECTIVE ACTION: The front of the PACS was secured to the tunnel balance system to level the PACS. This allowed the small wing to be tested but the data could only be taken over a very small range due to the PACS not being able to move.

PROBLEM: Q Effects on Parafoil Angle of Attack - It was observed during testing that the angle of attack not only is a function of the rigging geometry but also is a function of the dynamic pressure (Q). Therefore, there was not an easy way to measure the angle of attack during testing.
CORRECTIVE ACTION: The angle of attack was derived as a function of rigging geometry and dynamic pressure for data reduction and analysis purposes. The angle of attack was also measured and compared using video and still photographic techniques.

5.0 ANALYSIS OF RESULTS

The information in this section describes how the data was reduced after testing was completed.

5.1 ANGLE OF ATTACK SUMMARY

One of the basic differences between testing fabric wings and rigid structures is finding the wings angle of attack. With a rigid wing the angles can be measured directly by mounting sensors directly on the wing. Previous to this test it was thought that any instrumentation mounted in the wing would significantly change the shape of the wing, thus invalidating the test results. For this reason a inclinometer was not incorporated in the wing.

The angle of attack was derived as a function of the physical constants of the PACS and parafoil and of the variables measured during testing. The physical constants were the PACS plate hole geometry, parafoil suspension line geometry and parafoil chord length. The measured variables included; dynamic pressure (Q), angle between PACS top and bottom plates (δp), angle measured between front center suspension line and top plate (ϕj) and angle of the top plate relative to horizontal (αp).

A data base was compiled that consisted of geometric variables and aerodynamic coefficients measured during testing and was used in conjunction with a computer program to calculate the angle of attack for each data point. Figure 5.1-1 shows the angle of attack as a function of δp and dynamic pressure.

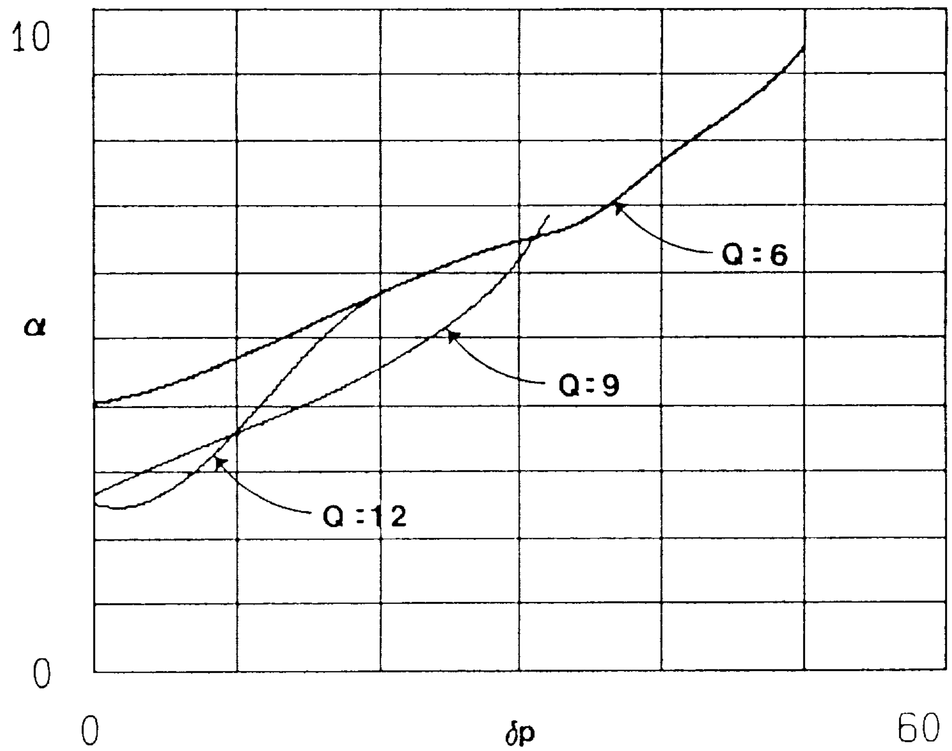

FIGURE 5.1-1, ANGLE OF ATTACK AS FUNCTION OF δ p AND DYNAMIC PRESSURE

The angle of attack was also measured using 70mm black and white and video photography. The method used was to place the cameras in the tunnel wall adjacent to where the wing would be flying. The wing tip was then photographed when each data point was taken. After testing was completed a grid was placed in the tunnel, in the same plane as the parafoil wing tip was flying, and photographed using the same two camera locations. The two films were superimposed and the angle of attack then directly measured (Figure 5.1-2).

ORIGINAL PAGE IS
OF POOR QUALITY

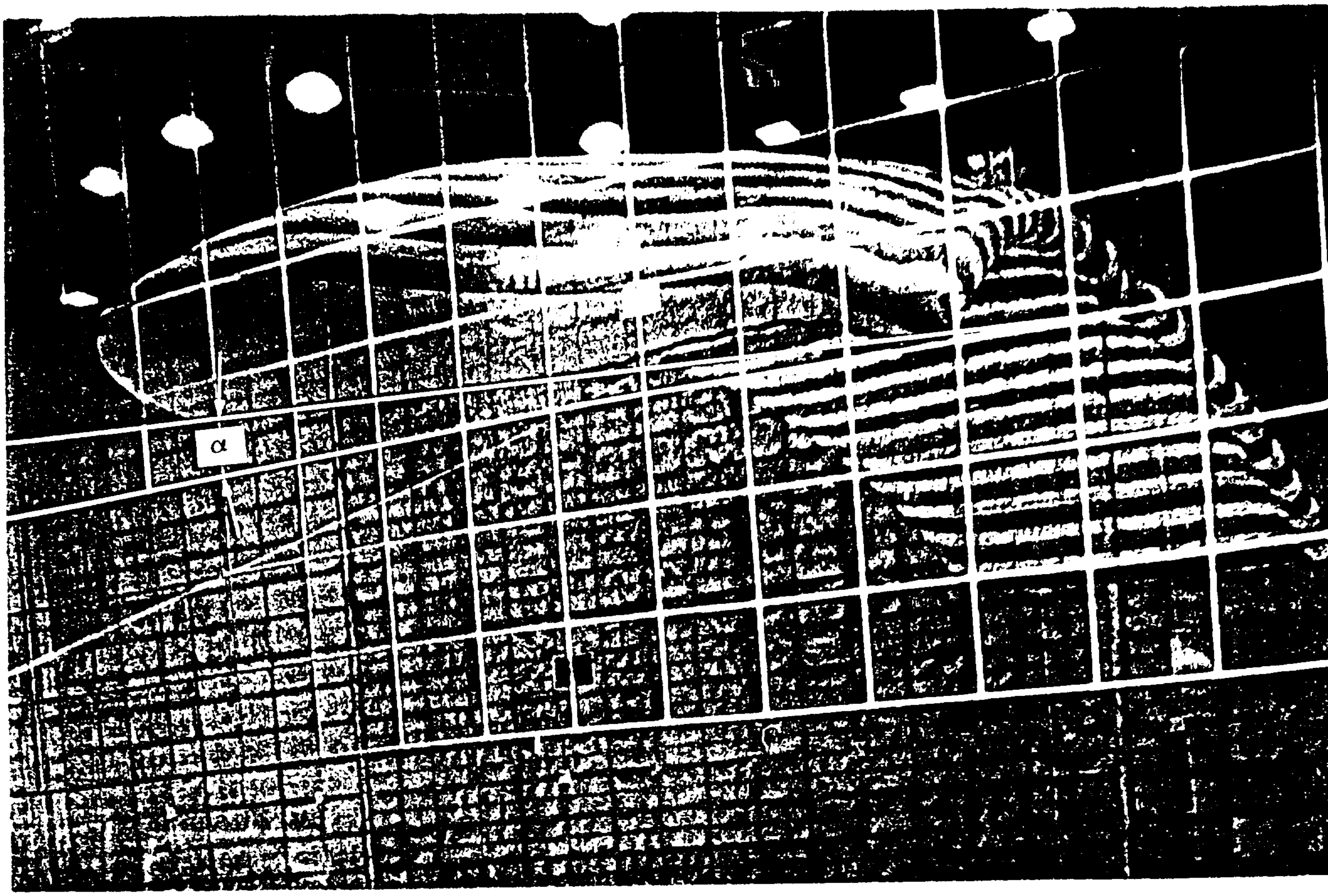

FIGURE 5.1-2, DIRECT MEASUREMENT OF ANGLE OF ATTACK

There were two problems with this method. The first problem was that the cameras had to be located in existing view ports that were located slightly aft and above the wing. The second problem encountered was that the wing distorted at high dynamic pressures. The distorted wing profile made it difficult to find the actual chord line of the parafoil therefore a average chordline was assumed.

Figure 5.1-3 shows planned versus actual angle measuring techniques. All of the measured values agree with calculated values to within 10%.

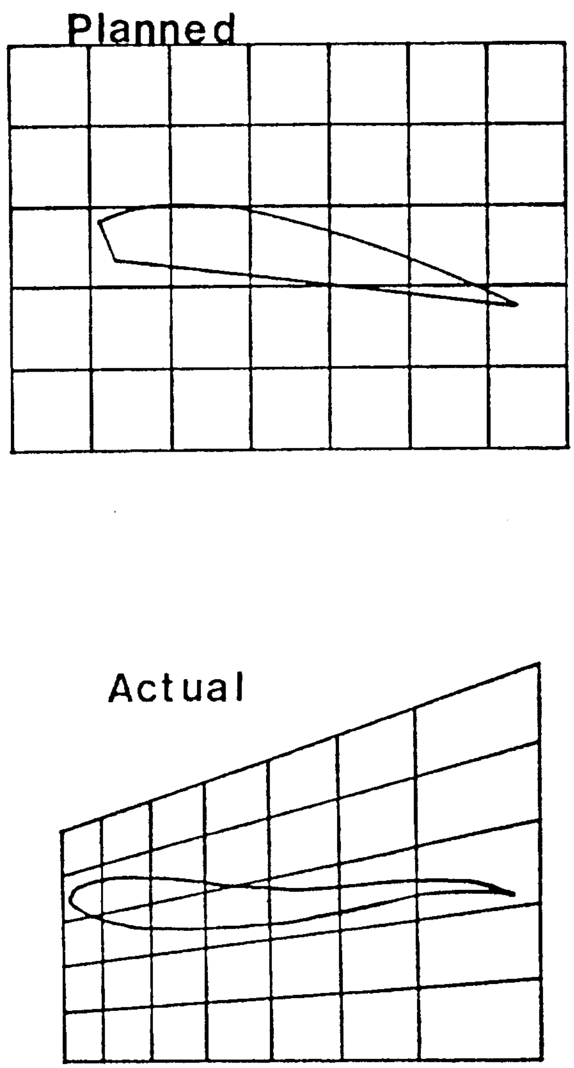

FIGURE 5.1-3, ANGLE OF ATTACK MEASURING TECHNIQUES PLANNED VS. ACTUAL

5.1.1 Angle of Attack Calculation

Figure 5.1-4 depicts the geometry used in determining parafoil angle of attack. Values for L_1, length of forward suspension line, and L_4, length of fourth suspension line, are constants to this configuration. The values for Cx, XX and Xf are also constant and are shown in the figure. The values of ϕ, δp, and αp, R, Ru, F, Fu, a, q_1 and q_2 vary for each set of test conditions.

To determine parafoil angle of attack the following set of equations are used:

$$\alpha = \alpha p - \phi + (180 - \theta_1 - \theta_2)$$

where:

$$\theta_1 = \cos^{-1}((Fu^2 + a^2 - XX^2)/(2\ Fu\ a))$$

$$\theta_2 = \cos^{-1}((Cx^2 + a^2 - Ru^2)/(2\ Cx\ a)$$

$$a = (Fu^2 + XX^2 - 2\ Fu\ XX \cos \phi)^{1/2}$$

To determine Fu and Ru the following is used:

$$Fu = L_1 - F$$
$$Ru = L_4 - R$$

Where:

$$L_1 = L_R(1) - L_p(1) + L_{DP}(1)$$
$$L_4 = L_R(4) - L_p(4) + L_{DP}(4)$$

Where LR is the line length from the parafoil to the confluence point, LP the length from the confluence point to the top plate and L_{DP} the length from the bottom plate to the top plate. From analysis conducted in Section 5.3:

$L_R(1) = 59.405$ ft $L_R(4) = 60.268$ ft
$L_p(1) = 11.880$ ft $L_p(4) = 12.020$ ft

To determine L_{DP}:

$$L_{DP} = (.3403 + 2(.3942 + x)^2 - 2(.3942 + x)(.3403 + (.3942 + x)^2)^{1/2} \cos(5 + \tan^{-1}(.5833/(.3942 + x))))^{1/2} + .0833$$

Where X is the longitudinal distance of the PACS hole location for the specific line. For line 1, X = 0.0 ft; for line 4, X = 0.5869 ft. Therefore,

$L_{DP}(1) = 0.701$ ft $L_{DP}(4) = 0.752$ ft

and the following are the resulting line lengths:

$L_1 = 48.2$ ft $L_4 = 49.0$ ft

The quantities L and R are functions of δp, the plate separation angle:

$$F(\delta p) = (.3403 + 2(.3942)^2 - 2(.3942)(.3403 + (.3942)^2)^{1/2} \cos((\delta p + 5) + \tan^{-1}(.5833/.3942)))^{1/2} + .0833$$

$$R(\delta p) = (.3403 + 2(0.9838)^2 - 2(0.9838)(.3403 + (0.9838)^2)^{1/2} \cos((\delta p + 5) + \tan^{-1}(.5838/0.938)))^{1/2} + .0833$$

Table 5.1-5 shows the quantities R, Ru, F, Fu as a function of δp.

$Cx = 2.948$ ft.

$xx = 0.590$ ft.

$xf = 0.3942$ ft

$L_1 = F + Fu$

$L_4 = R_4 + Ru_4$

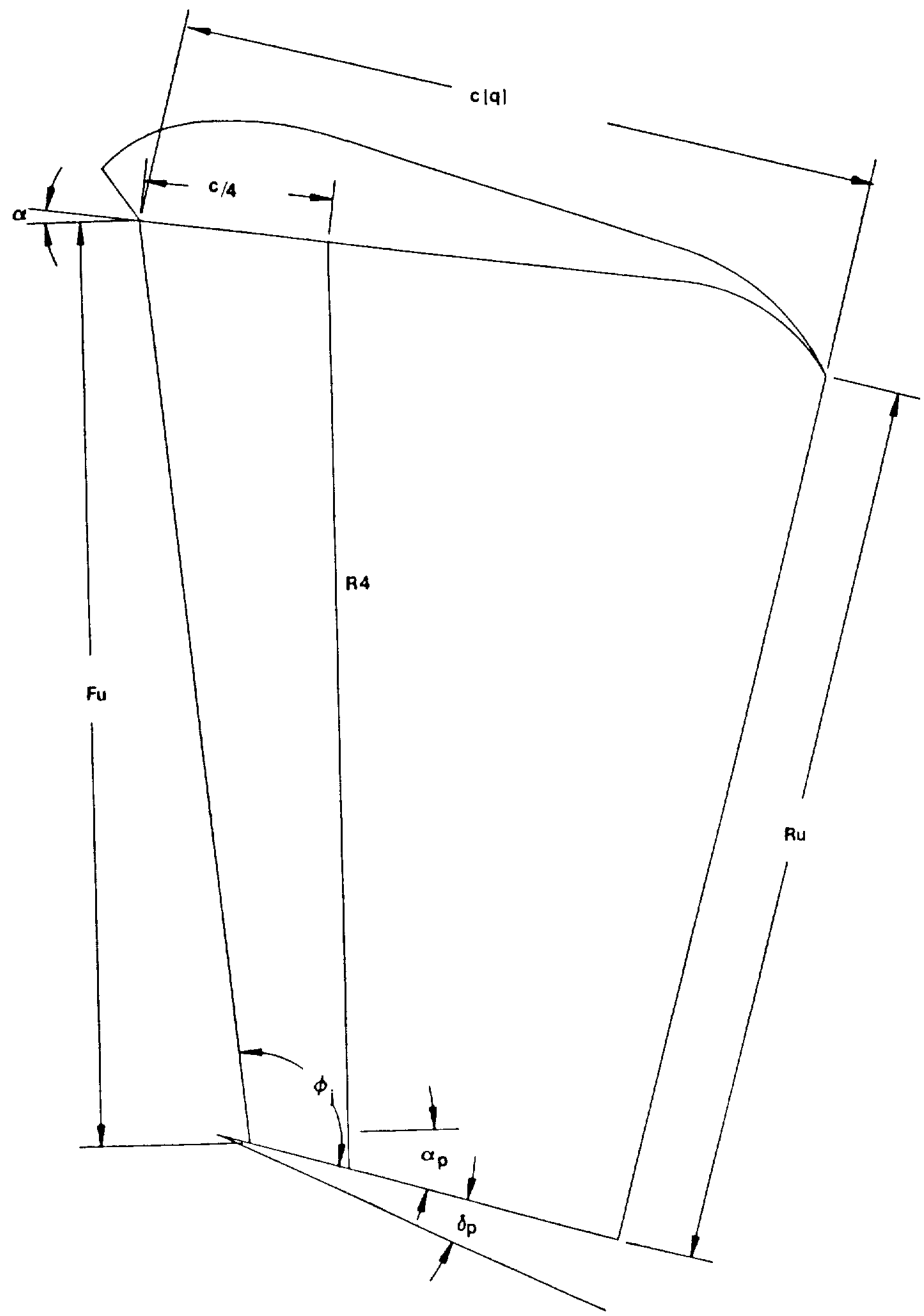

FIGURE 5.1-4, ANGLE OF ATTACK GEOMETRY

$\delta\rho$	R	RU	F	FU
0.0000	0.7524	48.4476	0.7010	47.9990
5.0000	0.8376	48.3624	0.7351	47.9649
10.0000	0.9219	48.2781	0.7688	47.9312
15.0000	1.0050	48.1950	0.8019	47.8981
20.0000	1.0866	48.1134	0.8341	47.8659
25.0000	1.1666	48.0334	0.8655	47.8345
30.0000	1.2446	47.9554	0.8959	47.8041
35.0000	1.3206	47.8794	0.9251	47.7749
40.0000	1.3944	47.8056	0.9531	47.7469
45.0000	1.4657	47.7343	0.9797	47.7203
50.0000	1.5345	47.6655	1.0050	47.6950
55.0000	1.6006	47.5994	1.0288	47.6712
60.0000	1.6639	47.5361	1.0511	47.6489
65.0000	1.7242	47.4758	1.0717	47.6283
70.0000	1.7815	47.4185	1.0907	47.6093
75.0000	1.8355	47.3645	1.1080	47.5920
80.0000	1.8863	47.3137	1.1236	47.5764
85.0000	1.9337	47.2663	1.1373	47.5627

TABLE 5.1-5, LINE LENGTH FUNCTIONS

5.1.3 Angle of Attack Results

Table 5.1-6 shows the resulting parafoil angles of attack for wind tunnel runs 1-17, along with values discussed in Section 5.1.2.

R	P	ALPHAP	DELTAP	FU	RU	XX	A	CX	THETA1	THETA2	ALPHA	PHI
1	3	2.31	29.75	47.81	47.96	0.59	47.75	2.95	0.70	92.29	4.99	84.33
1	4	-2.54	45.02	47.72	47.73	0.59	47.62	2.95	0.70	90.43	6.39	79.94
3	3	2.38	1.10	47.99	48.43	0.59	47.88	2.95	0.69	99.04	4.09	78.56
3	4	3.18	20.00	47.87	48.11	0.59	47.79	2.95	0.70	94.61	5.96	81.91
3	5	2.39	29.98	47.80	47.96	0.59	47.72	2.95	0.70	92.81	7.40	81.48
4	3	2.35	30.02	47.80	47.96	0.59	47.73	2.95	0.70	92.59	6.49	82.57
4	4	1.37	35.05	47.77	47.88	0.59	47.70	2.95	0.70	91.77	6.85	82.05
4	5	0.45	40.04	47.75	47.81	0.59	47.66	2.95	0.70	91.10	7.69	80.96
4	6	0.20	45.03	47.72	47.73	0.59	47.63	2.95	0.70	90.26	8.44	80.80
4	7	-0.50	50.03	47.69	47.67	0.59	47.59	2.95	0.70	89.62	9.42	79.76
5	3	-2.43	50.00	47.69	47.67	0.59	47.58	2.95	0.70	89.89	8.59	78.40
5	4	0.32	1.16	47.99	48.43	0.59	47.87	2.95	0.69	99.11	2.35	78.17
5	5	-2.46	12.30	47.92	48.24	0.59	47.78	2.95	0.69	97.23	3.29	76.34
6	3	-1.25	30.05	47.80	47.95	0.59	47.71	2.95	0.70	93.01	4.61	80.43
6	4	-4.19	30.03	47.80	47.95	0.59	47.67	2.95	0.69	93.71	4.52	76.89
6	5	-5.35	29.93	47.80	47.96	0.59	47.66	2.95	0.69	93.96	4.23	75.78
6	6	-5.43	29.84	47.81	47.96	0.59	47.66	2.95	0.69	94.06	4.54	75.28
6	7	-5.50	29.81	47.81	47.96	0.59	47.65	2.95	0.68	94.16	4.85	74.80
6	8	-5.54	29.78	47.81	47.96	0.59	47.64	2.95	0.68	94.52	6.29	72.97
9	3	0.73	1.10	47.99	48.43	0.59	47.87	2.95	0.69	99.13	2.79	78.12
9	4	-1.20	19.72	47.87	48.12	0.59	47.75	2.95	0.69	95.41	4.53	78.17
9	5	-1.15	25.01	47.83	48.03	0.59	47.72	2.95	0.69	94.31	5.22	78.62
9	6	-0.75	30.03	47.80	47.95	0.59	47.70	2.95	0.69	93.29	6.23	79.04
9	7	-0.23	31.79	47.79	47.93	0.59	47.69	2.95	0.70	92.90	6.80	79.37
9	8	0.27	25.01	47.83	48.03	0.59	47.74	2.95	0.70	94.04	5.53	80.01
9	9	-3.53	25.01	47.83	48.03	0.59	47.70	2.95	0.69	94.80	4.84	76.14
9	10	-5.44	24.86	47.84	48.04	0.59	47.68	2.95	0.68	96.23	4.56	74.09
9	11	-5.56	24.69	47.84	48.04	0.59	47.88	2.95	0.68	95.30	4.57	73.89
9	12	-5.66	24.57	47.84	48.04	0.59	47.87	2.95	0.68	95.43	4.88	73.35
9	13	-5.76	24.25	47.84	48.05	0.59	47.87	2.95	0.68	95.85	5.39	72.52
10	3	1.09	19.95	47.87	48.11	0.59	47.77	2.95	0.70	94.92	5.04	80.44
10	4	-2.24	19.94	47.87	48.11	0.59	47.74	2.95	0.69	95.52	4.16	77.39
10	5	-5.43	19.81	47.87	48.12	0.59	47.71	2.95	0.68	96.23	3.75	73.91
10	6	-5.58	19.69	47.87	48.12	0.59	47.71	2.95	0.68	96.29	3.71	73.74
10	7	-5.89	19.58	47.87	48.12	0.59	47.70	2.95	0.68	96.36	3.80	73.47
10	8	-5.78	19.51	47.87	48.12	0.59	47.70	2.95	0.68	96.56	4.46	72.52
11	3	0.87	19.79	47.87	48.12	0.59	47.78	2.95	0.70	94.82	4.27	81.08
11	4	1.44	24.84	47.84	48.04	0.59	47.75	2.95	0.70	93.81	5.82	81.31
11	5	-2.57	27.12	47.82	48.00	0.59	47.60	2.95	0.66	95.99	12.88	67.90
11	6	0.92	29.79	47.81	47.96	0.59	47.73	2.95	0.70	92.78	5.59	81.85
11	7	0.01	29.78	47.81	47.96	0.59	47.72	2.95	0.70	92.96	5.44	80.91
11	8	0.52	29.77	47.81	47.96	0.59	47.72	2.95	0.70	92.93	5.78	81.11
11	9	-3.14	29.83	47.81	47.96	0.59	47.68	2.95	0.69	93.71	5.19	77.27
11	10	0.29	29.64	47.81	47.96	0.59	47.72	2.95	0.70	92.96	5.58	81.05
11	11	-4.87	29.45	47.81	47.96	0.59	47.66	2.95	0.69	94.10	4.87	75.48
11	12	0.12	29.54	47.81	47.96	0.59	47.72	2.95	0.70	92.97	5.34	81.11
11	13	-5.44	29.22	47.81	47.97	0.59	47.66	2.95	0.68	94.30	4.93	74.64
11	14	0.29	29.34	47.81	47.97	0.59	47.72	2.95	0.70	92.99	5.43	81.17
12	3	1.44	29.99	47.80	47.96	0.59	47.74	2.95	0.70	92.52	5.28	82.93
12	4	-0.39	29.99	47.80	47.96	0.59	47.72	2.95	0.70	92.90	4.98	81.03
12	5	0.35	29.99	47.80	47.96	0.59	47.72	2.95	0.70	92.76	5.13	81.76
12	6	-3.72	30.05	47.80	47.95	0.59	47.68	2.95	0.69	93.67	4.84	77.08
12	7	0.24	30.06	47.80	47.95	0.59	47.72	2.95	0.70	92.79	5.24	81.51
12	8	-5.27	30.22	47.80	47.95	0.59	47.66	2.95	0.69	93.90	4.40	75.74
12	9	0.35	30.23	47.80	47.95	0.59	47.72	2.95	0.70	92.74	5.27	81.64
12	10	-5.44	30.42	47.80	47.95	0.59	47.65	2.95	0.68	93.99	4.79	75.09
12	11	2.01	19.93	47.87	48.11	0.59	47.79	2.95	0.70	94.59	4.62	82.10
12	12	0.98	19.93	47.87	48.11	0.59	47.78	2.95	0.70	94.78	4.35	81.15
12	13	1.55	19.90	47.87	48.11	0.59	47.78	2.95	0.70	94.69	4.54	81.82

TABLE 5.1-6, ANGLE OF ATTACK RESULTS

R	P	ALPHAP	DELTAP	FU	RU	XX	A	CX	THETA1	THETA2	ALPHA	PHI
12	14	0.87	19.93	47.87	48.11	0.59	47.78	2.95	0.70	94.78	4.27	81.12
12	15	1.81	19.95	47.87	48.11	0.59	47.79	2.95	0.70	94.62	4.38	81.91
12	16	-2.57	19.53	47.87	48.12	0.59	47.74	2.95	0.69	95.59	3.70	77.45
12	17	1.44	19.59	47.87	48.12	0.59	47.79	2.95	0.70	94.75	4.39	81.60
12	18	-3.49	20.03	47.87	48.11	0.59	47.73	2.95	0.69	95.66	3.58	76.60
12	19	1.73	20.06	47.87	48.11	0.59	47.79	2.95	0.70	94.61	4.58	81.84
12	20	-4.87	19.37	47.87	48.12	0.59	47.72	2.95	0.68	96.09	3.29	75.06
12	21	1.55	19.30	47.87	48.12	0.59	47.79	2.95	0.70	94.82	4.47	81.57
12	22	5.29	20.29	47.86	48.11	0.59	47.71	2.95	0.68	95.97	13.86	74.78
12	23	1.67	20.32	47.86	48.11	0.59	47.78	2.95	0.70	94.62	4.79	81.56
12	24	-5.50	19.21	47.87	48.13	0.59	47.71	2.95	0.68	96.31	3.41	74.10
12	25	1.44	19.35	47.87	48.12	0.59	47.79	2.95	0.70	94.84	4.51	81.39
12	26	-5.44	20.41	47.86	48.11	0.59	47.71	2.95	0.68	96.03	3.48	74.37
12	27	-2.88	1.07	47.99	48.43	0.59	47.84	2.95	0.68	99.84	2.02	74.60
12	28	-4.18	1.07	47.99	48.43	0.59	47.83	2.95	0.68	100.10	1.77	73.28
12	29	-5.44	1.00	47.99	48.43	0.59	47.82	2.95	0.67	100.30	1.28	72.30
12	30	-5.50	0.89	47.99	48.43	0.59	47.82	2.95	0.67	100.27	0.96	72.60
12	31	-5.62	0.84	47.99	48.43	0.59	47.82	2.95	0.67	100.25	0.70	72.76
12	32	-3.32	0.95	47.99	48.43	0.59	47.84	2.95	0.68	99.88	1.60	74.52
12	33	-3.32	0.96	47.99	48.43	0.59	47.84	2.95	0.68	99.91	1.76	74.33
12	34	-3.89	0.96	47.99	48.43	0.59	47.83	2.96	0.68	100.07	1.83	73.53
12	35	-3.32	0.95	47.99	48.43	0.59	47.84	2.95	0.68	99.93	1.81	74.26
12	36	-3.89	0.95	47.99	48.43	0.59	47.83	2.95	0.68	100.08	1.86	73.49
12	37	-3.32	0.95	47.99	48.43	0.59	47.84	2.95	0.88	99.92	1.78	74.30
12	38	-5.44	0.93	47.99	48.43	0.59	47.82	2.95	0.67	100.32	1.28	72.28
12	39	-3.55	0.93	47.99	48.43	0.59	47.84	2.95	0.68	99.95	1.63	74.19
12	40	-5.33	0.94	47.99	48.43	0.59	47.81	2.95	0.67	100.36	1.55	72.09
12	41	-3.15	0.95	47.99	48.43	0.59	47.84	2.95	0.68	99.92	1.96	74.29
12	42	-5.44	0.77	47.99	48.43	0.59	47.82	2.95	0.67	100.33	1.13	72.43
12	43	-3.72	0.79	47.99	48.43	0.59	47.84	2.95	0.68	99.96	1.39	74.25
12	44	-5.44	1.00	47.99	48.43	0.59	47.81	2.95	0.67	100.37	1.53	71.99
12	45	-3.43	1.04	47.99	48.43	0.59	47.83	2.95	0.68	99.96	1.90	74.04
12	46	-5.44	0.46	48.00	48.44	0.59	47.82	2.95	0.67	100.42	1.17	72.30
12	47	-3.37	0.53	48.00	48.44	0.59	47.84	2.95	0.68	100.03	1.75	74.17
12	48	-5.44	1.18	47.99	48.43	0.59	47.81	2.95	0.67	100.31	1.48	72.10
12	49	-4.87	1.06	47.99	48.43	0.59	47.82	2.96	0.67	100.25	1.69	72.51
12	50	-3.55	1.07	47.99	48.43	0.59	47.83	2.95	0.68	99.98	1.91	73.88
13	3	1.61	29.99	47.80	47.96	0.59	47.73	2.95	0.70	92.69	6.14	82.08
13	4	1.61	29.99	47.80	47.96	0.59	47.73	2.95	0.70	92.69	6.11	82.11
13	5	1.61	30.00	47.80	47.96	0.59	47.73	2.95	0.70	92.68	6.08	82.15
13	6	1.61	29.99	47.80	47.96	0.59	47.73	2.95	0.70	92.71	6.22	81.97
13	7	1.50	29.99	47.80	47.96	0.59	47.72	2.95	0.70	92.75	6.26	81.79
13	8	1.44	29.99	47.80	47.96	0.59	47.72	2.95	0.70	92.81	6.43	81.50
13	9	1.44	29.99	47.80	47.96	0.59	47.72	2.95	0.70	92.89	6.74	81.11
13	10	1.04	30.00	47.80	47.98	0.59	47.71	2.95	0.70	93.03	6.92	80.39
13	11	0.28	29.98	47.80	47.96	0.59	47.69	2.95	0.69	93.38	7.59	78.61
13	12	2.19	29.99	47.80	47.96	0.59	47.66	2.95	0.69	93.95	11.83	75.73
13	13	2.30	30.00	47.80	47.96	0.59	47.73	2.95	0.70	92.56	6.27	82.78
13	14	2.59	30.00	47.80	47.96	0.59	47.74	2.95	0.70	92.51	6.40	82.98
13	15	2.59	29.98	47.80	47.96	0.59	47.73	2.95	0.70	92.55	6.52	82.82
13	16	2.59	29.98	47.80	47.96	0.59	47.73	2.96	0.70	92.57	6.63	82.69
13	17	2.24	30.00	47.80	47.96	0.59	47.73	2.96	0.70	92.58	6.31	82.65
13	18	2.01	30.00	47.80	47.96	0.59	47.73	2.95	0.70	92.69	6.54	82.08
13	19	1.61	30.00	47.80	47.96	0.59	47.72	2.95	0.70	92.77	6.45	81.69
13	20	1.61	29.98	47.80	47.96	0.59	47.72	2.96	0.70	92.87	6.82	81.22
13	21	0.52	29.98	47.80	47.96	0.59	47.71	2.95	0.70	93.08	6.62	80.12
13	22	-0.28	29.99	47.80	47.98	0.59	47.70	2.95	0.70	93.25	6.50	79.28
13	23	-0.58	30.00	47.80	47.96	0.59	47.68	2.95	0.69	93.63	7.77	77.35
13	24	2.82	29.99	47.80	47.96	0.59	47.74	2.95	0.70	92.48	6.47	83.17
14	3	0.18	1.11	47.99	48.43	0.59	47.87	2.95	0.69	99.16	2.46	77.93
14	4	0.18	1.11	47.99	48.43	0.59	47.87	2.95	0.69	99.19	2.48	77.82

TABLE 5.1-6, ANGLE OF ATTACK RESULTS (CONTINUED)

R	P	ALPHAP	DELTAP	FU	RU	XX	A	CX	THETA1	THETA2	ALPHA	PHI
14	5	0.18	1.11	47.99	48.43	0.59	47.87	2.96	0.89	99.15	2.32	78.02
14	6	0.18	1.11	47.99	48.43	0.59	47.87	2.96	0.89	99.19	2.50	77.80
14	7	0.18	1.11	47.99	48.43	0.59	47.87	2.95	0.89	99.15	2.36	77.98
14	8	0.01	1.11	47.99	48.43	0.59	47.87	2.95	0.89	99.18	2.30	77.84
14	9	0.01	1.11	47.99	48.43	0.59	47.87	2.95	0.89	99.20	2.35	77.77
14	10	0.01	1.11	47.99	48.43	0.59	47.87	2.95	0.89	99.20	2.35	77.77
14	11	0.01	1.11	47.99	48.43	0.59	47.86	2.95	0.89	99.36	3.01	76.95
14	12	-1.14	1.11	47.99	48.43	0.59	47.85	2.95	0.88	99.54	2.80	76.03
14	13	0.01	1.11	47.99	48.43	0.59	47.84	2.95	0.88	99.70	4.36	75.27
14	14	0.52	1.11	47.99	48.43	0.59	47.87	2.95	0.89	99.11	2.53	78.19
14	15	0.52	1.12	47.99	48.43	0.59	47.88	2.95	0.89	99.08	2.43	78.32
14	16	0.52	1.11	47.99	48.43	0.59	47.87	2.95	0.89	99.12	2.56	78.15
14	17	0.52	1.11	47.99	48.43	0.59	47.87	2.95	0.89	99.11	2.54	78.18
14	18	0.52	1.11	47.99	48.43	0.59	47.87	2.95	0.89	99.12	2.55	78.16
14	19	0.52	1.11	47.99	48.43	0.59	47.87	2.95	0.89	99.19	2.82	77.82
14	20	0.52	1.11	47.99	48.43	0.59	47.87	2.95	0.89	99.17	2.78	77.88
14	21	0.01	1.11	47.99	48.43	0.59	47.87	2.95	0.89	99.21	2.42	77.69
14	22	-0.57	1.11	47.99	48.43	0.59	47.86	2.95	0.89	99.38	2.50	76.86
14	23	-0.85	1.11	47.99	48.43	0.59	47.85	2.96	0.88	99.54	2.89	76.03
14	24	-0.85	1.11	47.99	48.43	0.59	47.85	2.95	0.88	99.66	3.36	75.46
14	25	0.29	1.11	47.99	48.43	0.59	47.88	2.95	0.89	99.08	2.17	78.35
14	26	2.99	20.03	47.87	48.11	0.59	47.80	2.95	0.70	94.43	5.06	82.80
14	27	2.99	20.03	47.87	48.11	0.59	47.79	2.96	0.70	94.44	5.09	82.76
14	28	2.99	19.99	47.87	48.11	0.59	47.79	2.96	0.70	94.48	5.24	82.57
14	29	2.99	20.03	47.87	48.11	0.59	47.79	2.95	0.70	94.47	5.24	82.57
14	30	2.82	20.01	47.87	48.11	0.59	47.79	2.95	0.70	94.52	5.28	82.34
14	31	2.01	20.03	47.87	48.11	0.59	47.79	2.96	0.70	94.59	4.74	81.98
14	32	1.44	20.00	47.87	48.11	0.59	47.78	2.95	0.70	94.81	5.03	80.90
14	33	0.87	20.00	47.87	48.11	0.59	47.77	2.96	0.70	94.96	5.04	80.17
14	34	0.29	19.99	47.87	48.11	0.59	47.76	2.96	0.89	95.12	5.12	79.35
14	35	-0.85	19.99	47.87	48.11	0.59	47.74	2.95	0.89	95.46	5.35	77.65
14	36	-1.71	20.01	47.87	48.11	0.59	47.72	2.95	0.88	95.93	6.40	75.28
14	37	3.39	20.01	47.87	48.11	0.59	47.80	2.95	0.70	94.40	5.31	82.98
14	38	0.01	1.11	47.99	48.43	0.59	47.87	2.95	0.89	99.23	2.49	77.60
14	39	1.15	9.93	47.93	48.28	0.59	47.83	2.95	0.89	97.00	3.62	79.84
14	40	1.10	15.09	47.90	48.19	0.59	47.79	2.95	0.70	96.04	4.82	79.56
14	41	-2.28	19.91	47.87	48.11	0.59	47.72	2.96	0.89	95.91	6.67	75.46

TABLE 5.1-6, ANGLE OF ATTACK RESULTS (CONTINUED)

5.2 PACS WEIGHT TARE

The Parafoil Attitude Control System (PACS) was originally conceived to enable a parafoil to be tested through a range of rigging angles and to allow the parafoil to find its natural trim point. This concept consisted of a set of hinged plates to effect the change in rigging angle and a moveable pivot point (Xcp drive system) to allow the parafoil to fly at its natural trim angle without distorting the suspension system. The original design concept included an active counterweight system which would balance the PACS in both the X- and Z-axes thus keeping the center of gravity of the PACS at the pivot point no matter what the angle between the plates of the Xcp setting. This balanced system would reduce the effect of the PACS on the test article to only the dynamic moment of inertia of the system.

Due to time and budget constraints, the active counterweight system was replaced by a static counterweight. This static counterweight essentially only balanced the PACS in the X-axis at one angle between the plates and one Xcp setting. Because of this imbalance in the PACS, the test article was required to overcome the moment imposed about the pivot point by the weight of the PACS. This meant that the Xcp setting had to be increased to allow the parafoil normal force to overcome the increase in moment. During testing it was found that the travel of the Xcp drive system was insufficient to overcome this moment; thus the Xcp of the PACS could not be matched to the natural trim condition of the test article.

As a result of the imbalance of the PACS and the limited Xcp travel the data were compromised in two ways: (1) since the PACS could not match the natural trim condition of the test article, the parafoil suspension lines were slightly distorting the parafoil; and (2) the data included the moment created by the shift in the center of gravity (c.g.) of the PACS. The distortion of the parafoil was found to be minimal and could be considered within the accuracy of the rigging of the parafoil; however, the moment created by the PACS c.g. was found to be significant and required development of a methodology to modify the data to eliminate the effect of the PACS c.g. shift. This section documents the methodology which was developed to calculate the weight tare of the PACS.

5.2.1 Weight Tare Methodology

Since the weight of the PACS with no tunnel flow always acts in the vertical plane in line with the pivot point, it is possible to determine the weight centroid of the PACS at a given angle between the plates. This is done by setting the PACS at the positive and negative Xcp limits and measuring the angle of the top plate with respect to horizontal at each of the Xcp settings. Given this information for a range of angles between the plates (δ_p) a set of calibration curves for the weight centroid can be developed as a function of δ_p. Figure 5.2-1 below defines the nomenclature necessary to develop the equations to calculate the weight centroid.

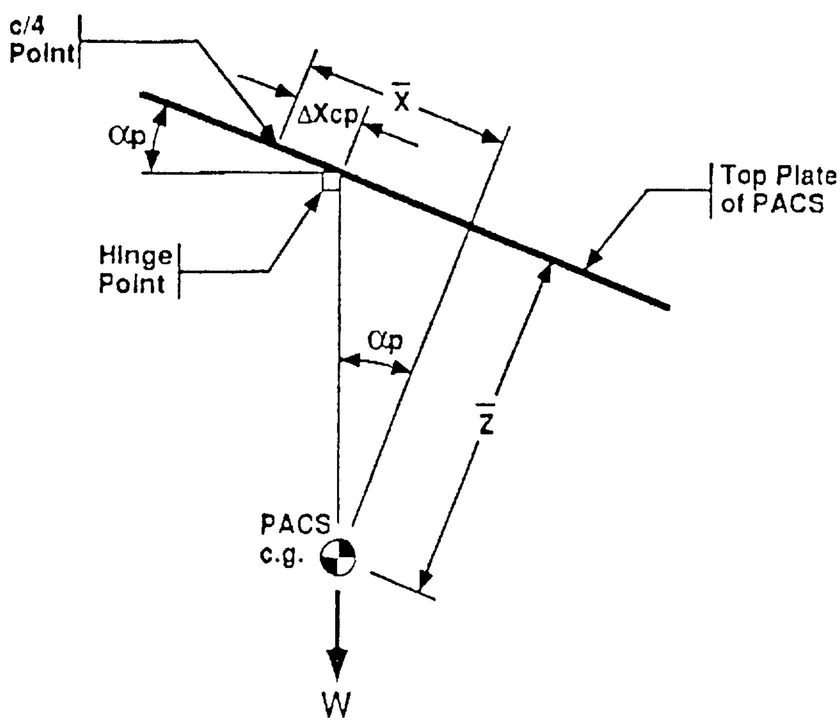

FIGURE 5.2-1, WEIGHT TARE NOMENCLATURE

The angle of the top plate (αp) is defined by the following equation.

$$\alpha p = \tan^{-1}((x-\Delta Xcp)/z)$$

For two ΔXcp locations the equation above can be transformed to the two equations below.

$$z \tan \alpha p_1 = x - \Delta Xcp_1$$
$$z \tan \alpha p_2 = x - \Delta Xcp_2$$

Subtracting these equations and solving for the Z-axis centroid location yields the following equation.

$$z = (\Delta Xcp_2 - \Delta Xcp_1)/(\tan \alpha p1 - \tan \alpha p2)$$

Substituting the above equation into the original equation yields the following equation for the X-axis centroid location.

$$x = ((\Delta Xcp_2 - \Delta Xcp_1)/(\tan \alpha p1 - \tan \alpha p2))\tan \alpha p1 + \Delta Xcp_1$$

This weight tare calibration was performed post-test at discrete values for the angle between the PACS plate ($\delta_p = 1^o, 5^o, 10^o,...,50^o, 55^o, 59^o$). These data were used to develop the weight tare calibration.

5.2.2 Inclinometer Calibration

When the weight tare calibration was performed it was discovered that the angle of the top plate exceeded the calibration range of the inclinometer used to measure the angle. A calibration of the inclinometer was performed to extend the calibrated range of the inclinometer. It was originally felt that this calibration might be questionable and outside the linear range of the inclinometer; however when the measured data were compared to the original calibration as shown below, the data showed a very good correlation.

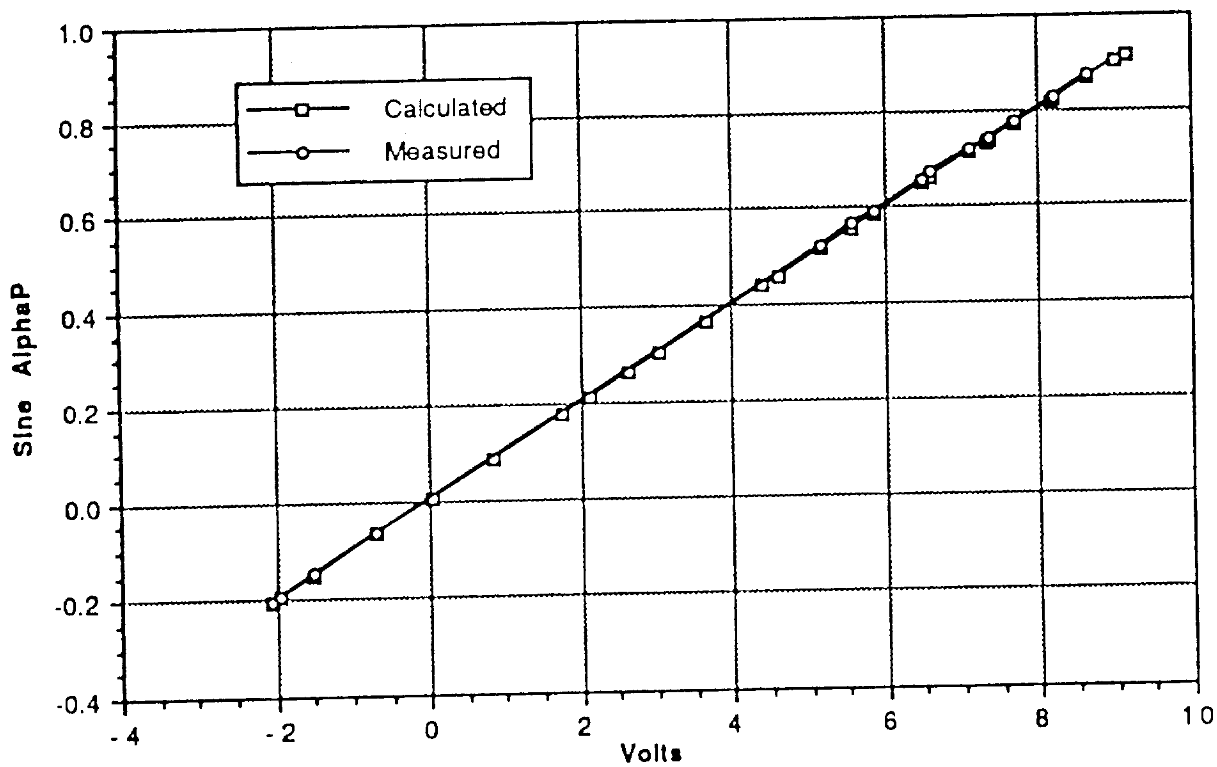

FIGURE 5.2-2, INCLINOMETER CALIBRATION

5.2.3 Weight Tare Calibration

Table 5.2-3 and Figure 5.2-4 were developed using the equations developed in the weight tare methodology section, the data obtained in the weight tare calibration, and the original inclinometer calibration. Due to the small plate angle changes with changes in Xcp at $\delta_p = 1^o$ and 5^o, the trigonometric tangent function accuracy cause these data to be questionable, therefore they were removed from the data base.

Point #	Lpot (In)	DelP (deg)	Xcp (In)	Output (volts)	Calc Sine	Calc AlphaP	Zbar	Xbar
1			-2.500	2.118	0.2118	12.2259		
2	0.027	1	-2.505	7.373	0.7375	47.5194	-19.8377	-24.1688
3	0.027	1	3.932	8.167	0.8169	54.7799		
5	0.211	5	-2.501	9.142	0.9145	66.1330	5.4176	9.7435
4	0.211	5	3.933	7.312	0.7314	47.0042	4.6507	8.0103
28	0.211	5	3.938	6.586	0.6588	41.2061		
6	0.507	10	-2.501	9.025	0.9028	64.5261	4.5154	6.9768
27	0.507	10	3.938	5.582	0.5583	33.9400		
7	0.871	15	-2.501	8.655	0.8658	59.9701	5.3189	6.7004
26	0.871	15	3.939	4.607	0.4608	27.4374		
8	1.296	20	-2.501	8.200	0.8202	55.1092	6.1812	6.3626
25	1.296	20	3.939	3.650	0.3650	21.4098		
9	1.775	25	-2.501	7.683	0.7685	50.2212	6.9533	5.8509
24	1.775	25	3.940	2.650	0.2650	15.3664		
10	2.301	30	-2.501	7.100	0.7102	45.2507	7.7676	5.3349
23	2.301	30	3.940	1.768	0.1767	10.1805		
11	2.866	35	-2.501	6.486	0.6488	40.4486	8.3721	4.6365
22	2.866	35	3.940	0.830	0.0829	4.7557		
12	3.463	40	-2.501	5.845	0.5846	35.7773	8.9790	3.9695
21	3.463	40	3.941	0.033	0.0032	0.1817		
13	4.085	45	-2.501	5.151	0.5152	31.0111	9.6171	3.2801
20	4.085	45	3.941	-0.684	-0.0686	-3.9314		
14	4.727	50	-2.501	4.397	0.4398	26.0892	10.0489	2.4195
19	4.727	50	3.941	-1.495	-0.1497	-8.6095		
15	5.378	55	-2.501	3.659	0.3659	21.4652	10.9141	1.7905
18	5.378	55	3.941	-1.931	-0.1933	-11.1465		
16	5.905	59	-2.501	3.030	0.3030	17.6383	12.2237	1.3856
17	5.905	59	3.937	-2.041	-0.2043	-11.7899		

TABLE 5.2-3, PACS CENTER OF GRAVITY CALCULATIONS

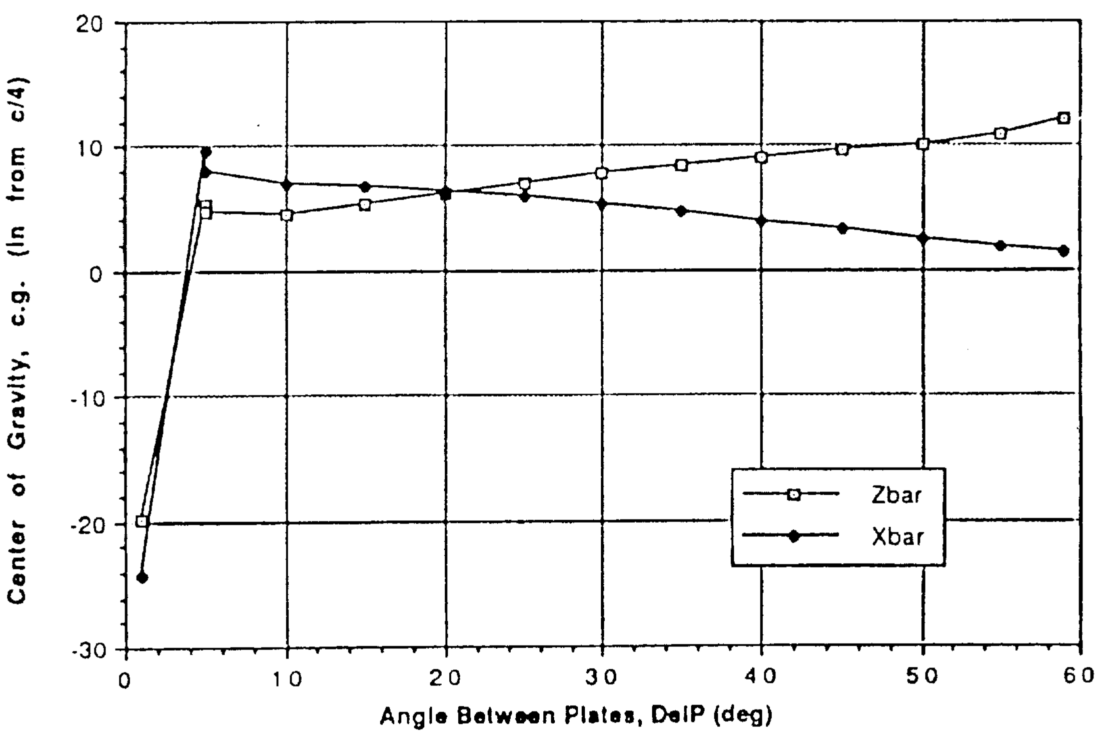

FIGURE 5.2-4, PACS CENTER OF GRAVITY LOCATION

5.2.4 Induced Moment

As mentioned earlier when the test article is "flying" it must overcome the moment induced by the offset in the PACS center of gravity. Figure 5.2-5 below depicts the nomenclature which defines this phenomenon.

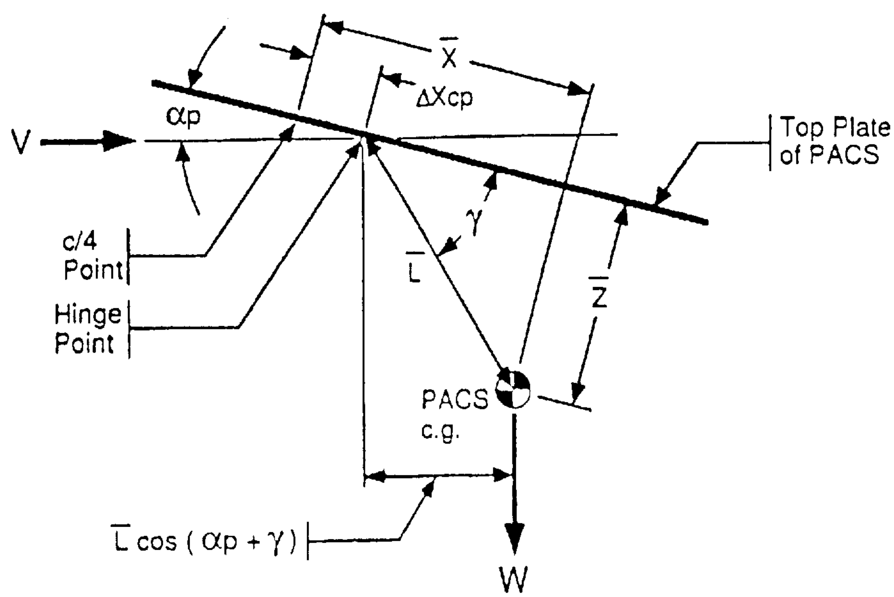

FIGURE 5.2-5, INDUCED MOMENT NOMENCLATURE

The distance from the pivot point to the PACS c.g. is given by the following equation.

$$L = ((x - \Delta Xcp)^2 + (z)^2)^{1/2}$$

The angle between the top plate of the PACS, the pivot point, and the PACS c.g. is determined by the following equation.

$$\gamma = \tan^{-1}(z/(x-\Delta Xcp))$$

The induced moment is therefore determined by the following equation.

$$\Delta M_{PACS(c.g.)} = W_{PACS} L \sin(\alpha_p + \gamma)$$

This methodology was applied to all the data and the induced moment, due to the offset in the PACS c.g., was removed from the data.

5.3 SUSPENSION LINE LIFT AND DRAG STUDY

A study was conducted to determine the percentage of vehicle lift and drag due to the suspension lines. Originally a value of 15% was quoted for the line drag value, which is normal for an average parafoil setup. However, due to the number of lines found in the ARS Parafoil (960) a new study was conducted. To conduct this study the configuration and data were taken from the 20 x 60 ft parafoil tested at NASA Ames Research Center in August 1988.

5.3.1 Parafoil Configuration

The parafoil configuration, shown in Figure 5.3-1, is the 20 x 60 ft, 1/3 scale model. In estimating the line lift and drag, since the parafoil is laterally symmetrical, half the model was analyzed. (The final values were then doubled.) The test case chosen was at $\alpha = 0.0$, L/D = 2.90. Figure 5.3-2 shows the longitudinal line geometry at the test case.

ORIGINAL PAGE IS
OF POOR QUALITY

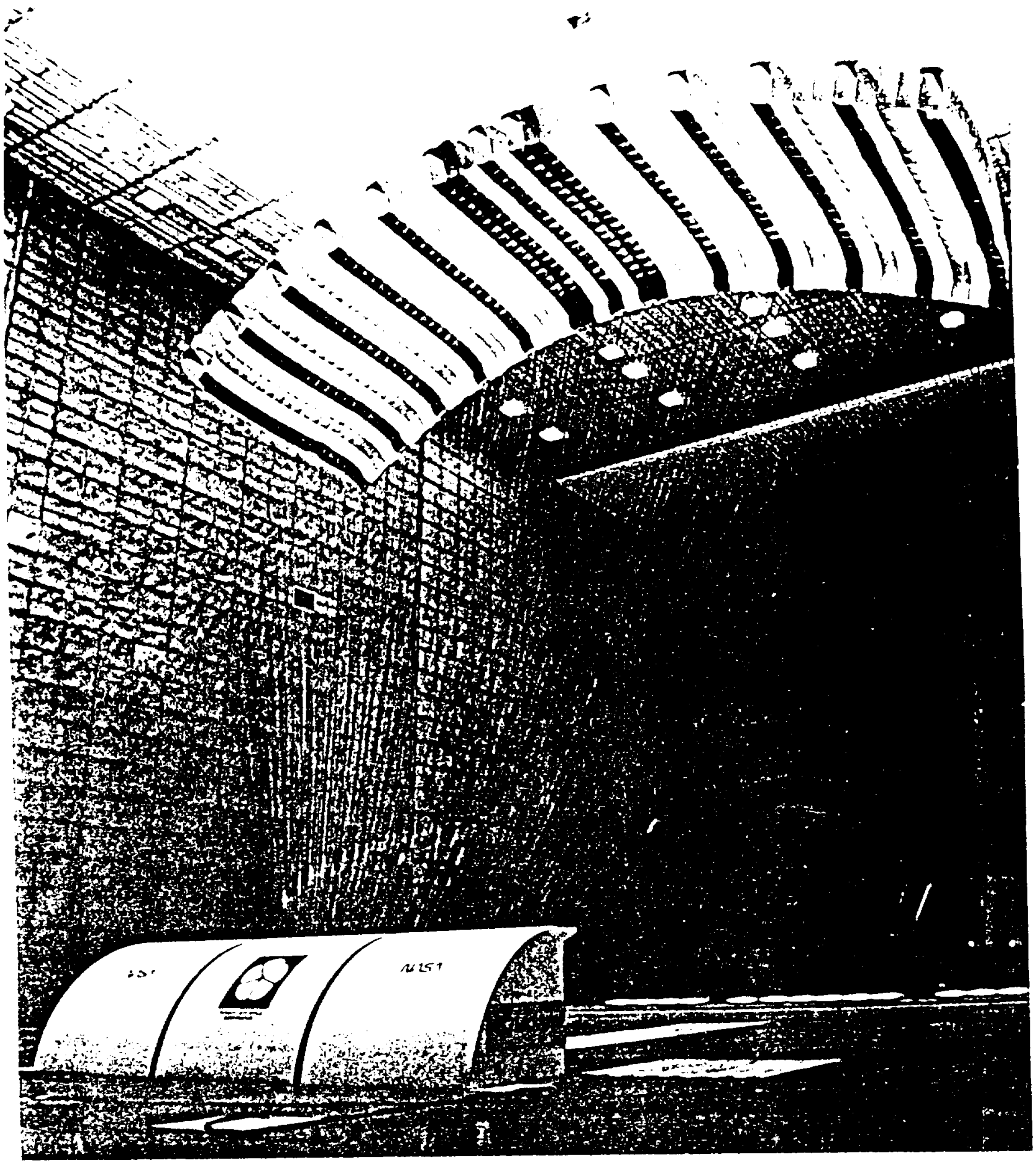

FIGURE 5.3-1, 20 FT X 60 FT PARAFOIL
1/3 SCALE MODEL

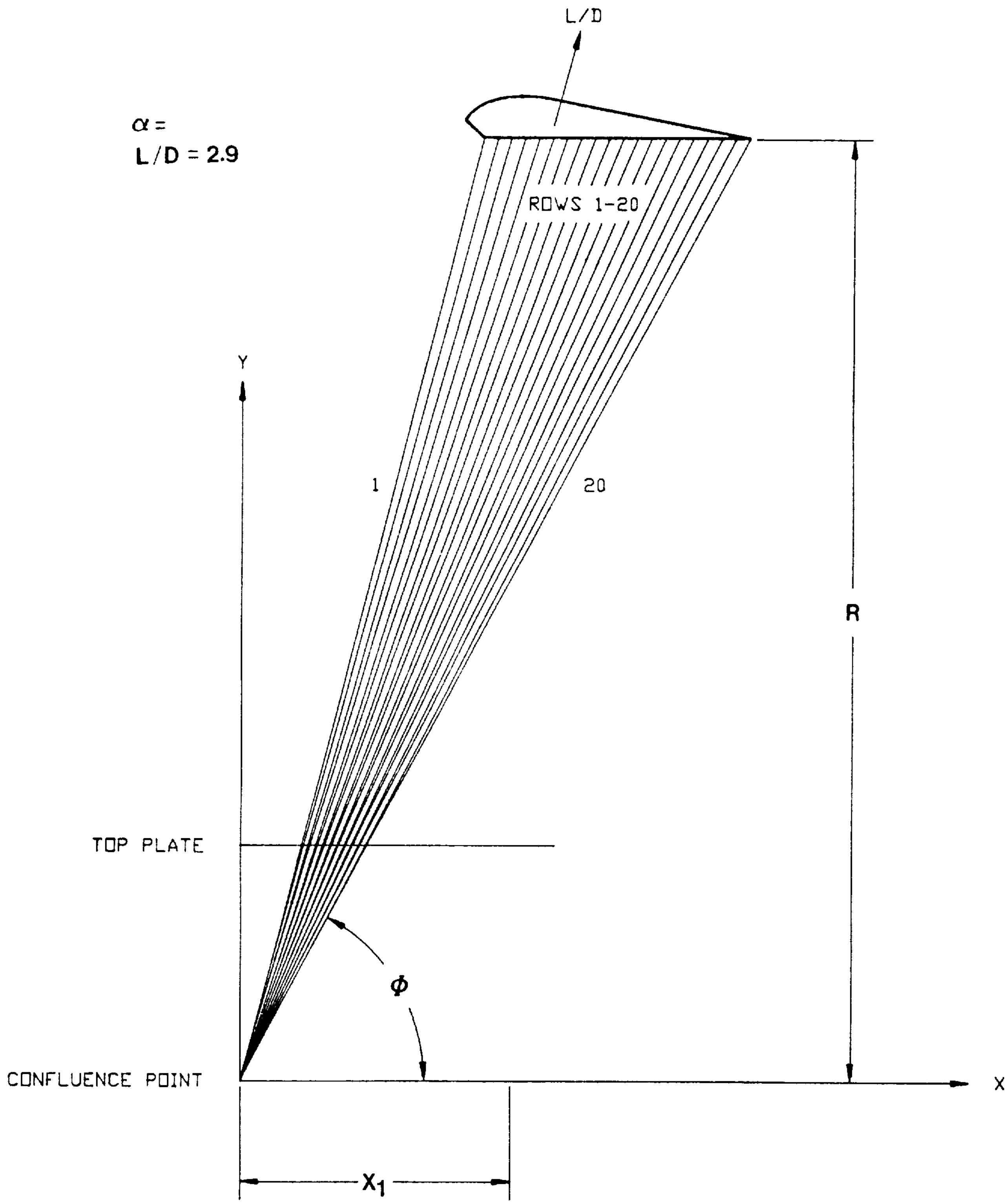

FIGURE 5.3-2, LONGITUDINAL LINE GEOMETRY

5.3.2 Drag Coefficient Estimate

As a means of comparison to the wind tunnel test case, which lists aero coefficients, a C_D for the suspension lines had to be determined. In Fluid Dynamic Drag (Hoerner, 1965) the Cross Flow Principle is used, which determines coefficients for flow around wires and cables. Figure 5.3-3 depicts the nomenclature for the Cross Flow Principle. To determine C_D the following equations are used:

$C_{D1} = 1.10 \sin^3(\alpha)$	A_{ref} = LxD of line ($A_{ref}1$)
$C_{D2} = C_{D1} * A_{ref}1/A_{ref}2$	A_{ref} = ΣLxD for lines ($A_{ref}2$)
$C_{D3} = C_{D2} * A_{ref}2/A_{ref}3$	A_{ref} = A_{ref} Parafoil ($A_{ref}3$)

where C_{D1} is the Drag Coefficient based on each line's reference area, C_{D2} the Drag Coefficient based on the total line reference area (105.87 ft^2), C_{D3} the Drag Coefficient based on the parafoil reference area (1200 ft^2) and ϕ is the angle of attack. Table 5.3-7 lists the values calculated for the angle ϕ, and Table 5.3-8 the values for $A_{ref}1$.

In the equations above the line diameter, D, was assumed to be 4.458×10^{-3} ft, or the average diameter of the lines under load. In determining the length, L, only the line length exposed to the flow was used. The following equation was used to obtain this length.

$$LA = LR - LP$$

where LR is the length from the parafoil to the confluence point, LP the length from confluence point to the top plate, and LA the exposed length (see Figure 5.3-4). Tables 5.3-9 to 5.3-11 give values calculated for the line lengths, LA.

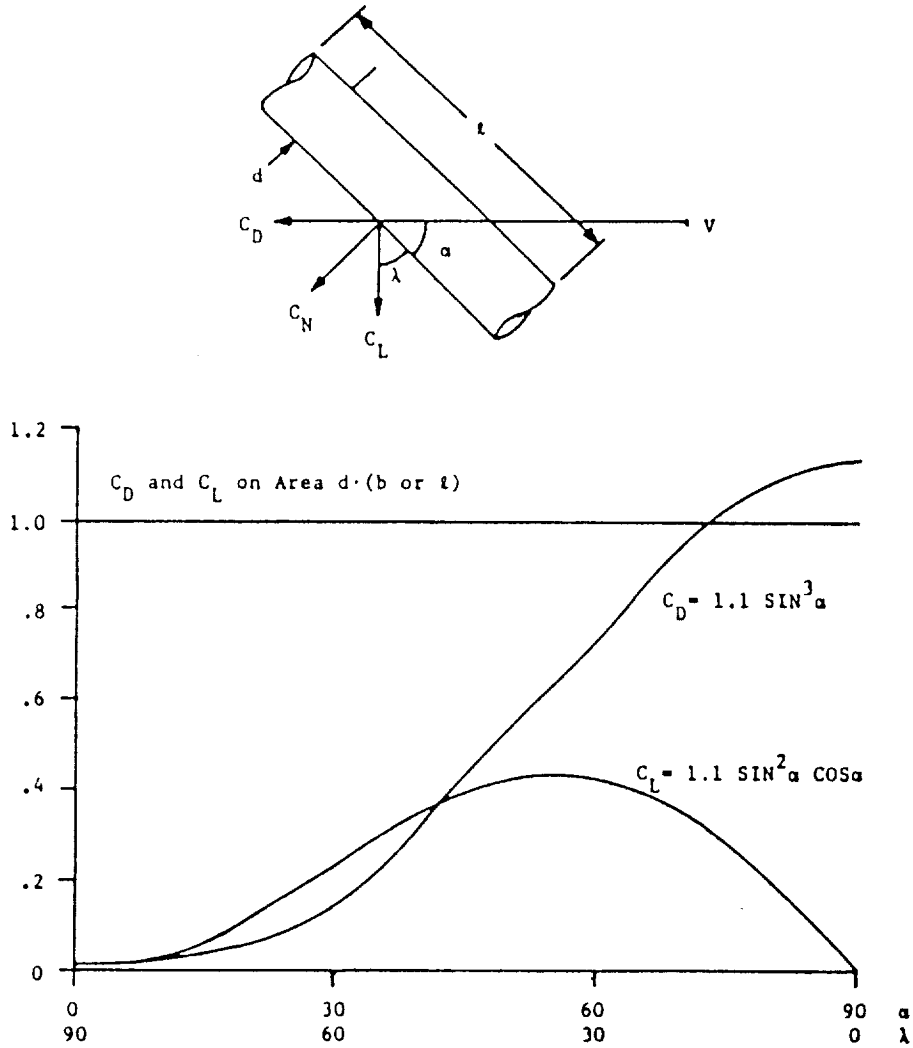

FIGURE 5.3-3, CROSS FLOW PRINCIPLE

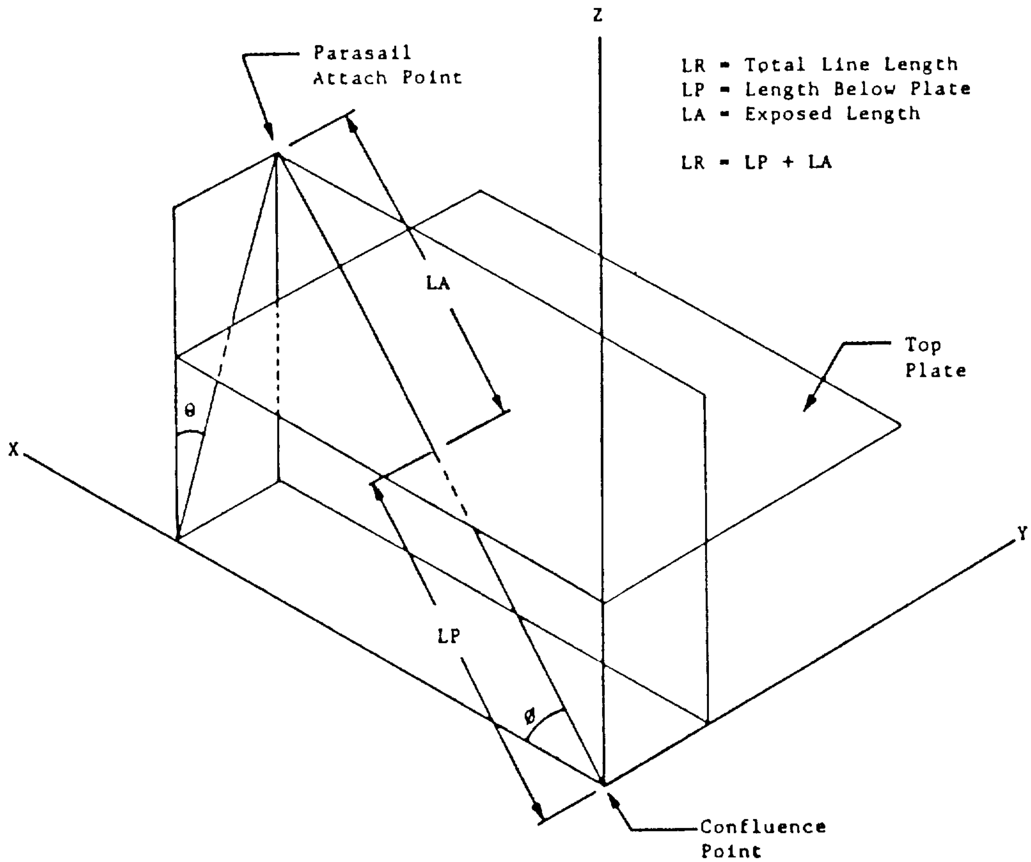

FIGURE 5.3-4, LINE LENGTH NOMENCLATURE

5.3.3 Drag Coefficient Results

Drag coefficients were calculated using equations derived in Section 5.3.2. The results for C_{D1}, C_{D2} and C_{D3} can be found in Tables 5.3-6, 5.3-7 and 5.3-8 respectively. The total C_D's for the lines were found to be the following:

$$C_{D2T} = 1.73709 \quad \text{(based on } A_{ref}2\text{)}$$
$$C_{D3T} = 0.15326 \quad \text{(based on } A_{ref}3\text{)}$$

5.3.4 Lift Coefficient Estimate

A C_L for the suspension lines also had to be determined for comparison purposes. The same Cross Flow principle found in Fluid Dynamic Drag (Hoerner 1965)[2] is used. Figure 5.3-3 depicts the nomenclature for the Cross Flow Principle, and Figure 5.3-5 depicts the geometry for determining C_L. The following set of equations are used in calculating C_L:

$$C_{L1} = 1.10 \sin^2(\phi) * \cos(\phi) * \cos(\theta) \qquad A_{ref} = A_{ref}1$$
$$C_{L2} = C_{L1} * A_{ref}1/A_{ref}2 \qquad A_{ref} = A_{ref}2$$
$$C_{L3} = C_{L2} * A_{ref}2/A_{ref}3 \qquad A_{ref} = A_{ref}3$$

where C_{L1} is the Lift Coefficient based on each line's reference area, C_{L2} with Lift Coefficient based on the total line reference area (105.87 ft^2), C_{L3} the Lift Coefficient based on the parafoil reference area (1200 ft^2), ϕ is the angle of attack, and θ is the rotation angle in the YZ plane. Table 5.3-1 lists the values calculated for the angle ϕ, Table 5.3-9 the values for angle θ, and Table 5.3-3 the values for $A_{ref}1$.

In the equations above the line diameter, D, was assumed to be 4.458×10^{-3} ft, or the average diameter of the lines under load. In determining the length, L, only exposed the line length discussed in Section 5.3.2 was used.

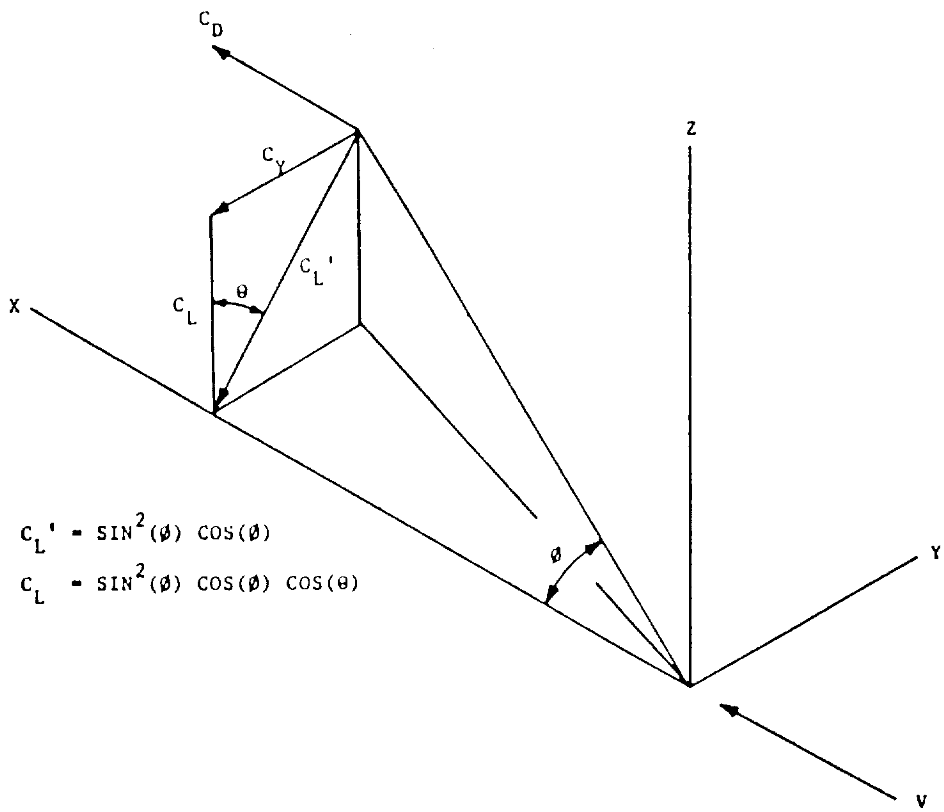

FIGURE 5.3-5, LIFT COEFFICIENT GEOMETRY

5.3.5 Lift Coefficient Results

Lift coefficients were calculated using equations developed in section 5.3.4. The results for C_{L1}, C_{L2} and C_{L3} can be found in Tables 5.3-10, 5.3-11 and 5.3-12 respectively.

The total C_L's for the lines were found to be the following:

C_{L2T} = -0.66988 (based on $A_{ref}2$)
C_{L3T} = -0.05910 (based on $A_{ref}3$)

NOTE: The negative sign reflects that the line lift acts in the opposite direction of parafoil lift.

5.3.6 Comparison to Test Data

To determine the percentage of drag due to the lines a test point from the wind tunnel was selected having a similar set of parafoil attitude conditions. Shown in Figure 5.3-6 is the selected point with an α_p = 0.2 and an L/D of 2.93. As the figure shows:

C_D = 0.315895

and for the lines:

C_{D3T} = 0.15236

Therefore:

C_D Lines = 48.5% of total drag

In determining the percentage of lift due to the lines, the same test condition shown in Figure 5.3-6 was used. As the figure shows:

$$C_L = 0.927782$$

and for the lines:

$$C_{L3T} = -0.05910$$

Therefore:

$$C_L \text{ Lines} = 6.4\% \text{ of total Lift (negative sense)}$$

```
0RUN   4      POINT  6   ACQUIRED  9/12/88 AT 17:33: 1     DATE PRINTED 10/13/88    TIME PRINTED 15:32:03     CONF  1.0   VER 3
------------------------------------------------------------------------------------------------------------------------------------
0TUNNEL CONDITIONS                                              PACS                                   CONTROL LINES   CONTROL,C
---------------------                                           ------                                -------------------------
  PRESSURES   TEMPERATURES   VELOCITIES     MISCELLANEOUS         ANGLES      CENTER OF PRESSURE
                                                                -------------
BARO  14.6640   TT    62.8   VKTS   42.61  RH   68.7          | ALPHAP   0.20 |   XCP   3.887       1     -0.1     1      0.0
                                                                -------------
PT     0.0180                MTUN  0.0642  RHO   .233847E-02    JPHI    93.01     DISTANCES          2     -1.1     2     -0.2
PS     0.0304                                                   PHI     80.80    LPOT  21.666        CTL1   0.053
Q      6.0463                                                   THETA   85.35                        CTL2   0.082
                                                                DELTAP  45.03
TETHER LINES                                                     TETHER,C
--------------                                                   ---------
1    -0.2  2    -0.5  3     0.0  4    -0.1                       1     0.0  2    -0.1   3     0.0  4     0.0
RISERS                                                           RISERS,C
--------                                                         ---------
1    21.3  5    18.4  9    43.7  13   32.9  17   18.4            1     3.6  5     3.0   9     7.2 13     5.4  17    3.0
2    22.1  6    36.6  10  126.6  14   36.2  18   13.1            2     3.6  6     6.0   10   20.9 14     6.0  18    2.2
3    27.2  7    32.8  11   47.9  15   23.9  19   11.5            3     4.5  7     5.4   11    7.9 15     3.9  19    1.9
4    34.3  8     6.8  12   43.0  16   15.9  20    5.1            4     5.7  8     1.1   12    7.1 16     2.6  20    0.8
0WIND TUNNEL BALANCE LOADS AND COEFFICEINTS -- MODEL
-----------------------------------------------------
LIFTU    6732.  PITCHU   -813.  LIFTC    6732.  PITCHC   -813.  L/D        2.937    ----------------
                                                                                    | CL   0.927782 |  CMY  -0.005681
DRAGU    2292.  YAWU     -130.  DRAGC    2292.  YAWC     -130.  DELMCG   8236.58    ----------------
                                                                                    | CD   0.315895 |  CMZ  -0.006299
SIDEU    -156.  ROLLU    -517.  SIDEC    -156.  ROLLC    -517.                      ----------------
                                                                                      CY  -0.021501    CMX  -0.001187
```

FIGURE 5.3-6, WIND TUNNEL TEST CASE

ORIGINAL PAGE IS
OF POOR QUALITY

Chordwise Riser Line No.

Spanwise Riser Line No.	1	2	3	4	5	6	7	8	9	10
1	76.26561	75.34832	74.43865	73.53695	72.64356	71.75879	70.88293	70.01626	69.15902	68.31144
2	76.26561	75.34832	74.43865	73.53695	72.64356	71.75879	70.88293	70.01626	69.15902	68.31144
3	76.26561	75.34832	74.43865	73.53695	72.64356	71.75879	70.88293	70.01626	69.15902	68.31144
4	76.26561	75.34832	74.43865	73.53695	72.64356	71.75879	70.88293	70.01626	69.15902	68.31144
5	76.26561	75.34832	74.43865	73.53695	72.64356	71.75879	70.88293	70.01626	69.15902	68.31144
6	76.26561	75.34832	74.43865	73.53695	72.64356	71.75879	70.88293	70.01626	69.15902	68.31144
7	76.26561	75.34832	74.43865	73.53695	72.64356	71.75879	70.88293	70.01626	69.15902	68.31144
8	76.26561	75.34832	74.43865	73.53695	72.64356	71.75879	70.88293	70.01626	69.15902	68.31144
9	76.26561	75.34832	74.43865	73.53695	72.64356	71.75879	70.88293	70.01626	69.15902	68.31144
10	76.26561	75.34832	74.43865	73.53695	72.64356	71.75879	70.88293	70.01626	69.15902	68.31144
11	76.26561	75.34832	74.43865	73.53695	72.64356	71.75879	70.88293	70.01626	69.15902	68.31144
12	76.26561	75.34832	74.43865	73.53695	72.64356	71.75879	70.88293	70.01626	69.15902	68.31144
13	76.26561	75.34832	74.43865	73.53695	72.64356	71.75879	70.88293	70.01626	69.15902	68.31144
14	76.26561	75.34832	74.43865	73.53695	72.64356	71.75879	70.88293	70.01626	69.15902	68.31144
15	76.26561	75.34832	74.43865	73.53695	72.64356	71.75879	70.88293	70.01626	69.15902	68.31144
16	76.26561	75.34832	74.43865	73.53695	72.64356	71.75879	70.88293	70.01626	69.15902	68.31144
17	76.26561	75.34832	74.43865	73.53695	72.64356	71.75879	70.88293	70.01626	69.15902	68.31144
18	76.26561	75.34832	74.43865	73.53695	72.64356	71.75879	70.88293	70.01626	69.15902	68.31144
19	76.26561	75.34832	74.43865	73.53695	72.64356	71.75879	70.88293	70.01626	69.15902	68.31144
20	76.26561	75.34832	74.43865	73.53695	72.64356	71.75879	70.88293	70.01626	69.15902	68.31144
21	76.26561	75.34832	74.43865	73.53695	72.64356	71.75879	70.88293	70.01626	69.15902	68.31144
22	76.26561	75.34832	74.43865	73.53695	72.64356	71.75879	70.88293	70.01626	69.15902	68.31144
23	76.26561	75.34832	74.43865	73.53695	72.64356	71.75879	70.88293	70.01626	69.15902	68.31144
24	76.26561	75.34832	74.43865	73.53695	72.64356	71.75879	70.88293	70.01626	69.15902	68.31144

Spanwise Riser Line No.	11	12	13	14	15	16	17	18	19	20
1	67.47371	66.64602	65.82852	65.02137	64.22467	63.43852	62.66302	61.89822	61.14416	60.40689
2	67.47371	66.64602	65.82852	65.02137	64.22467	63.43852	62.66302	61.89822	61.14416	60.40689
3	67.47371	66.64602	65.82852	65.02137	64.22467	63.43852	62.66302	61.89822	61.14416	60.40689
4	67.47371	66.64602	65.82852	65.02137	64.22467	63.43852	62.66302	61.89822	61.14416	60.40689
5	67.47371	66.64602	65.82852	65.02137	64.22467	63.43852	62.66302	61.89822	61.14416	60.40689
6	67.47371	66.64602	65.82852	65.02137	64.22467	63.43852	62.66302	61.89822	61.14416	60.40689
7	67.47371	66.64602	65.82852	65.02137	64.22467	63.43852	62.66302	61.89822	61.14416	60.40689
8	67.47371	66.64602	65.82852	65.02137	64.22467	63.43852	62.66302	61.89822	61.14416	60.40689
9	67.47371	66.64602	65.82852	65.02137	64.22467	63.43852	62.66302	61.89822	61.14416	60.40689
10	67.47371	66.64602	65.82852	65.02137	64.22467	63.43852	62.66302	61.89822	61.14416	60.40689
11	67.47371	66.64602	65.82852	65.02137	64.22467	63.43852	62.66302	61.89822	61.14416	60.40689
12	67.47371	66.64602	65.82852	65.02137	64.22467	63.43852	62.66302	61.89822	61.14416	60.40689
13	67.47371	66.64602	65.82852	65.02137	64.22467	63.43852	62.66302	61.89822	61.14416	60.40689
14	67.47371	66.64602	65.82852	65.02137	64.22467	63.43852	62.66302	61.89822	61.14416	60.40689
15	67.47371	66.64602	65.82852	65.02137	64.22467	63.43852	62.66302	61.89822	61.14416	60.40689
16	67.47371	66.64602	65.82852	65.02137	64.22467	63.43852	62.66302	61.89822	61.14416	60.40689
17	67.47371	66.64602	65.82852	65.02137	64.22467	63.43852	62.66302	61.89822	61.14416	60.40689
18	67.47371	66.64602	65.82852	65.02137	64.22467	63.43852	62.66302	61.89822	61.14416	60.40689
19	67.47371	66.64602	65.82852	65.02137	64.22467	63.43852	62.66302	61.89822	61.14416	60.40689
20	67.47371	66.64602	65.82852	65.02137	64.22467	63.43852	62.66302	61.89822	61.14416	60.40689
21	67.47371	66.64602	65.82852	65.02137	64.22467	63.43852	62.66302	61.89822	61.14416	60.40689
22	67.47371	66.64602	65.82852	65.02137	64.22467	63.43852	62.66302	61.89822	61.14416	60.40689
23	67.47371	66.64602	65.82852	65.02137	64.22467	63.43852	62.66302	61.89822	61.14416	60.40689
24	67.47371	66.64602	65.82852	65.02137	64.22467	63.43852	62.66302	61.89822	61.14416	60.406891

TABLE 5.3-7, PHI (LONGITUDINAL LINE ANGLE), deg

Chordwise Riser Line No.

Spanwise Riser Line No.

	1	2	3	4	5	6	7	8	9	10
1	0.21179	0.21262	0.21350	0.21444	0.21543	0.21648	0.21757	0.21872	0.21991	0.22116
2	0.21179	0.21262	0.21350	0.21444	0.21543	0.21648	0.21757	0.21872	0.21991	0.22116
3	0.21179	0.21262	0.21350	0.21444	0.21543	0.21648	0.21757	0.21872	0.21991	0.22116
4	0.21167	0.21250	0.21339	0.21432	0.21532	0.21636	0.21745	0.21860	0.21979	0.22104
5	0.21167	0.21250	0.21339	0.21432	0.21532	0.21636	0.21745	0.21860	0.21979	0.22104
6	0.21167	0.21250	0.21339	0.21432	0.21532	0.21636	0.21745	0.21860	0.21979	0.22104
7	0.21134	0.21217	0.21306	0.21400	0.21499	0.21603	0.21712	0.21827	0.21946	0.22070
8	0.21134	0.21217	0.21306	0.21400	0.21499	0.21603	0.21712	0.21827	0.21946	0.22070
9	0.21134	0.21217	0.21306	0.21400	0.21499	0.21603	0.21712	0.21827	0.21946	0.22070
10	0.21080	0.21163	0.21251	0.21345	0.21444	0.21548	0.21657	0.21771	0.21891	0.22015
11	0.21080	0.21163	0.21251	0.21345	0.21444	0.21548	0.21657	0.21771	0.21891	0.22015
12	0.21080	0.21163	0.21251	0.21345	0.21444	0.21548	0.21657	0.21771	0.21891	0.22015
13	0.21004	0.21086	0.21174	0.21268	0.21366	0.21470	0.21579	0.21693	0.21812	0.21936
14	0.21004	0.21086	0.21174	0.21268	0.21366	0.21470	0.21579	0.21693	0.21812	0.21936
15	0.21004	0.21086	0.21174	0.21268	0.21366	0.21470	0.21579	0.21693	0.21812	0.21936
16	0.20903	0.20985	0.21073	0.21166	0.21265	0.21368	0.21476	0.21590	0.21708	0.21832
17	0.20903	0.20985	0.21073	0.21166	0.21265	0.21368	0.21476	0.21590	0.21708	0.21832
18	0.20903	0.20985	0.21073	0.21166	0.21265	0.21368	0.21476	0.21590	0.21708	0.21832
19	0.20776	0.20858	0.20946	0.21038	0.21136	0.21239	0.21347	0.21460	0.21578	0.21701
20	0.20776	0.20858	0.20946	0.21038	0.21136	0.21239	0.21347	0.21460	0.21578	0.21701
21	0.20776	0.20858	0.20946	0.21038	0.21136	0.21239	0.21347	0.21460	0.21578	0.21701
22	0.20620	0.20702	0.20789	0.20881	0.20978	0.21081	0.21188	0.21301	0.21418	0.21540
23	0.20620	0.20702	0.20789	0.20881	0.20978	0.21081	0.21188	0.21301	0.21418	0.21540
24	0.20620	0.20702	0.20789	0.20881	0.20978	0.21081	0.21188	0.21301	0.21418	0.21540

Spanwise Riser Line No.

	11	12	13	14	15	16	17	18	19	20
1	0.22246	0.22379	0.22518	0.22661	0.22809	0.22961	0.23118	0.23279	0.23443	0.23612
2	0.22246	0.22379	0.22518	0.22661	0.22809	0.22961	0.23118	0.23279	0.23443	0.23612
3	0.22246	0.22379	0.22518	0.22661	0.22809	0.22961	0.23118	0.23279	0.23443	0.23612
4	0.22233	0.22367	0.22506	0.22649	0.22797	0.22949	0.23105	0.23266	0.23431	0.23600
5	0.22233	0.22367	0.22506	0.22649	0.22797	0.22949	0.23105	0.23266	0.23431	0.23600
6	0.22233	0.22367	0.22506	0.22649	0.22797	0.22949	0.23105	0.23266	0.23431	0.23600
7	0.22199	0.22333	0.22472	0.22615	0.22762	0.22914	0.23071	0.23231	0.23396	0.23564
8	0.22199	0.22333	0.22472	0.22615	0.22762	0.22914	0.23071	0.23231	0.23396	0.23564
9	0.22199	0.22333	0.22472	0.22615	0.22762	0.22914	0.23071	0.23231	0.23396	0.23564
10	0.22144	0.22277	0.22415	0.22558	0.22705	0.22857	0.23013	0.23173	0.23337	0.23506
11	0.22144	0.22277	0.22415	0.22558	0.22705	0.22857	0.23013	0.23173	0.23337	0.23506
12	0.22144	0.22277	0.22415	0.22558	0.22705	0.22857	0.23013	0.23173	0.23337	0.23506
13	0.22064	0.22197	0.22335	0.22478	0.22624	0.22776	0.22931	0.23091	0.23254	0.23422
14	0.22064	0.22197	0.22335	0.22478	0.22624	0.22776	0.22931	0.23091	0.23254	0.23422
15	0.22064	0.22197	0.22335	0.22478	0.22624	0.22776	0.22931	0.23091	0.23254	0.23422
16	0.21960	0.22093	0.22230	0.22372	0.22518	0.22669	0.22823	0.22982	0.23145	0.23313
17	0.21960	0.22093	0.22230	0.22372	0.22518	0.22669	0.22823	0.22982	0.23145	0.23313
18	0.21960	0.22093	0.22230	0.22372	0.22518	0.22669	0.22823	0.22982	0.23145	0.23313
19	0.21828	0.21960	0.22097	0.22238	0.22384	0.22534	0.22688	0.22920	0.23008	0.23174
20	0.21828	0.21960	0.22097	0.22238	0.22384	0.22534	0.22688	0.22920	0.23008	0.23174
21	0.21828	0.21960	0.22097	0.22238	0.22384	0.22534	0.22688	0.22920	0.23008	0.23174
22	0.21667	0.21798	0.21934	0.22074	0.22219	0.22368	0.22521	0.22678	0.22840	0.23005
23	0.21667	0.21798	0.21934	0.22074	0.22219	0.22368	0.22521	0.22678	0.22840	0.23005
24	0.21667	0.21798	0.21934	0.22074	0.22219	0.22368	0.22521	0.22678	0.22840	0.23005

TABLE 5.3-8, AREF1 (LINE REFERENCE AREA), ft^2

Chordwise Riser Line No.

Spanwise Riser Line No.

	1	2	3	4	5	6	7	8	9	10
1	59.38813	59.62969	59.88520	60.15628	60.44212	60.74252	61.05725	61.38611	61.72886	62.08527
2	59.38813	59.62969	59.88520	60.15628	60.44212	60.74252	61.05725	61.38611	61.72886	62.08527
3	59.38813	59.62969	59.88520	60.15628	60.44212	60.74252	61.05725	61.38611	61.72886	62.08527
4	59.38813	59.62969	59.88520	60.15628	60.44212	60.74252	61.05725	61.38611	61.72886	62.08527
5	59.38813	59.62969	59.88520	60.15628	60.44212	60.74252	61.05725	61.38611	61.72886	62.08527
6	59.38813	59.62969	59.88520	60.15628	60.44212	60.74252	61.05725	61.38611	61.72886	62.08527
7	59.38813	59.62969	59.88520	60.15628	60.44212	60.74252	61.05725	61.38611	61.72886	62.08527
8	59.38813	59.62969	59.88520	60.15628	60.44212	60.74252	61.05725	61.38611	61.72886	62.08527
9	59.38813	59.62969	59.88520	60.15628	60.44212	60.74252	61.05725	61.38611	61.72886	62.08527
10	59.38813	59.62969	59.88520	60.15628	60.44212	60.74252	61.05725	61.38611	61.72886	62.08527
11	59.38813	59.62969	59.88520	60.15628	60.44212	60.74252	61.05725	61.38611	61.72886	62.08527
12	59.38813	59.62969	59.88520	60.15628	60.44212	60.74252	61.05725	61.38611	61.72886	62.08527
13	59.38813	59.62969	59.88520	60.15628	60.44212	60.74252	61.05725	61.38611	61.72886	62.08527
14	59.38813	59.62969	59.88520	60.15628	60.44212	60.74252	61.05725	61.38611	61.72886	62.08527
15	59.38813	59.62969	59.88520	60.15628	60.44212	60.74252	61.05725	61.38611	61.72886	62.08527
16	59.38813	59.62969	59.88520	60.15628	60.44212	60.74252	61.05725	61.38611	61.72886	62.08527
17	59.38813	59.62969	59.88520	60.15628	60.44212	60.74252	61.05725	61.38611	61.72886	62.08527
18	59.38813	59.62969	59.88520	60.15628	60.44212	60.74252	61.05725	61.38611	61.72886	62.08527
19	59.38813	59.62969	59.88520	60.15628	60.44212	60.74252	61.05725	61.38611	61.72886	62.08527
20	59.38813	59.62969	59.88520	60.15628	60.44212	60.74252	61.05725	61.38611	61.72886	62.08527
21	59.38813	59.62969	59.88520	60.15628	60.44212	60.74252	61.05725	61.38611	61.72886	62.08527
22	59.38813	59.62969	59.88520	60.15628	60.44212	60.74252	61.05725	61.38611	61.72886	62.08527
23	59.38813	59.62969	59.88520	60.15628	60.44212	60.74252	61.05725	61.38611	61.72886	62.08527
24	59.38813	59.62969	59.88520	60.15628	60.44212	60.74252	61.05725	61.38611	61.72886	62.08527

Spanwise Riser Line No.

	11	12	13	14	15	16	17	18	19	20
1	62.45511	62.83815	63.23414	63.64284	64.06401	64.49740	64.94277	65.39987	65.86847	66.34831
2	62.45511	62.83815	63.23414	63.64284	64.06401	64.49740	64.94277	65.39987	65.86847	66.34831
3	62.45511	62.83815	63.23414	63.64284	64.06401	64.49740	64.94277	65.39987	65.86847	66.34831
4	62.45511	62.83815	63.23414	63.64284	64.06401	64.49740	64.94277	65.39987	65.86847	66.34831
5	62.45511	62.83815	63.23414	63.64284	64.06401	64.49740	64.94277	65.39987	65.86847	66.34831
6	62.45511	62.83815	63.23414	63.64284	64.06401	64.49740	64.94277	65.39987	65.86847	66.34831
7	62.45511	62.83815	63.23414	63.64284	64.06401	64.49740	64.94277	65.39987	65.86847	66.34831
8	62.45511	62.83815	63.23414	63.64284	64.06401	64.49740	64.94277	65.39987	65.86847	66.34831
9	62.45511	62.83815	63.23414	63.64284	64.06401	64.49740	64.94277	65.39987	65.86847	66.34831
10	62.45511	62.83815	63.23414	63.64284	64.06401	64.49740	64.94277	65.39987	65.86847	66.34831
11	62.45511	62.83815	63.23414	63.64284	64.06401	64.49740	64.94277	65.39987	65.86847	66.34831
12	62.45511	62.83815	63.23414	63.64284	64.06401	64.49740	64.94277	65.39987	65.86847	66.34831
13	62.45511	62.83815	63.23414	63.64284	64.06401	64.49740	64.94277	65.39987	65.86847	66.34831
14	62.45511	62.83815	63.23414	63.64284	64.06401	64.49740	64.94277	65.39987	65.86847	66.34831
15	62.45511	62.83815	63.23414	63.64284	64.06401	64.49740	64.94277	65.39987	65.86847	66.34831
16	62.45511	62.83815	63.23414	63.64284	64.06401	64.49740	64.94277	65.39987	65.86847	66.34831
17	62.45511	62.83815	63.23414	63.64284	64.06401	64.49740	64.94277	65.39987	65.86847	66.34831
18	62.45511	62.83815	63.23414	63.64284	64.06401	64.49740	64.94277	65.39987	65.86847	66.34831
19	62.45511	62.83815	63.23414	63.64284	64.06401	64.49740	64.94277	65.39987	65.86847	66.34831
20	62.45511	62.83815	63.23414	63.64284	64.06401	64.49740	64.94277	65.39987	65.86847	66.34831
21	62.45511	62.83815	63.23414	63.64284	64.06401	64.49740	64.94277	65.39987	65.86847	66.34831
22	62.45511	62.83815	63.23414	63.64284	64.06401	64.49740	64.94277	65.39987	65.86847	66.34831
23	62.45511	62.83815	63.23414	63.64284	64.06401	64.49740	64.94277	65.39987	65.86847	66.34831
24	62.45511	62.83815	63.23414	63.64284	64.06401	64.49740	64.94277	65.39987	65.86847	66.34831

TABLE 5.3-9, LR (LENGTH TO CONFLUENCE POINT), ft

Chordwise Riser Line No.

Spanwise Riser Line No.	1	2	3	4	5	6	7	8	9	10
1	11.88099	11.93558	11.99317	12.05366	12.11707	12.18329	12.25233	12.32409	12.39855	12.47570
2	11.88099	11.93558	11.99317	12.05366	12.11707	12.18329	12.25233	12.32409	12.39855	12.47570
3	11.88099	11.93558	11.99317	12.05366	12.11707	12.18329	12.25233	12.32409	12.39855	12.47570
4	11.90715	11.96182	12.01945	12.08004	12.14352	12.20982	12.27896	12.35085	12.42541	12.50266
5	11.90715	11.96182	12.01945	12.08004	12.14352	12.20982	12.27896	12.35085	12.42541	12.50266
6	11.90715	11.96182	12.01945	12.08004	12.14352	12.20982	12.27896	12.35085	12.42541	12.50266
7	11.98018	12.03503	12.09285	12.15365	12.21734	12.28392	12.35330	12.42547	12.50038	12.57792
8	11.98018	12.03503	12.09285	12.15365	12.21734	12.28392	12.35330	12.42547	12.50038	12.57792
9	11.98018	12.03503	12.09285	12.15365	12.21734	12.28392	12.35330	12.42547	12.50038	12.57792
10	12.10148	12.15660	12.21478	12.27591	12.33999	12.40700	12.47683	12.54945	12.62487	12.70296
11	12.10148	12.15660	12.21478	12.27591	12.33999	12.40700	12.47683	12.54945	12.62487	12.70296
12	12.10148	12.15660	12.21478	12.27591	12.33999	12.40700	12.47683	12.54945	12.62487	12.70296
13	12.27345	12.32898	12.38761	12.44925	12.51387	12.58147	12.65192	12.72522	12.80136	12.88021
14	12.27345	12.32898	12.38761	12.44925	12.51387	12.58147	12.65192	12.72522	12.80136	12.88021
15	12.27345	12.32898	12.38761	12.44925	12.51387	12.58147	12.65192	12.72522	12.80136	12.88021
16	12.49949	12.55557	12.61478	12.67707	12.74242	12.81080	12.88209	12.95629	13.03334	13.11320
17	12.49949	12.55557	12.61478	12.67707	12.74242	12.81080	12.88209	12.95629	13.03334	13.11320
18	12.49949	12.55557	12.61478	12.67707	12.74242	12.81080	12.88209	12.95629	13.03334	13.11320
19	12.78432	12.84109	12.90104	12.96418	13.03042	13.09976	13.17209	13.24742	13.32569	13.40678
20	12.78432	12.84109	12.90104	12.96418	13.03042	13.09976	13.17209	13.24742	13.32569	13.40678
21	12.78432	12.84109	12.90104	12.96418	13.03042	13.09976	13.17209	13.24742	13.32569	13.40678
22	13.13417	13.19178	13.25266	13.31683	13.38421	13.45472	13.52837	13.60505	13.68477	13.76746
23	13.13417	13.19178	13.25266	13.31683	13.38421	13.45472	13.52837	13.60505	13.68477	13.76746
24	13.13417	13.19178	13.25266	13.31683	13.38421	13.45472	13.52837	13.60505	13.68477	13.76746

Spanwise Riser Line No.	11	12	13	14	15	16	17	18	19	20
1	12.55542	12.63773	12.72250	12.80972	12.89940	12.99138	13.08572	13.18226	13.28100	13.38197
2	12.55542	12.63773	12.72250	12.80972	12.89940	12.99138	13.08572	13.18226	13.28100	13.38197
3	12.55542	12.63773	12.72250	12.80972	12.89940	12.99138	13.08572	13.18226	13.28100	13.38197
4	12.58253	12.66495	12.74985	12.83725	12.92700	13.01918	13.11366	13.21041	13.30931	13.41043
5	12.58253	12.66495	12.74985	12.83725	12.92700	13.01918	13.11366	13.21041	13.30931	13.41043
6	12.58253	12.66495	12.74985	12.83725	12.92700	13.01918	13.11366	13.21041	13.30931	13.41043
7	12.65813	12.74088	12.82619	12.91399	13.00416	13.09676	13.19164	13.28885	13.38823	13.48984
8	12.65813	12.74088	12.82619	12.91399	13.00416	13.09676	13.19164	13.28885	13.38823	13.48984
9	12.65813	12.74088	12.82619	12.91399	13.00416	13.09676	13.19164	13.28885	13.38823	13.48984
10	12.78371	12.86700	12.95300	13.04141	13.13228	13.22559	13.32121	13.41914	13.51937	13.62175
11	12.78371	12.86700	12.95300	13.04141	13.13228	13.22559	13.32121	13.41914	13.51937	13.62175
12	12.78371	12.86700	12.95300	13.04141	13.13228	13.22559	13.32121	13.41914	13.51937	13.62175
13	12.96175	13.04594	13.13277	13.22210	13.31393	13.40824	13.50490	13.60390	13.70523	13.80876
14	12.96175	13.04594	13.13277	13.22210	13.31393	13.40824	13.50490	13.60390	13.70523	13.80876
15	12.96175	13.04594	13.13277	13.22210	13.31393	13.40824	13.50490	13.60390	13.70523	13.80876
16	13.19580	13.28111	13.36900	13.45961	13.55271	13.64834	13.74637	13.84679	13.94955	14.05459
17	13.19580	13.28111	13.36900	13.45961	13.55271	13.64834	13.74637	13.84679	13.94955	14.05459
18	13.19580	13.28111	13.36900	13.45961	13.55271	13.64834	13.74637	13.84679	13.94955	14.05459
19	13.49074	13.57742	13.66687	13.75897	13.85364	13.95091	14.05064	13.98661	14.25745	14.36442
20	13.49074	13.57742	13.66687	13.75897	13.85364	13.95091	14.05064	13.98661	14.25745	14.36442
21	13.49074	13.57742	13.66687	13.75897	13.85364	13.95091	14.05064	13.98661	14.25745	14.36442
22	13.85301	13.94145	14.03269	14.12663	14.22330	14.32256	14.42445	14.52887	14.63570	14.74501
23	13.85301	13.94145	14.03269	14.12663	14.22330	14.32256	14.42445	14.52887	14.63570	14.74501
24	13.85301	13.94145	14.03269	14.12663	14.22330	14.32256	14.42445	14.52887	14.63570	14.74501

TABLE 5.3-10, LP (LENGTH OF CONFLUENCE POINT TO TOP PLATE), ft

Chordwise Riser Line No.

Spanwise Riser Line No.	1	2	3	4	5	6	7	8	9	10
1	47.50714	47.69351	47.89203	48.10262	48.32505	48.55923	48.80492	49.06201	49.33030	49.60957
2	47.50714	47.69351	47.89203	48.10262	48.32505	48.55923	48.80492	49.06201	49.33030	49.60957
3	47.50714	47.69351	47.89203	48.10262	48.32505	48.55923	48.80492	49.06201	49.33030	49.60957
4	47.48098	47.66726	47.86575	48.07624	48.29859	48.53269	48.77829	49.03526	49.30345	49.58261
5	47.48098	47.66726	47.86575	48.07624	48.29859	48.53269	48.77829	49.03526	49.30345	49.58261
6	47.48098	47.66726	47.86575	48.07624	48.29859	48.53269	48.77829	49.03526	49.30345	49.58261
7	47.40795	47.59466	47.79235	48.00262	48.22478	48.45859	48.70396	48.96063	49.22848	49.50735
8	47.40795	47.59466	47.79235	48.00262	48.22478	48.45859	48.70396	48.96063	49.22848	49.50735
9	47.40795	47.59466	47.79235	48.00262	48.22478	48.45859	48.70396	48.96063	49.22848	49.50735
10	47.28665	47.47248	47.67042	47.88036	48.10213	48.33551	48.58043	48.83665	49.10398	49.38231
11	47.28665	47.47248	47.67042	47.88036	48.10213	48.33551	48.58043	48.83665	49.10398	49.38231
12	47.28665	47.47248	47.67042	47.88036	48.10213	48.33551	48.58043	48.83665	49.10398	49.38231
13	47.11468	47.30610	47.49759	47.70703	47.92825	48.16105	48.40533	48.66088	48.92750	49.20506
14	47.11468	47.30610	47.49759	47.70703	47.92825	48.16105	48.40533	48.66088	48.92750	49.20506
15	47.11468	47.30610	47.49759	47.70703	47.92825	48.16105	48.40533	48.66088	48.92750	49.20506
16	46.88864	47.07352	47.27042	47.47920	47.69970	47.93172	48.17516	48.42982	48.69552	48.97208
17	46.88864	47.07352	47.27042	47.47920	47.69970	47.93172	48.17516	48.42982	48.69552	48.97208
18	46.88864	47.07352	47.27042	47.47920	47.69970	47.93172	48.17516	48.42982	48.69552	48.97208
19	46.60381	46.78806	46.98416	47.19209	47.41170	47.64276	47.88517	48.13869	48.40317	48.67849
20	46.60381	46.78806	46.98416	47.19209	47.41170	47.64276	47.88517	48.13869	48.40317	48.67849
21	46.60381	46.78806	46.98416	47.19209	47.41170	47.64276	47.88517	48.13869	48.40317	48.67849
22	46.25396	46.43730	46.63254	46.83945	47.05791	47.28780	47.52888	47.78106	48.04408	48.31781
23	46.25396	46.43730	46.63254	46.83945	47.05791	47.28780	47.52888	47.78106	48.04408	48.31781
24	46.25396	46.43730	46.63254	46.83945	47.05791	47.28780	47.52888	47.78106	48.04408	48.31781

Spanwise Riser Line No.	11	12	13	14	15	16	17	18	19	20
1	49.89970	50.20042	50.51164	50.83312	51.16461	51.50602	51.85705	52.21761	52.58741	52.96634
2	49.89970	50.20042	50.51164	50.83312	51.16461	51.50602	51.85705	52.21761	52.58741	52.96634
3	49.89970	50.20042	50.51164	50.83312	51.16461	51.50602	51.85705	52.21761	52.58741	52.96634
4	49.87259	50.17320	50.48429	50.80559	51.13695	51.47822	51.82911	52.18947	52.55916	52.93788
5	49.87259	50.17320	50.48429	50.80559	51.13695	51.47822	51.82911	52.18947	52.55916	52.93788
6	49.87259	50.17320	50.48429	50.80559	51.13695	51.47822	51.82911	52.18947	52.55916	52.93788
7	49.79698	50.09727	50.40795	50.72885	51.05984	51.40063	51.75113	52.11103	52.48024	52.85847
8	49.79698	50.09727	50.40795	50.72885	51.05984	51.40063	51.75113	52.11103	52.48024	52.85847
9	49.79698	50.09727	50.40795	50.72885	51.05984	51.40063	51.75113	52.11103	52.48024	52.85847
10	49.67141	49.97109	50.28114	50.60143	50.93173	51.27181	51.62156	51.98074	52.34910	52.72656
11	49.67141	49.97109	50.28114	50.60143	50.93173	51.27181	51.62156	51.98074	52.34910	52.72656
12	49.67141	49.97109	50.28114	50.60143	50.93173	51.27181	51.62156	51.98074	52.34910	52.72656
13	49.49336	49.79221	50.10137	50.42074	50.75008	51.08916	51.43787	51.79598	52.16324	52.53955
14	49.49336	49.79221	50.10137	50.42074	50.75008	51.08916	51.43787	51.79598	52.16324	52.53955
15	49.49336	49.79221	50.10137	50.42074	50.75008	51.08916	51.43787	51.79598	52.16324	52.53955
16	49.25931	49.55704	49.86508	50.18323	50.51130	50.84906	51.19640	51.55308	51.91892	52.29372
17	49.25931	49.55704	49.86508	50.18323	50.51130	50.84906	51.19640	51.55308	51.91892	52.29372
18	49.25931	49.55704	49.86508	50.18323	50.51130	50.84906	51.19640	51.55308	51.91892	52.29372
19	48.96438	49.26073	49.56727	49.88387	50.21037	50.54648	50.89213	51.41326	51.61102	51.98389
20	48.96438	49.26073	49.56727	49.88387	50.21037	50.54648	50.89213	51.41326	51.61102	51.98389
21	48.96438	49.26073	49.56727	49.88387	50.21037	50.54648	50.89213	51.41326	51.61102	51.98389
22	48.60211	48.89670	49.20145	49.51621	49.84071	50.17484	50.51832	50.87101	51.23276	51.60330
23	48.60211	48.89670	49.20145	49.51621	49.84071	50.17484	50.51832	50.87101	51.23276	51.60330
24	48.60211	48.89670	49.20145	49.51621	49.84071	50.17484	50.51832	50.87101	51.23276	51.60330

TABLE 5.3-11, LA (EXPOSED LENGTH), ft

Chordwise Riser Line No.

Spanwise Riser Line No.	1	2	3	4	5	6	7	8	9	10
1	1.00831	0.99614	0.98341	0.97018	0.95648	0.94236	0.92786	0.91303	0.89790	0.88253
2	1.00831	0.99614	0.98341	0.97018	0.95648	0.94236	0.92786	0.91303	0.89790	0.88253
3	1.00831	0.99614	0.98341	0.97018	0.95648	0.94236	0.92786	0.91303	0.89790	0.88253
4	1.00831	0.99614	0.98341	0.97018	0.95648	0.94236	0.92786	0.91303	0.89790	0.88253
5	1.00831	0.99614	0.98341	0.97018	0.95648	0.94236	0.92786	0.91303	0.89790	0.88253
6	1.00831	0.99614	0.98341	0.97018	0.95648	0.94236	0.92786	0.91303	0.89790	0.88253
7	1.00831	0.99614	0.98341	0.97018	0.95648	0.94236	0.92786	0.91303	0.89790	0.88253
8	1.00831	0.99614	0.98341	0.97018	0.95648	0.94236	0.92786	0.91303	0.89790	0.88253
9	1.00831	0.99614	0.98341	0.97018	0.95648	0.94236	0.92786	0.91303	0.89790	0.88253
10	1.00831	0.99614	0.98341	0.97018	0.95648	0.94236	0.92786	0.91303	0.89790	0.88253
11	1.00831	0.99614	0.98341	0.97018	0.95648	0.94236	0.92786	0.91303	0.89790	0.88253
12	1.00831	0.99614	0.98341	0.97018	0.95648	0.94236	0.92786	0.91303	0.89790	0.88253
13	1.00831	0.99614	0.98341	0.97018	0.95648	0.94236	0.92786	0.91303	0.89790	0.88253
14	1.00831	0.99614	0.98341	0.97018	0.95648	0.94236	0.92786	0.91303	0.89790	0.88253
15	1.00831	0.99614	0.98341	0.97018	0.95648	0.94236	0.92786	0.91303	0.89790	0.88253
16	1.00831	0.99614	0.98341	0.97018	0.95648	0.94236	0.92786	0.91303	0.89790	0.88253
17	1.00831	0.99614	0.98341	0.97018	0.95648	0.94236	0.92786	0.91303	0.89790	0.88253
18	1.00831	0.99614	0.98341	0.97018	0.95648	0.94236	0.92786	0.91303	0.89790	0.88253
19	1.00831	0.99614	0.98341	0.97018	0.95648	0.94236	0.92786	0.91303	0.89790	0.88253
20	1.00831	0.99614	0.98341	0.97018	0.95648	0.94236	0.92786	0.91303	0.89790	0.88253
21	1.00831	0.99614	0.98341	0.97018	0.95648	0.94236	0.92786	0.91303	0.89790	0.88253
22	1.00831	0.99614	0.98341	0.97018	0.95648	0.94236	0.92786	0.91303	0.89790	0.88253
23	1.00831	0.99614	0.98341	0.97018	0.95648	0.94236	0.92786	0.91303	0.89790	0.88253
24	1.00831	0.99614	0.98341	0.97018	0.95648	0.94236	0.92786	0.91303	0.89790	0.88253

Spanwise Riser Line No.	11	12	13	14	15	16	17	18	19	20
1	0.86694	0.85119	0.83530	0.81931	0.80325	0.78717	0.77109	0.75503	0.73903	0.72311
2	0.86694	0.85119	0.83530	0.81931	0.80325	0.78717	0.77109	0.75503	0.73903	0.72311
3	0.86694	0.85119	0.83530	0.81931	0.80325	0.78717	0.77109	0.75503	0.73903	0.72311
4	0.86694	0.85119	0.83530	0.81931	0.80325	0.78717	0.77109	0.75503	0.73903	0.72311
5	0.86694	0.85119	0.83530	0.81931	0.80325	0.78717	0.77109	0.75503	0.73903	0.72311
6	0.86694	0.85119	0.83530	0.81931	0.80325	0.78717	0.77109	0.75503	0.73903	0.72311
7	0.86694	0.85119	0.83530	0.81931	0.80325	0.78717	0.77109	0.75503	0.73903	0.72311
8	0.86694	0.85119	0.83530	0.81931	0.80325	0.78717	0.77109	0.75503	0.73903	0.72311
9	0.86694	0.85119	0.83530	0.81931	0.80325	0.78717	0.77109	0.75503	0.73903	0.72311
10	0.86694	0.85119	0.83530	0.81931	0.80325	0.78717	0.77109	0.75503	0.73903	0.72311
11	0.86694	0.85119	0.83530	0.81931	0.80325	0.78717	0.77109	0.75503	0.73903	0.72311
12	0.86694	0.85119	0.83530	0.81931	0.80325	0.78717	0.77109	0.75503	0.73903	0.72311
13	0.86694	0.85119	0.83530	0.81931	0.80325	0.78717	0.77109	0.75503	0.73903	0.72311
14	0.86694	0.85119	0.83530	0.81931	0.80325	0.78717	0.77109	0.75503	0.73903	0.72311
15	0.86694	0.85119	0.83530	0.81931	0.80325	0.78717	0.77109	0.75503	0.73903	0.72311
16	0.86694	0.85119	0.83530	0.81931	0.80325	0.78717	0.77109	0.75503	0.73903	0.72311
17	0.86694	0.85119	0.83530	0.81931	0.80325	0.78717	0.77109	0.75503	0.73903	0.72311
18	0.86694	0.85119	0.83530	0.81931	0.80325	0.78717	0.77109	0.75503	0.73903	0.72311
19	0.86694	0.85119	0.83530	0.81931	0.80325	0.78717	0.77109	0.75503	0.73903	0.72311
20	0.86694	0.85119	0.83530	0.81931	0.80325	0.78717	0.77109	0.75503	0.73903	0.72311
21	0.86694	0.85119	0.83530	0.81931	0.80325	0.78717	0.77109	0.75503	0.73903	0.72311
22	0.86694	0.85119	0.83530	0.81931	0.80325	0.78717	0.77109	0.75503	0.73903	0.72311
23	0.86694	0.85119	0.83530	0.81931	0.80325	0.78717	0.77109	0.75503	0.73903	0.72311
24	0.86694	0.85119	0.83530	0.81931	0.80325	0.78717	0.77109	0.75503	0.73903	0.72311

TABLE 5.3-12, CDI (DRAG COEFFICIENT BASED ON INDIVIDUAL REF AREA)

Chordwise Riser Line No.

Spanwise Riser Line No.	1	2	3	4	5	6	7	8	9	10
1	0.00202	0.00200	0.00198	0.00197	0.00195	0.00193	0.00191	0.00189	0.00187	0.00184
2	0.00202	0.00200	0.00198	0.00197	0.00195	0.00193	0.00191	0.00189	0.00187	0.00184
3	0.00202	0.00200	0.00198	0.00197	0.00195	0.00193	0.00191	0.00189	0.00187	0.00184
4	0.00202	0.00200	0.00198	0.00196	0.00195	0.00193	0.00191	0.00189	0.00186	0.00184
5	0.00202	0.00200	0.00198	0.00196	0.00195	0.00193	0.00191	0.00189	0.00186	0.00184
6	0.00202	0.00200	0.00198	0.00196	0.00195	0.00193	0.00191	0.00189	0.00186	0.00184
7	0.00201	0.00200	0.00198	0.00196	0.00194	0.00192	0.00190	0.00188	0.00186	0.00184
8	0.00201	0.00200	0.00198	0.00196	0.00194	0.00192	0.00190	0.00188	0.00186	0.00184
9	0.00201	0.00200	0.00198	0.00196	0.00194	0.00192	0.00190	0.00188	0.00186	0.00184
10	0.00201	0.00199	0.00197	0.00196	0.00194	0.00192	0.00190	0.00188	0.00186	0.00184
11	0.00201	0.00199	0.00197	0.00196	0.00194	0.00192	0.00190	0.00188	0.00186	0.00184
12	0.00201	0.00199	0.00197	0.00196	0.00194	0.00192	0.00190	0.00188	0.00186	0.00184
13	0.00200	0.00198	0.00197	0.00195	0.00193	0.00191	0.00189	0.00187	0.00185	0.00183
14	0.00200	0.00198	0.00197	0.00195	0.00193	0.00191	0.00189	0.00187	0.00185	0.00183
15	0.00200	0.00198	0.00197	0.00195	0.00193	0.00191	0.00189	0.00187	0.00185	0.00183
16	0.00199	0.00197	0.00196	0.00194	0.00192	0.00190	0.00188	0.00186	0.00184	0.00182
17	0.00199	0.00197	0.00196	0.00194	0.00192	0.00190	0.00188	0.00186	0.00184	0.00182
18	0.00199	0.00197	0.00196	0.00194	0.00192	0.00190	0.00188	0.00186	0.00184	0.00182
19	0.00198	0.00196	0.00195	0.00193	0.00191	0.00189	0.00187	0.00185	0.00183	0.00181
20	0.00198	0.00196	0.00195	0.00193	0.00191	0.00189	0.00187	0.00185	0.00183	0.00181
21	0.00198	0.00196	0.00195	0.00193	0.00191	0.00189	0.00187	0.00185	0.00183	0.00181
22	0.00196	0.00195	0.00193	0.00191	0.00190	0.00188	0.00186	0.00184	0.00182	0.00180
23	0.00196	0.00195	0.00193	0.00191	0.00190	0.00188	0.00186	0.00184	0.00182	0.00180
24	0.00196	0.00195	0.00193	0.00191	0.00190	0.00188	0.00186	0.00184	0.00182	0.00180

Spanwise Riser Line No.	11	12	13	14	15	16	17	18	19	20
1	0.00182	0.00180	0.00178	0.00175	0.00173	0.00171	0.00168	0.00166	0.00164	0.00161
2	0.00182	0.00180	0.00178	0.00175	0.00173	0.00171	0.00168	0.00166	0.00164	0.00161
3	0.00182	0.00180	0.00178	0.00175	0.00173	0.00171	0.00168	0.00166	0.00164	0.00161
4	0.00182	0.00180	0.00178	0.00175	0.00173	0.00171	0.00168	0.00166	0.00164	0.00161
5	0.00182	0.00180	0.00178	0.00175	0.00173	0.00171	0.00168	0.00166	0.00164	0.00161
6	0.00182	0.00180	0.00178	0.00175	0.00173	0.00171	0.00168	0.00166	0.00164	0.00161
7	0.00182	0.00180	0.00177	0.00175	0.00173	0.00170	0.00168	0.00166	0.00163	0.00161
8	0.00182	0.00180	0.00177	0.00175	0.00173	0.00170	0.00168	0.00166	0.00163	0.00161
9	0.00182	0.00180	0.00177	0.00175	0.00173	0.00170	0.00168	0.00166	0.00163	0.00161
10	0.00181	0.00179	0.00177	0.00175	0.00172	0.00170	0.00168	0.00165	0.00163	0.00161
11	0.00181	0.00179	0.00177	0.00175	0.00172	0.00170	0.00168	0.00165	0.00163	0.00161
12	0.00181	0.00179	0.00177	0.00175	0.00172	0.00170	0.00168	0.00165	0.00163	0.00161
13	0.00181	0.00178	0.00176	0.00174	0.00172	0.00169	0.00167	0.00165	0.00162	0.00160
14	0.00181	0.00178	0.00176	0.00174	0.00172	0.00169	0.00167	0.00165	0.00162	0.00160
15	0.00181	0.00178	0.00176	0.00174	0.00172	0.00169	0.00167	0.00165	0.00162	0.00160
16	0.00180	0.00178	0.00175	0.00173	0.00171	0.00169	0.00166	0.00164	0.00162	0.00159
17	0.00180	0.00178	0.00175	0.00173	0.00171	0.00169	0.00166	0.00164	0.00162	0.00159
18	0.00180	0.00178	0.00175	0.00173	0.00171	0.00169	0.00166	0.00164	0.00162	0.00159
19	0.00179	0.00177	0.00174	0.00172	0.00170	0.00168	0.00165	0.00163	0.00161	0.00158
20	0.00179	0.00177	0.00174	0.00172	0.00170	0.00168	0.00165	0.00163	0.00161	0.00158
21	0.00179	0.00177	0.00174	0.00172	0.00170	0.00168	0.00165	0.00163	0.00161	0.00158
22	0.00177	0.00175	0.00173	0.00171	0.00169	0.00166	0.00164	0.00162	0.00159	0.00157
23	0.00177	0.00175	0.00173	0.00171	0.00169	0.00166	0.00164	0.00162	0.00159	0.00157
24	0.00177	0.00175	0.00173	0.00171	0.00169	0.00166	0.00164	0.00162	0.00159	0.00157

TABLE 5.3-13, CD2 (DRAG COEFFICIENT BASED ON TOTAL LINE REF AREA)

Chordwise Riser Line No.

Spanwise Riser Line No.	1	2	3	4	5	6	7	8	9	10
1	0.00018	0.00018	0.00017	0.00017	0.00017	0.00017	0.00017	0.00017	0.00016	0.00016
2	0.00018	0.00018	0.00017	0.00017	0.00017	0.00017	0.00017	0.00017	0.00016	0.00016
3	0.00018	0.00018	0.00017	0.00017	0.00017	0.00017	0.00017	0.00017	0.00016	0.00016
4	0.00018	0.00018	0.00017	0.00017	0.00017	0.00017	0.00017	0.00017	0.00016	0.00016
5	0.00018	0.00018	0.00017	0.00017	0.00017	0.00017	0.00017	0.00017	0.00016	0.00016
6	0.00018	0.00018	0.00017	0.00017	0.00017	0.00017	0.00017	0.00017	0.00016	0.00016
7	0.00018	0.00018	0.00017	0.00017	0.00017	0.00017	0.00017	0.00017	0.00016	0.00016
8	0.00018	0.00018	0.00017	0.00017	0.00017	0.00017	0.00017	0.00017	0.00016	0.00016
9	0.00018	0.00018	0.00017	0.00017	0.00017	0.00017	0.00017	0.00017	0.00016	0.00016
10	0.00018	0.00018	0.00017	0.00017	0.00017	0.00017	0.00017	0.00017	0.00016	0.00016
11	0.00018	0.00018	0.00017	0.00017	0.00017	0.00017	0.00017	0.00017	0.00016	0.00016
12	0.00018	0.00018	0.00017	0.00017	0.00017	0.00017	0.00017	0.00017	0.00016	0.00016
13	0.00018	0.00018	0.00017	0.00017	0.00017	0.00017	0.00017	0.00017	0.00016	0.00016
14	0.00018	0.00018	0.00017	0.00017	0.00017	0.00017	0.00017	0.00017	0.00016	0.00016
15	0.00018	0.00018	0.00017	0.00017	0.00017	0.00017	0.00017	0.00017	0.00016	0.00016
16	0.00018	0.00017	0.00017	0.00017	0.00017	0.00017	0.00017	0.00016	0.00016	0.00016
17	0.00018	0.00017	0.00017	0.00017	0.00017	0.00017	0.00017	0.00016	0.00016	0.00016
18	0.00018	0.00017	0.00017	0.00017	0.00017	0.00017	0.00017	0.00016	0.00016	0.00016
19	0.00017	0.00017	0.00017	0.00017	0.00017	0.00017	0.00017	0.00016	0.00016	0.00016
20	0.00017	0.00017	0.00017	0.00017	0.00017	0.00017	0.00017	0.00016	0.00016	0.00016
21	0.00017	0.00017	0.00017	0.00017	0.00017	0.00017	0.00017	0.00016	0.00016	0.00016
22	0.00017	0.00017	0.00017	0.00017	0.00017	0.00017	0.00016	0.00016	0.00016	0.00016
23	0.00017	0.00017	0.00017	0.00017	0.00017	0.00017	0.00016	0.00016	0.00016	0.00016
24	0.00017	0.00017	0.00017	0.00017	0.00017	0.00017	0.00016	0.00016	0.00016	0.00016

Spanwise Riser Line No.	11	12	13	14	15	16	17	18	19	20
1	0.00016	0.00016	0.00016	0.00015	0.00015	0.00015	0.00015	0.00015	0.00014	0.00014
2	0.00016	0.00016	0.00016	0.00015	0.00015	0.00015	0.00015	0.00015	0.00014	0.00014
3	0.00016	0.00016	0.00016	0.00015	0.00015	0.00015	0.00015	0.00015	0.00014	0.00014
4	0.00016	0.00016	0.00016	0.00015	0.00015	0.00015	0.00015	0.00015	0.00014	0.00014
5	0.00016	0.00016	0.00016	0.00015	0.00015	0.00015	0.00015	0.00015	0.00014	0.00014
6	0.00016	0.00016	0.00016	0.00015	0.00015	0.00015	0.00015	0.00015	0.00014	0.00014
7	0.00016	0.00016	0.00016	0.00015	0.00015	0.00015	0.00015	0.00015	0.00014	0.00014
8	0.00016	0.00016	0.00016	0.00015	0.00015	0.00015	0.00015	0.00015	0.00014	0.00014
9	0.00016	0.00016	0.00016	0.00015	0.00015	0.00015	0.00015	0.00015	0.00014	0.00014
10	0.00016	0.00016	0.00016	0.00015	0.00015	0.00015	0.00015	0.00015	0.00014	0.00014
11	0.00016	0.00016	0.00016	0.00015	0.00015	0.00015	0.00015	0.00015	0.00014	0.00014
12	0.00016	0.00016	0.00016	0.00015	0.00015	0.00015	0.00015	0.00015	0.00014	0.00014
13	0.00016	0.00016	0.00016	0.00015	0.00015	0.00015	0.00015	0.00015	0.00014	0.00014
14	0.00016	0.00016	0.00016	0.00015	0.00015	0.00015	0.00015	0.00015	0.00014	0.00014
15	0.00016	0.00016	0.00016	0.00015	0.00015	0.00015	0.00015	0.00015	0.00014	0.00014
16	0.00016	0.00016	0.00015	0.00015	0.00015	0.00015	0.00015	0.00014	0.00014	0.00014
17	0.00016	0.00016	0.00015	0.00015	0.00015	0.00015	0.00015	0.00014	0.00014	0.00014
18	0.00016	0.00016	0.00015	0.00015	0.00015	0.00015	0.00015	0.00014	0.00014	0.00014
19	0.00016	0.00016	0.00015	0.00015	0.00015	0.00015	0.00015	0.00014	0.00014	0.00014
20	0.00016	0.00016	0.00015	0.00015	0.00015	0.00015	0.00015	0.00014	0.00014	0.00014
21	0.00016	0.00016	0.00015	0.00015	0.00015	0.00015	0.00015	0.00014	0.00014	0.00014
22	0.00016	0.00015	0.00015	0.00015	0.00015	0.00015	0.00014	0.00014	0.00014	0.00014
23	0.00016	0.00015	0.00015	0.00015	0.00015	0.00015	0.00014	0.00014	0.00014	0.00014
24	0.00016	0.00015	0.00015	0.00015	0.00015	0.00015	0.00014	0.00014	0.00014	0.00014

TABLE 5.3-14, CD3 (DRAG COEFFICIENT BASED ON PARAFOIL REF AREA)

Chordwise Riser Line No.

Spanwise Riser Line No.	1	2	3	4	5	6	7	8	9	10
1	-0.97500	-0.97500	-0.97500	-0.97500	-0.97500	-0.97500	-0.97500	-0.97500	-0.97500	-0.97500
2	0.22500	0.22500	0.22500	0.22500	0.22500	0.22500	0.22500	0.22500	0.22500	0.22500
3	1.42500	1.42500	1.42500	1.42500	1.42500	1.42500	1.42500	1.42500	1.42500	1.42500
4	2.62500	2.62500	2.62500	2.62500	2.62500	2.62500	2.62500	2.62500	2.62500	2.62500
5	3.82500	3.82500	3.82500	3.82500	3.82500	3.82500	3.82500	3.82500	3.82500	3.82500
6	5.02500	5.02500	5.02500	5.02500	5.02500	5.02500	5.02500	5.02500	5.02500	5.02500
7	6.22500	6.22500	6.22500	6.22500	6.22500	6.22500	6.22500	6.22500	6.22500	6.22500
8	7.42500	7.42500	7.42500	7.42500	7.42500	7.42500	7.42500	7.42500	7.42500	7.42500
9	8.62500	8.62500	8.62500	8.62500	8.62500	8.62500	8.62500	8.62500	8.62500	8.62500
10	9.82500	9.82500	9.82500	9.82500	9.82500	9.82500	9.82500	9.82500	9.82500	9.82500
11	11.02500	11.02500	11.02500	11.02500	11.02500	11.02500	11.02500	11.02500	11.02500	11.02500
12	12.22500	12.22500	12.22500	12.22500	12.22500	12.22500	12.22500	12.22500	12.22500	12.22500
13	13.42500	13.42500	13.42500	13.42500	13.42500	13.42500	13.42500	13.42500	13.42500	13.42500
14	14.62500	14.62500	14.62500	14.62500	14.62500	14.62500	14.62500	14.62500	14.62500	14.62500
15	15.82500	15.82500	15.82500	15.82500	15.82500	15.82500	15.82500	15.82500	15.82500	15.82500
16	17.02500	17.02500	17.02500	17.02500	17.02500	17.02500	17.02500	17.02500	17.02500	17.02500
17	18.22500	18.22500	18.22500	18.22500	18.22500	18.22500	18.22500	18.22500	18.22500	18.22500
18	19.42500	19.42500	19.42500	19.42500	19.42500	19.42500	19.42500	19.42500	19.42500	19.42500
19	20.62500	20.62500	20.62500	20.62500	20.62500	20.62500	20.62500	20.62500	20.62500	20.62500
20	21.82500	21.82500	21.82500	21.82500	21.82500	21.82500	21.82500	21.82500	21.82500	21.82500
21	23.02500	23.02500	23.02500	23.02500	23.02500	23.02500	23.02500	23.02500	23.02500	23.02500
22	24.22500	24.22500	24.22500	24.22500	24.22500	24.22500	24.22500	24.22500	24.22500	24.22500
23	25.42500	25.42500	25.42500	25.42500	25.42500	25.42500	25.42500	25.42500	25.42500	25.42500
24	26.62500	26.62500	26.62500	26.62500	26.62500	26.62500	26.62500	26.62500	26.62500	26.62500

Spanwise Riser Line No.	11	12	13	14	15	16	17	18	19	20
1	-0.97500	-0.97500	-0.97500	-0.97500	-0.97500	-0.97500	-0.97500	-0.97500	-0.97500	-0.97500
2	0.22500	0.22500	0.22500	0.22500	0.22500	0.22500	0.22500	0.22500	0.22500	0.22500
3	1.42500	1.42500	1.42500	1.42500	1.42500	1.42500	1.42500	1.42500	1.42500	1.42500
4	2.62500	2.62500	2.62500	2.62500	2.62500	2.62500	2.62500	2.62500	2.62500	2.62500
5	3.82500	3.82500	3.82500	3.82500	3.82500	3.82500	3.82500	3.82500	3.82500	3.82500
6	5.02500	5.02500	5.02500	5.02500	5.02500	5.02500	5.02500	5.02500	5.02500	5.02500
7	6.22500	6.22500	6.22500	6.22500	6.22500	6.22500	6.22500	6.22500	6.22500	6.22500
8	7.42500	7.42500	7.42500	7.42500	7.42500	7.42500	7.42500	7.42500	7.42500	7.42500
9	8.62500	8.62500	8.62500	8.62500	8.62500	8.62500	8.62500	8.62500	8.62500	8.62500
10	9.82500	9.82500	9.82500	9.82500	9.82500	9.82500	9.82500	9.82500	9.82500	9.82500
11	11.02500	11.02500	11.02500	11.02500	11.02500	11.02500	11.02500	11.02500	11.02500	11.02500
12	12.22500	12.22500	12.22500	12.22500	12.22500	12.22500	12.22500	12.22500	12.22500	12.22500
13	13.42500	13.42500	13.42500	13.42500	13.42500	13.42500	13.42500	13.42500	13.42500	13.42500
14	14.62500	14.62500	14.62500	14.62500	14.62500	14.62500	14.62500	14.62500	14.62500	14.62500
15	15.82500	15.82500	15.82500	15.82500	15.82500	15.82500	15.82500	15.82500	15.82500	15.82500
16	17.02500	17.02500	17.02500	17.02500	17.02500	17.02500	17.02500	17.02500	17.02500	17.02500
17	18.22500	18.22500	18.22500	18.22500	18.22500	18.22500	18.22500	18.22500	18.22500	18.22500
18	19.42500	19.42500	19.42500	19.42500	19.42500	19.42500	19.42500	19.42500	19.42500	19.42500
19	20.62500	20.62500	20.62500	20.62500	20.62500	20.62500	20.62500	20.62500	20.62500	20.62500
20	21.82500	21.82500	21.82500	21.82500	21.82500	21.82500	21.82500	21.82500	21.82500	21.82500
21	23.02500	23.02500	23.02500	23.02500	23.02500	23.02500	23.02500	23.02500	23.02500	23.02500
22	24.22500	24.22500	24.22500	24.22500	24.22500	24.22500	24.22500	24.22500	24.22500	24.22500
23	25.42500	25.42500	25.42500	25.42500	25.42500	25.42500	25.42500	25.42500	25.42500	25.42500
24	26.62500	26.62500	26.62500	26.62500	26.62500	26.62500	26.62500	26.62500	26.62500	26.62500

TABLE 5.3-15, THETA (FRONTAL ANGLE YZ PLANE), deg

Chordwise Riser Line No.

Spanwise Riser Line No.	1	2	3	4	5	6	7	8	9	10
1	-0.24641	-0.26040	-0.27382	-0.28666	-0.29890	-0.31054	-0.32156	-0.33197	-0.34177	-0.35096
2	-0.24644	-0.26043	-0.27386	-0.28670	-0.29894	-0.31058	-0.32161	-0.33202	-0.34181	-0.35099
3	-0.24637	-0.26035	-0.27377	-0.28661	-0.29885	-0.31049	-0.32151	-0.33192	-0.34171	-0.35089
4	-0.24618	-0.26016	-0.27357	-0.28640	-0.29863	-0.31026	-0.32127	-0.33167	-0.34146	-0.35063
5	-0.24589	-0.25985	-0.27325	-0.28606	-0.29828	-0.30989	-0.32089	-0.33128	-0.34106	-0.35022
6	-0.24549	-0.25943	-0.27281	-0.28560	-0.29780	-0.30939	-0.32037	-0.33075	-0.34050	-0.34965
7	-0.24499	-0.25890	-0.27224	-0.28501	-0.29718	-0.30875	-0.31971	-0.33006	-0.33980	-0.34893
8	-0.24438	-0.25825	-0.27156	-0.28430	-0.29644	-0.30798	-0.31891	-0.32924	-0.33895	-0.34805
9	-0.24365	-0.25749	-0.27076	-0.28346	-0.29556	-0.30707	-3.31797	-0.32827	-0.33795	-0.34703
10	-0.24283	-0.25662	-0.26984	-0.28250	-0.29456	-0.30603	-0.31689	-0.32715	-0.33680	-0.34585
11	-0.24189	-0.25563	-0.26880	-0.28141	-0.29343	-0.30485	-0.31567	-0.32589	-0.33551	-0.34452
12	-0.24085	-0.25453	-0.26765	-0.28020	-0.29217	-0.30354	-0.31432	-0.32449	-0.33407	-0.34304
13	-0.23971	-0.25332	-0.26638	-0.27887	-0.29078	-0.30210	-0.31282	-0.32295	-0.33248	-0.34141
14	-0.23846	-0.25200	-0.26499	-0.27741	-0.28926	-0.30052	-0.31119	-0.32126	-0.33074	-0.33962
15	-0.23710	-0.25058	-0.26348	-0.27583	-0.28761	-0.29881	-0.30942	-0.31944	-0.32886	-0.33769
16	-0.23564	-0.24902	-0.26186	-0.27414	-0.28584	-0.29697	-0.30752	-0.31747	-0.32684	-0.33562
17	-0.23408	-0.24737	-0.26012	-0.27232	-0.28395	-0.29500	-0.30548	-0.31537	-0.32467	-0.33339
18	-0.23241	-0.24561	-0.25827	-0.27038	-0.28193	-0.29290	-0.30330	-0.31312	-0.32236	-0.33102
19	-0.23065	-0.24374	-0.25631	-0.26832	-0.27978	-0.29068	-0.30100	-0.31074	-0.31991	-0.32850
20	-0.22878	-0.24177	-0.25423	-0.26615	-0.27752	-0.28832	-0.29856	-0.30822	-0.31732	-0.32584
21	-0.22681	-0.23969	-0.25204	-0.26386	-0.27513	-0.28584	-0.29599	-0.30557	-0.31459	-0.32303
22	-0.22474	-0.23750	-0.24974	-0.26145	-0.27262	-0.28323	-0.29329	-0.30278	-0.31172	-0.32009
23	-0.22257	-0.23521	-0.24734	-0.25893	-0.26999	-0.28050	-0.29046	-0.29987	-0.30871	-0.31700
24	-0.22031	-0.23282	-0.24482	-0.25630	-0.26724	-0.27765	-0.28751	-0.29681	-0.30557	-0.31378

Spanwise Riser Line No.	11	12	13	14	15	16	17	18	19	20
1	-0.35951	-0.36748	-0.37484	-0.38162	-0.38783	-0.39347	-0.39856	-0.40312	-0.40716	-0.41071
2	-0.35956	-0.36753	-0.37489	-0.38167	-0.38788	-0.39352	-0.39861	-0.40318	-0.40722	-0.41077
3	-0.35946	-0.36742	-0.37478	-0.38156	-0.38776	-0.39340	-0.39849	-0.40305	-0.40710	-0.41064
4	-0.35919	-0.36714	-0.37450	-0.38128	-0.38747	-0.39311	-0.39820	-0.40276	-0.40680	-0.41034
5	-0.35877	-0.36671	-0.37406	-0.38083	-0.38702	-0.39265	-0.39773	-0.40228	-0.40632	-0.40985
6	-0.35818	-0.36612	-0.37346	-0.38021	-0.38639	-0.39201	-0.39709	-0.40163	-0.40566	-0.40919
7	-0.35745	-0.36536	-0.37269	-0.37943	-0.38559	-0.39120	-0.39627	-0.40080	-0.40482	-0.40835
8	-0.35655	-0.36445	-0.37175	-0.37848	-0.38463	-0.39022	-0.39527	-0.39980	-0.40381	-0.40733
9	-0.35550	-0.36337	-0.37066	-0.37736	-0.38349	-0.38907	-0.39411	-0.39862	-0.40262	-0.40612
10	-0.35429	-0.36214	-0.36940	-0.37608	-0.38219	-0.38775	-0.39277	-0.39727	-0.40125	-0.40475
11	-0.35293	-0.36075	-0.36798	-0.37463	-0.38072	-0.38626	-0.39126	-0.39574	-0.39971	-0.40319
12	-0.35141	-0.35920	-0.36640	-0.37302	-0.37909	-0.38460	-0.38958	-0.39404	-0.39799	-0.40145
13	-0.34974	-0.35749	-0.36465	-0.37125	-0.37728	-0.38277	-0.38772	-0.39216	-0.39610	-0.39955
14	-0.34792	-0.35562	-0.36275	-0.36931	-0.37531	-0.38077	-0.38570	-0.39012	-0.39403	-0.39746
15	-0.34594	-0.35360	-0.36069	-0.36721	-0.37318	-0.37861	-0.38351	-0.38790	-0.39179	-0.39520
16	-0.34381	-0.35142	-0.35847	-0.36495	-0.37088	-0.37628	-0.38115	-0.38551	-0.38938	-0.39277
17	-0.34153	-0.34909	-0.35609	-0.36253	-0.36842	-0.37378	-0.37862	-0.38295	-0.38680	-0.39016
18	-0.33910	-0.34661	-0.35356	-0.35995	-0.36580	-0.37112	-0.37593	-0.38023	-0.38404	-0.38739
19	-0.33652	-0.34397	-0.35087	-0.35721	-0.36302	-0.36830	-0.37307	-0.37734	-0.38112	-0.38444
20	-0.33379	-0.34119	-0.34803	-0.35432	-0.36008	-0.36532	-0.37005	-0.37428	-0.37804	-0.38133
21	-0.33092	-0.33825	-0.34503	-0.35127	-0.35698	-0.36217	-0.36686	-0.37106	-0.37478	-0.37805
22	-0.32790	-0.33517	-0.34188	-0.34807	-0.35372	-0.35887	-0.36352	-0.36768	-0.37136	-0.37460
23	-0.32474	-0.33193	-0.33859	-0.34471	-0.35031	-0.35541	-0.36001	-0.36413	-0.36778	-0.37099
24	-0.32144	-0.32856	-0.33514	-0.34120	-0.34675	-0.35179	-0.35635	-0.36043	-0.36404	-0.36721

TABLE 5.3-16, CL1 (BASED ON INDIVIDUAL REF AREA)

Chordwise Riser Line No.

Spanwise Riser Line No.	1	2	3	4	5	6	7	8	9	10
1	-0.00049	-0.00052	-0.00055	-0.00058	-0.00061	-0.00063	-0.00066	-0.00069	-0.00071	-0.00073
2	-0.00049	-0.00052	-0.00055	-0.00058	-0.00061	-0.00064	-0.00066	-0.00069	-0.00071	-0.00073
3	-0.00049	-0.00052	-0.00055	-0.00058	-0.00061	-0.00063	-0.00066	-0.00069	-0.00071	-0.00073
4	-0.00049	-0.00052	-0.00055	-0.00058	-0.00061	-0.00063	-0.00066	-0.00068	-0.00071	-0.00073
5	-0.00049	-0.00052	-0.00055	-0.00058	-0.00061	-0.00063	-0.00066	-0.00068	-0.00071	-0.00073
6	-0.00049	-0.00052	-0.00055	-0.00058	-0.00061	-0.00063	-0.00066	-0.00068	-0.00071	-0.00073
7	-0.00049	-0.00052	-0.00055	-0.00058	-0.00060	-0.00063	-0.00066	-0.00068	-0.00070	-0.00073
8	-0.00049	-0.00052	-0.00055	-0.00057	-0.00060	-0.00063	-0.00065	-0.00068	-0.00070	-0.00073
9	-0.00049	-0.00052	-0.00054	-0.00057	-0.00060	-0.00063	-0.00065	-0.00068	-0.00070	-0.00072
10	-0.00048	-0.00051	-0.00054	-0.00057	-0.00060	-0.00062	-0.00065	-0.00067	-0.00070	-0.00072
11	-0.00048	-0.00051	-0.00054	-0.00057	-0.00059	-0.00062	-0.00065	-0.00067	-0.00069	-0.00072
12	-0.00048	-0.00051	-0.00054	-0.00056	-0.00059	-0.00062	-0.00064	-0.00067	-0.00069	-0.00071
13	-0.00048	-0.00050	-0.00053	-0.00056	-0.00059	-0.00061	-0.00064	-0.00066	-0.00068	-0.00071
14	-0.00047	-0.00050	-0.00053	-0.00056	-0.00058	-0.00061	-0.00063	-0.00066	-0.00068	-0.00070
15	-0.00047	-0.00050	-0.00053	-0.00055	-0.00058	-0.00061	-0.00063	-0.00065	-0.00068	-0.00070
16	-0.00047	-0.00049	-0.00052	-0.00055	-0.00057	-0.00060	-0.00062	-0.00065	-0.00067	-0.00069
17	-0.00046	-0.00049	-0.00052	-0.00054	-0.00057	-0.00060	-0.00062	-0.00064	-0.00067	-0.00069
18	-0.00046	-0.00049	-0.00051	-0.00054	-0.00057	-0.00059	-0.00062	-0.00064	-0.00066	-0.00068
19	-0.00045	-0.00048	-0.00051	-0.00053	-0.00056	-0.00058	-0.00061	-0.00063	-0.00065	-0.00067
20	-0.00045	-0.00048	-0.00050	-0.00053	-0.00055	-0.00058	-0.00060	-0.00062	-0.00065	-0.00067
21	-0.00045	-0.00047	-0.00050	-0.00052	-0.00055	-0.00057	-0.00060	-0.00062	-0.00064	-0.00066
22	-0.00044	-0.00046	-0.00049	-0.00052	-0.00054	-0.00056	-0.00059	-0.00061	-0.00063	-0.00065
23	-0.00043	-0.00046	-0.00049	-0.00051	-0.00053	-0.00056	-0.00058	-0.00060	-0.00062	-0.00064
24	-0.00043	-0.00046	-0.00048	-0.00051	-0.00053	-0.00055	-0.00058	-0.00060	-0.00062	-0.00064

Spanwise Riser Line No.	11	12	13	14	15	16	17	18	19	20
1	-0.00076	-0.00078	-0.00080	-0.00082	-0.00084	-0.00085	-0.00087	-0.00089	-0.00090	-0.00092
2	-0.00076	-0.00078	-0.00080	-0.00082	-0.00084	-0.00085	-0.00087	-0.00089	-0.00090	-0.00092
3	-0.00076	-0.00078	-0.00080	-0.00082	-0.00084	-0.00085	-0.00087	-0.00089	-0.00090	-0.00092
4	-0.00075	-0.00078	-0.00080	-0.00082	-0.00083	-0.00086	-0.00087	-0.00089	-0.00090	-0.00091
5	-0.00075	-0.00077	-0.00080	-0.00081	-0.00083	-0.00085	-0.00087	-0.00088	-0.00090	-0.00091
6	-0.00075	-0.00077	-0.00079	-0.00081	-0.00083	-0.00085	-0.00087	-0.00088	-0.00090	-0.00091
7	-0.00075	-0.00077	-0.00079	-0.00081	-0.00083	-0.00085	-0.00086	-0.00088	-0.00089	-0.00091
8	-0.00075	-0.00077	-0.00079	-0.00081	-0.00083	-0.00084	-0.00086	-0.00088	-0.00089	-0.00091
9	-0.00075	-0.00077	-0.00079	-0.00081	-0.00082	-0.00084	-0.00086	-0.00087	-0.00089	-0.00090
10	-0.00074	-0.00076	-0.00078	-0.00080	-0.00082	-0.00084	-0.00085	-0.00087	-0.00088	-0.00090
11	-0.00074	-0.00076	-0.00078	-0.00080	-0.00082	-0.00083	-0.00085	-0.00087	-0.00088	-0.00090
12	-0.00073	-0.00076	-0.00078	-0.00079	-0.00081	-0.00083	-0.00085	-0.00086	-0.00088	-0.00089
13	-0.00073	-0.00075	-0.00077	-0.00079	-0.00081	-0.00082	-0.00084	-0.00086	-0.00087	-0.00088
14	-0.00073	-0.00075	-0.00077	-0.00078	-0.00080	-0.00082	-0.00084	-0.00085	-0.00087	-0.00088
15	-0.00072	-0.00074	-0.00076	-0.00078	-0.00080	-0.00081	-0.00083	-0.00085	-0.00086	-0.00087
16	-0.00071	-0.00073	-0.00075	-0.00077	-0.00079	-0.00081	-0.00082	-0.00084	-0.00085	-0.00086
17	-0.00071	-0.00073	-0.00075	-0.00077	-0.00078	-0.00080	-0.00082	-0.00083	-0.00085	-0.00086
18	-0.00070	-0.00072	-0.00074	-0.00076	-0.00078	-0.00079	-0.00081	-0.00083	-0.00084	-0.00085
19	-0.00069	-0.00071	-0.00073	-0.00075	-0.00077	-0.00078	-0.00080	-0.00082	-0.00083	-0.00084
20	-0.00069	-0.00071	-0.00073	-0.00074	-0.00076	-0.00078	-0.00079	-0.00081	-0.00082	-0.00083
21	-0.00068	-0.00070	-0.00072	-0.00074	-0.00075	-0.00077	-0.00079	-0.00080	-0.00081	-0.00083
22	-0.00067	-0.00069	-0.00071	-0.00073	-0.00074	-0.00076	-0.00077	-0.00079	-0.00080	-0.00081
23	-0.00066	-0.00068	-0.00070	-0.00072	-0.00074	-0.00075	-0.00077	-0.00078	-0.00079	-0.00081
24	-0.00066	-0.00068	-0.00069	-0.00071	-0.00073	-0.00074	-0.00076	-0.00077	-0.00079	-0.00080

TABLE 5.3-17, CL2 (BASED ON LINE REF AREA)

Chordwise Riser Line No.

Spanwise Riser Line No.	1	2	3	4	5	6	7	8	9	10
1	-0.00004	-0.00005	-0.00005	-0.00005	-0.00005	-0.00006	-0.00006	-0.00006	-0.00006	-0.00006
2	-0.00004	-0.00005	-0.00005	-0.00005	-0.00005	-0.00006	-0.00006	-0.00006	-0.00006	-0.00006
3	-0.00004	-0.00005	-0.00005	-0.00005	-0.00005	-0.00006	-0.00006	-0.00006	-0.00006	-0.00006
4	-0.00004	-0.00005	-0.00005	-0.00005	-0.00005	-0.00006	-0.00006	-0.00006	-0.00006	-0.00006
5	-0.00004	-0.00005	-0.00005	-0.00005	-0.00005	-0.00006	-0.00006	-0.00006	-0.00006	-0.00006
6	-0.00004	-0.00005	-0.00005	-0.00005	-0.00005	-0.00006	-0.00006	-0.00006	-0.00006	-0.00006
7	-0.00004	-0.00005	-0.00005	-0.00005	-0.00005	-0.00006	-0.00006	-0.00006	-0.00006	-0.00006
8	-0.00004	-0.00005	-0.00005	-0.00005	-0.00005	-0.00006	-0.00006	-0.00006	-0.00006	-0.00006
9	-0.00004	-0.00005	-0.00005	-0.00005	-0.00005	-0.00006	-0.00006	-0.00006	-0.00006	-0.00006
10	-0.00004	-0.00005	-0.00005	-0.00005	-0.00005	-0.00005	-0.00006	-0.00006	-0.00006	-0.00006
11	-0.00004	-0.00005	-0.00005	-0.00005	-0.00005	-0.00005	-0.00006	-0.00006	-0.00006	-0.00006
12	-0.00004	-0.00004	-0.00005	-0.00005	-0.00005	-0.00005	-0.00006	-0.00006	-0.00006	-0.00006
13	-0.00004	-0.00004	-0.00005	-0.00005	-0.00005	-0.00005	-0.00006	-0.00006	-0.00006	-0.00006
14	-0.00004	-0.00004	-0.00005	-0.00005	-0.00005	-0.00005	-0.00006	-0.00006	-0.00006	-0.00006
15	-0.00004	-0.00004	-0.00005	-0.00005	-0.00005	-0.00005	-0.00006	-0.00006	-0.00006	-0.00006
16	-0.00004	-0.00004	-0.00005	-0.00005	-0.00005	-0.00005	-0.00006	-0.00006	-0.00006	-0.00006
17	-0.00004	-0.00004	-0.00005	-0.00005	-0.00005	-0.00005	-0.00005	-0.00006	-0.00006	-0.00006
18	-0.00004	-0.00004	-0.00005	-0.00005	-0.00005	-0.00005	-0.00005	-0.00006	-0.00006	-0.00006
19	-0.00004	-0.00004	-0.00004	-0.00005	-0.00005	-0.00005	-0.00005	-0.00006	-0.00006	-0.00006
20	-0.00004	-0.00004	-0.00004	-0.00005	-0.00005	-0.00005	-0.00005	-0.00006	-0.00006	-0.00006
21	-0.00004	-0.00004	-0.00004	-0.00005	-0.00005	-0.00005	-0.00005	-0.00005	-0.00006	-0.00006
22	-0.00004	-0.00004	-0.00004	-0.00005	-0.00005	-0.00005	-0.00005	-0.00005	-0.00006	-0.00006
23	-0.00004	-0.00004	-0.00004	-0.00005	-0.00005	-0.00005	-0.00005	-0.00005	-0.00006	-0.00006
24	-0.00004	-0.00004	-0.00004	-0.00004	-0.00005	-0.00005	-0.00005	-0.00005	-0.00005	-0.00006

Spanwise Riser Line No.	11	12	13	14	15	16	17	18	19	20
1	-0.00007	-0.00007	-0.00007	-0.00007	-0.00007	-0.00008	-0.00008	-0.00008	-0.00008	-0.00008
2	-0.00007	-0.00007	-0.00007	-0.00007	-0.00007	-0.00008	-0.00008	-0.00008	-0.00008	-0.00008
3	-0.00007	-0.00007	-0.00007	-0.00007	-0.00007	-0.00008	-0.00008	-0.00008	-0.00008	-0.00008
4	-0.00007	-0.00007	-0.00007	-0.00007	-0.00007	-0.00008	-0.00008	-0.00008	-0.00008	-0.00008
5	-0.00007	-0.00007	-0.00007	-0.00007	-0.00007	-0.00008	-0.00008	-0.00008	-0.00008	-0.00008
6	-0.00007	-0.00007	-0.00007	-0.00007	-0.00007	-0.00007	-0.00008	-0.00008	-0.00008	-0.00008
7	-0.00007	-0.00007	-0.00007	-0.00007	-0.00007	-0.00007	-0.00008	-0.00008	-0.00008	-0.00008
8	-0.00007	-0.00007	-0.00007	-0.00007	-0.00007	-0.00007	-0.00008	-0.00008	-0.00008	-0.00008
9	-0.00007	-0.00007	-0.00007	-0.00007	-0.00007	-0.00007	-0.00008	-0.00008	-0.00008	-0.00008
10	-0.00007	-0.00007	-0.00007	-0.00007	-0.00007	-0.00007	-0.00008	-0.00008	-0.00008	-0.00008
11	-0.00007	-0.00007	-0.00007	-0.00007	-0.00007	-0.00007	-0.00008	-0.00008	-0.00008	-0.00008
12	-0.00006	-0.00007	-0.00007	-0.00007	-0.00007	-0.00007	-0.00007	-0.00008	-0.00008	-0.00008
13	-0.00006	-0.00007	-0.00007	-0.00007	-0.00007	-0.00007	-0.00007	-0.00008	-0.00008	-0.00008
14	-0.00006	-0.00007	-0.00007	-0.00007	-0.00007	-0.00007	-0.00007	-0.00008	-0.00008	-0.00008
15	-0.00006	-0.00007	-0.00007	-0.00007	-0.00007	-0.00007	-0.00007	-0.00007	-0.00008	-0.00008
16	-0.00006	-0.00006	-0.00007	-0.00007	-0.00007	-0.00007	-0.00007	-0.00007	-0.00008	-0.00008
17	-0.00006	-0.00006	-0.00007	-0.00007	-0.00007	-0.00007	-0.00007	-0.00007	-0.00007	-0.00008
18	-0.00006	-0.00006	-0.00007	-0.00007	-0.00007	-0.00007	-0.00007	-0.00007	-0.00007	-0.00008
19	-0.00006	-0.00006	-0.00006	-0.00007	-0.00007	-0.00007	-0.00007	-0.00007	-0.00007	-0.00008
20	-0.00006	-0.00006	-0.00006	-0.00007	-0.00007	-0.00007	-0.00007	-0.00007	-0.00007	-0.00007
21	-0.00006	-0.00006	-0.00006	-0.00007	-0.00007	-0.00007	-0.00007	-0.00007	-0.00007	-0.00007
22	-0.00006	-0.00006	-0.00006	-0.00006	-0.00007	-0.00007	-0.00007	-0.00007	-0.00007	-0.00007
23	-0.00006	-0.00006	-0.00006	-0.00006	-0.00006	-0.00007	-0.00007	-0.00007	-0.00007	-0.00007
24	-0.00006	-0.00006	-0.00006	-0.00006	-0.00006	-0.00007	-0.00007	-0.00007	-0.00007	-0.00007

TABLE 5.3-18, CL3 (BASED ON PARAFOIL REF AREA)

ORIGINAL PAGE IS
OF POOR QUALITY

5.4 LATERAL STABILITY STUDY

When the 20 x 60 ft parafoil was tested in the NASA-Ames wind tunnel, four tether lines were attached to constrain the model in roll and yaw, as shown in Figure 5.4-1. Aerodynamic forces and moments were measured through the balance located in the tunnel floor. Missing from these balance measurements were the forces transmitted via the tether lines. The purpose of this study is to include these forces and their contributions to aerodynamic force and moment coefficients.

5.4.1 Resolving Tether Forces

During the wind tunnel test, a load cell was placed on each of the tether lines to measure line tension. To simplify the process of solving for these forces, the first step is to resolve the direction of the lines into unit vectors (UV_1, UV_2, UV_3, UV_4) as shown in Figure 5.4-1. As previously mentioned, the model was constrained in roll and yaw; however, it was allowed to move in pitch with this assumption; the unit vectors are functions of α and the forces are resolved as follows:

$$T_1 \cdot UV_1(\alpha) = T_1x + T_1y + T_1z$$
$$T_2 \cdot UV_2(\alpha) = T_2x + T_2y + T_2z$$
$$T_3 \cdot UV_3(\alpha) = T_3x + T_3y + T_3z$$
$$T_4 \cdot UV_4(\alpha) = T_4x + T_4y + T_4z$$

where T_1 to T_4 are the line tensions, UV_1 to UV_4 the unit vectors, and Tx, Ty and Tz the component forces. (See Figure 5.4-2 for a depiction of these forces.)

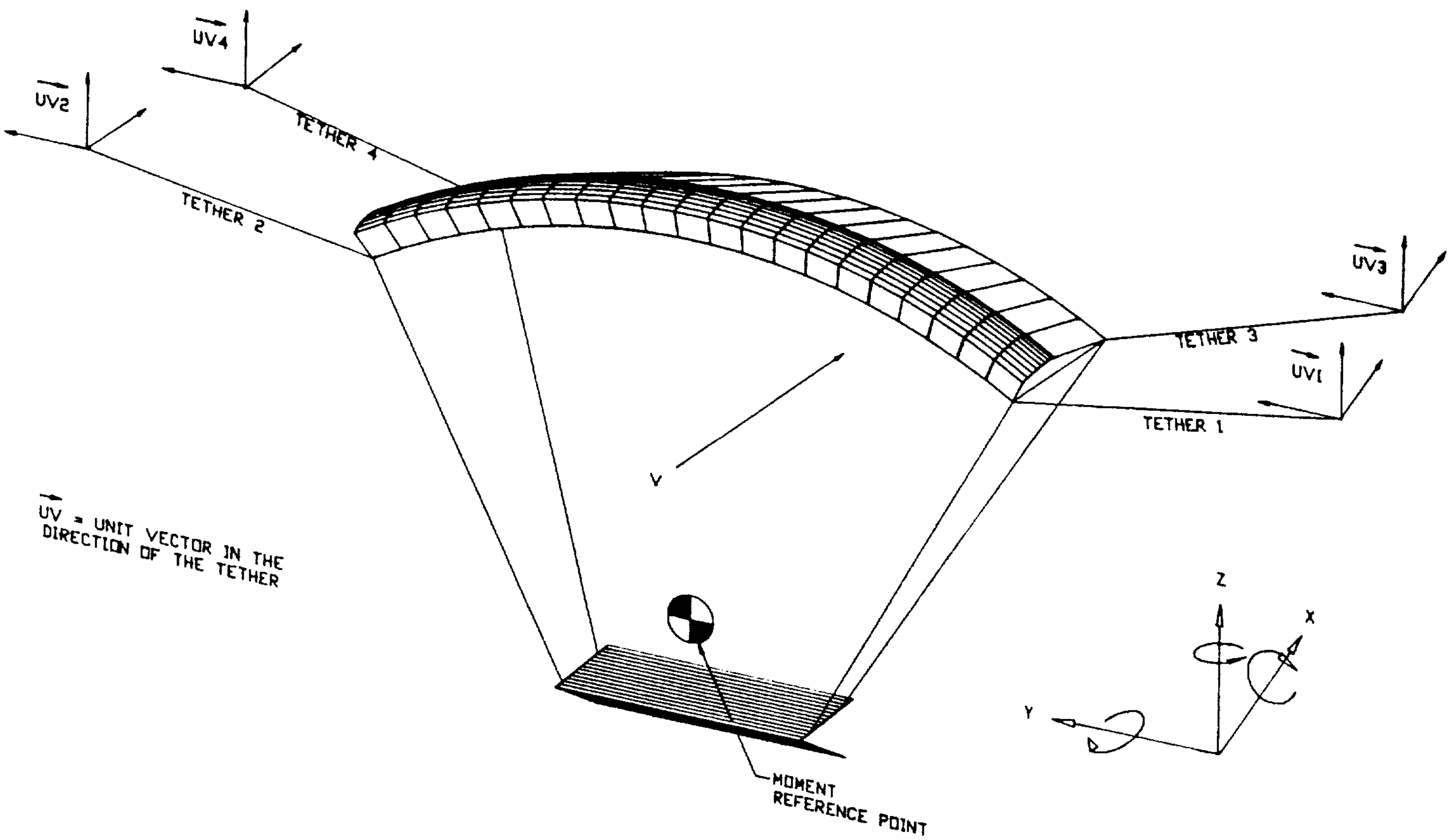

FIGURE 5.4-1, TETHER NOMENCLATURE

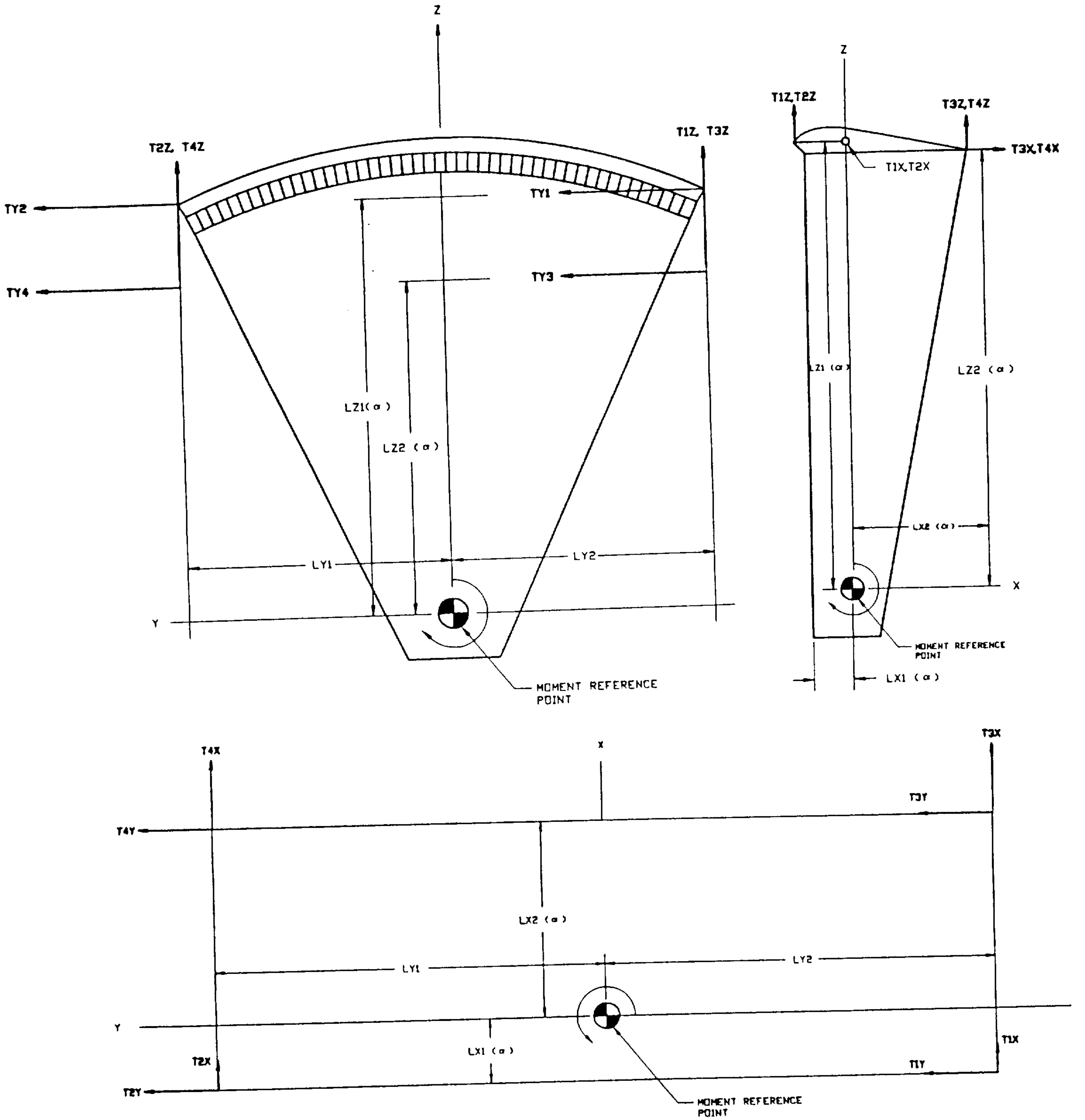

FIGURE 5.4-2, TETHER FORCE AND MOMENT COMPONENTS

5.4.2 Tether Aerodynamic Force Contributions

To add the tether force increments to the measured aerodynamic force obtained from the wind tunnel test the following is used:

$$\Delta D_T = T_1x + T_2x + T_3x + T_4x \; (\Delta \text{ Drag})$$
$$\Delta L_T = T_1z + T_2z + T_3z + T_4z \; (\Delta \text{ Lift})$$
$$\Delta S_T = T_1y + T_2y + T_3y + T_4y \; (\Delta \text{ Side Force})$$

To translate into coefficient form:

$$C_{DT} = \Delta D_T/qA_{REF}$$
$$C_{LT} = \Delta L_T/qA_{REF}$$
$$C_{ST} = \Delta S_T/qA_{REF}$$

where q is the dynamic pressure and A_{REF} the reference area of the parafoil (1200 ft^2).

5.4.3 Tether Aerodynamic Moment Contributions

To add the tether moment increments to the measured values obtained from the test the following is used:

$$\Delta M_{xT} = -(T_1y + T_2y)L_{z1}(\alpha) - (T_3y + T_4y)L_{z2}(\alpha) + (T_2z + T_4z)L_{y1} - (T_1z + T_3z)L_{y2}$$

$$\Delta M_{yT} = (T_1x + T_2x)L_{z1}(\alpha) + (T_3x + T_4x)L_{z2}(\alpha) + (T_1z + T_2z)L_{x1}(\alpha) - (T_3z + T_4z)L_{x2}(\alpha)$$

$$\Delta M_{zT} = (T_3x + T_1x)L_{y2} - (T_2x + T_4x)L_{y1} + (T_3y + T_4y)L_{x2}(\alpha) - (T_2y + T_1y)L_{x1}(\alpha)$$

To translate into coefficient form:

$$C_{MxT} = \Delta M_{xT}/(q\, A_{REF}\, L_{REF})$$
$$C_{MyT} = \Delta M_{yT}/(q\, A_{REF}\, L_{REF})$$
$$C_{MzT} = \Delta M_{zT}/(q\, A_{REF}\, L_{REF})$$

where q is the dynamic pressure, A_{REF} the parafoil reference area (1200 ft^2) and L_{REF} the reference length of 20 ft for lateral and 60 ft for longitudinal.

5.4.4 Moment Arm Determination

This section follows the development of equations used in determining the moment arms, as seen in Figure 5.4-2. As stated previously, the model is assumed to be constrained in roll and yaw, but is free to pitch. The moment arms Lz_1, Lz_2, Lx_1 and Lx_2 are therefore all functions of θ_1, θ_2, α and αp. The moment arms Ly_1 and Ly_2 are assumed constant. For the remainder of this section follow Figures 5.4-3 and 5.4-4.

Given:

cx, xx, LL, b, R, LL	(Constant)
αp, ϕ, δp, XCG1, XCG2	(Per Test Basis)

Calculated:

$$a = (Fu^2 + xx^2 - 2\, Fu\, xx \cos\theta)^{1/2}$$
$$\theta_1 = \cos^{-1}((Fu^2 + a^2 - xx^2)/(2\, Fu\, a))$$
$$\theta_2 = \cos^{-1}((Cx^2 + a^2 - Ru^2)/(2\, Cx\, a))$$
$$\alpha = \alpha p - \phi + (180 - \theta_1 - \theta_2)$$

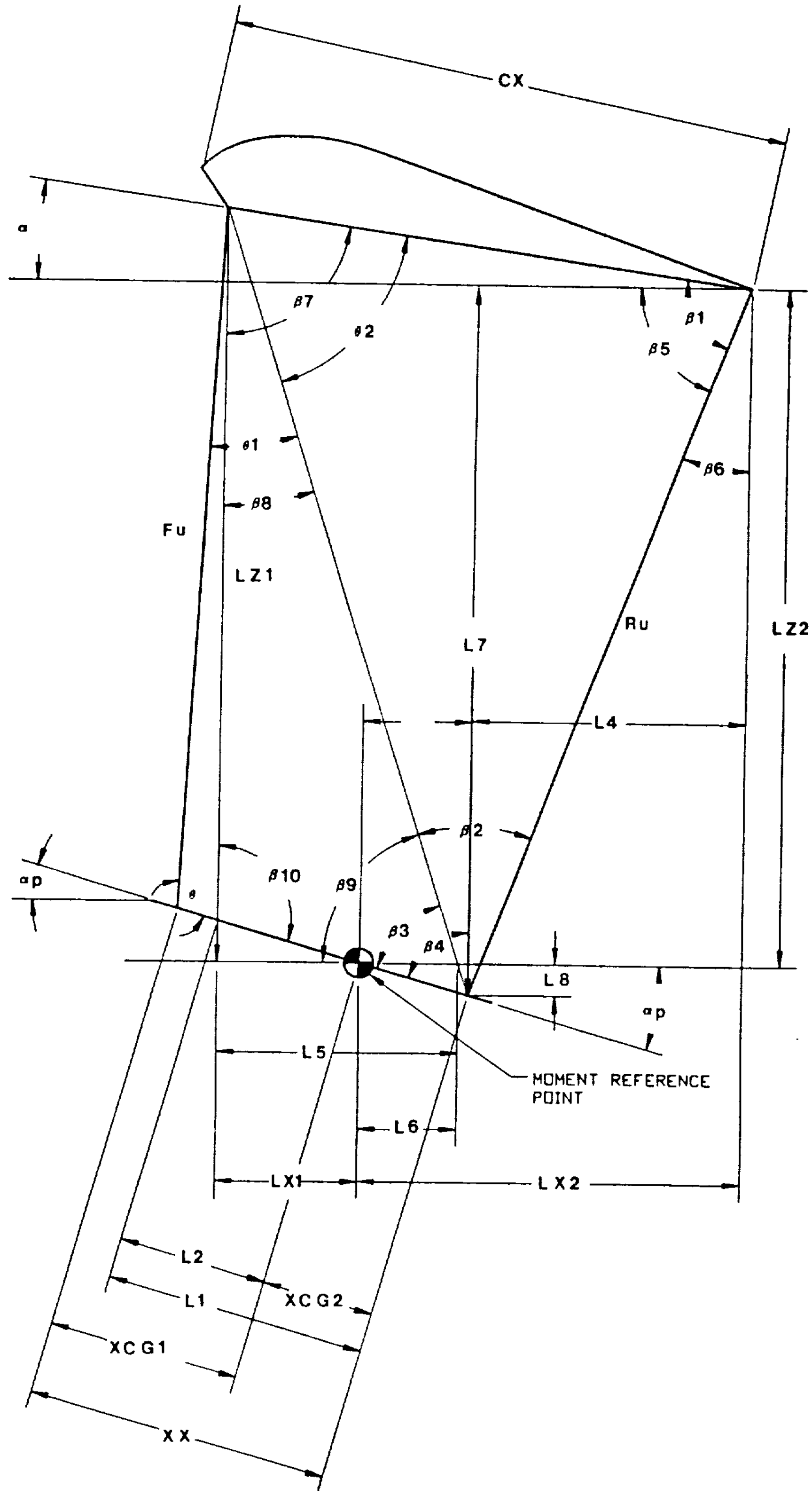

FIGURE 5.4-3, MOMENT ARM GEOMETRY

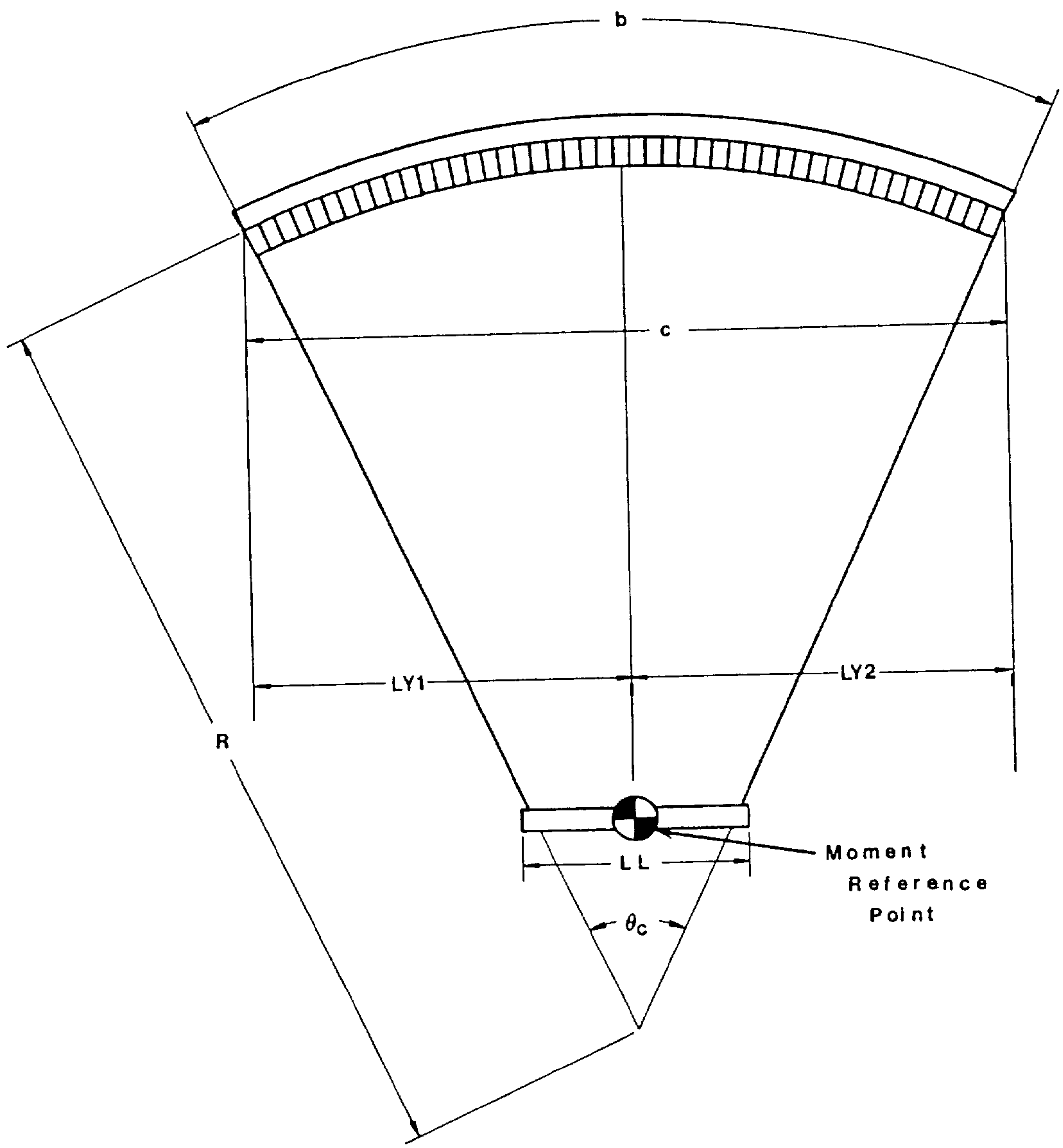

FIGURE 5.4-4, MOMENT ARM GEOMETRY

where the values of Fu, length of forward most suspension line and Ru, length of the rearmost suspension line were defined in a previous study as:

$$Ru = 53.995 - (.3403 + 2(4.1285)^2 - 2(4.1285)(.3403 + (4.1285)^2)^{1/2} \cos((\delta p + 5) + \tan^{-1}(.5833/4.1285)))^{1/2} + .0833$$

$$Fu = 48.209 - (.3403 + 2(.3942)^2 - 2(.3942)(.3403 + (.3942)^2)^{1/2} \cos((\delta p + 5) + \tan^{-1}(.5833/.3942)))^{1/2} + .0833$$

Continuing for the b angles and using the law of sines:

$$\alpha/\sin \beta_1 = Cx/\sin \beta_2 = Ru/\sin \theta_2$$

$$\alpha/\sin \theta = xx/\sin \theta_1 = Fu/\sin \beta_3$$

$$\beta_1 = \sin^{-1}((a \sin \theta_2)/Ru)$$

$$\beta_2 = \sin^{-1}((Cx \sin \theta_2)/Ru)$$

$$\beta_3 = \sin^{-1}((Fu \sin \theta_1)/XX)$$

$$\beta_4 = 90 - \alpha\rho$$

$$\beta_5 = \beta_1 - \alpha$$

$$\beta_6 = 90 - \beta_5$$

$$\beta_7 = 90 - \alpha$$

$$\beta_8 = \beta_7 - \theta_2$$

$$\beta_9 = 90 - \beta_8$$

$$\beta_{10} = 180 - \beta_3 - \beta_8$$

For the length calculations and using the law of sines:

$$\alpha/\sin\beta_{10} = L_1/\sin \beta_8$$

$$L_1 = (a \sin \beta_8)/\sin \beta_{10}$$

$$L_2 = L_1 - XCG2$$

$$L_3 = LCG2 \cos \alpha p$$

$$L_4 = Ru \cos \beta_5$$

$$L_5 = a \sin \beta_8$$

$$L_6 = L_5 - L_2 \cos \alpha p$$

$$\Lambda_7 = Ru \sin \beta_5$$

$$L_8 = XCG_2 \sin \alpha p$$

$$\theta C = b/R$$

$$C = 2R \sin (\theta C/2)$$

Solving for the moment arms:

$$Lx_1 = L_2 \cos \alpha p$$
$$Lx_2 = L_3 + L_4$$
$$Lz_1 = (L_5^2 + a^2)^{1/2}$$
$$Lz_2 = L_7 - L_8$$
$$Ly_1 = c/2$$
$$Ly_2 = c/2$$

Solving and substituting in terms of the "given" values:

$$Lx_1 = ((a \sin (90 - \alpha - \theta 2))/(\sin (90 - \sin^{-1}(Fu \sin \theta 1/xx)) + \alpha + \theta 2) - XCG2) \cos (\alpha p)$$
$$Lx_2 = XCG2 \cos \alpha p + Ru \cos (\sin^{-1}(a \sin \theta 2/Ru) - \alpha)$$
$$Lz_1 = ((a \sin (90 - \alpha - \theta 2))^2 + a^2)^{1/2}$$
$$Lz_2 = Ru \sin (\sin^{-1}(Fu \sin \theta 2/xx) - \alpha) - XCG2 \sin \alpha p$$
$$Ly_1 = R \sin (\theta c/2)$$
$$Ly_2 = R \sin (\theta c/2)$$

5.5 PARAFOIL SCALING EFFECTS

During the Advanced Recovery System (ARS) wind tunnel test at the National Full-scale Aerodynamic Complex, two different parafoils were tested. The largest of the two (20' x 60') was the primary model and was so chosen in order to have the majority of the measured data as close to the full scale drop test size as is possible in the confines of the 80' x 120' test section. The smaller parafoil model was sized in order to be able to evaluate the effects of different size. This would allow corrections to be calculated to properly estimate full scale flight values using the data from the larger parafoil mode.

During the test it was observed that the parafoil assumed a shape that was different from the original design contours. Although not entirely unexpected, it was concluded the magnitude of these distortions precluded the test article from properly modeling the intended design. This in itself is not detrimental because it can be assumed that the full scale parafoil will also distort under load. The problem is that the models and the full scale parafoils may not distort in the same way or in the same relative amount. Comparison between the two different size models can give insight to this.

It can be concluded that if the two models did not distort in the same way, a proper analysis of the scaling effects cannot be done without determining the effects (parametrically in the wind tunnel) of each of the different distortions. Since it is impractical to measure actual distortions and impossible, from the data obtained, to derive individual contributions, an analytical approach was taken to evaluating the effect of the parafoil model distortions.

5.5.1 Configuration Changes

During the test of the parafoil models, there were seven different distortions identified. The cause of each distortion was determined as was the effect of each distortion.

5.5.1.1 Leading Edge Distortion

During the test the leading edge of the parafoil was observed to be deflected up (Figure 5.5-1). The condition seemed to be worse at higher dynamic pressures. Because of the parafoil configuration and suspension line attachment location the front suspension line of each chordwise row had approximately twice the load as the next several lines behind it. This is verified by the load cell data. The front suspension line has approximately two times the surface area acting upon it as do any of the other lines.

Although the Kevlar lines that were used have a very low modulus of elasticity, they did stretch and the difference in stretch between the front lines and the ones behind them, allowed the leading edge to deflect up.

Line stretch is dependent on the load being applied and the elasticity of the line.

Aerodynamic load is the function of dynamic pressure (q) and characteristic area (S).

> The intent during the test was for q to be the same for both parafoil models (sizes) and data are available for comparisons at equal q.
>
> S is four times as large for the larger parafoil as it is for the smaller parafoil.

Line elasticity is dependent on the material, the line diameter and the style or weave. All three of these were identical for the two parafoil models.

Therefore, the leading edge deflection is four times as much for the larger parafoil as it is for the smaller parafoil though the linear dimension is only twice as large. The relative distortion is therefore twice as much in the larger parafoil as it is in the smaller one.

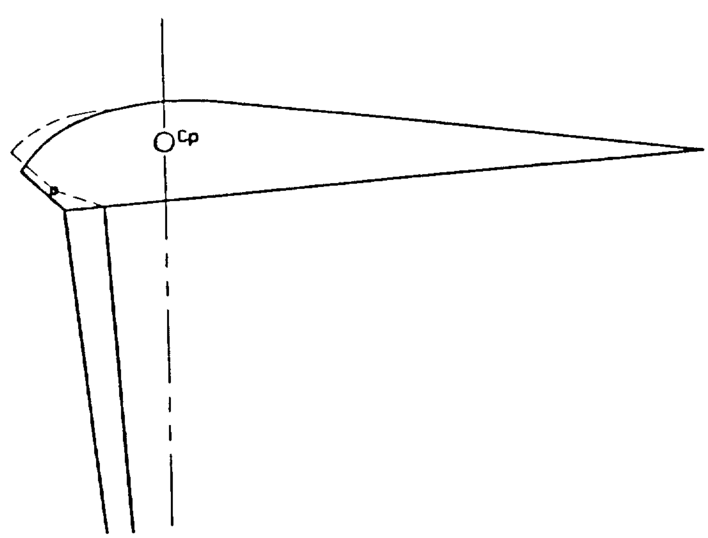

FIGURE 5.5-1, LEADING EDGE DISTORTION

5.5.1.2 Chordwise Foreshortening

Parafoils are rigged such that the payload is positioned forward and the front suspension lines are much closer to being perpendicular to the bottom surface which causes the parafoil to foreshorten (Figure 5.5-2). The foreshortening in turn allows the lines to reach above the nominal attach point producing a convex curve to the bottom surface of the parafoil.

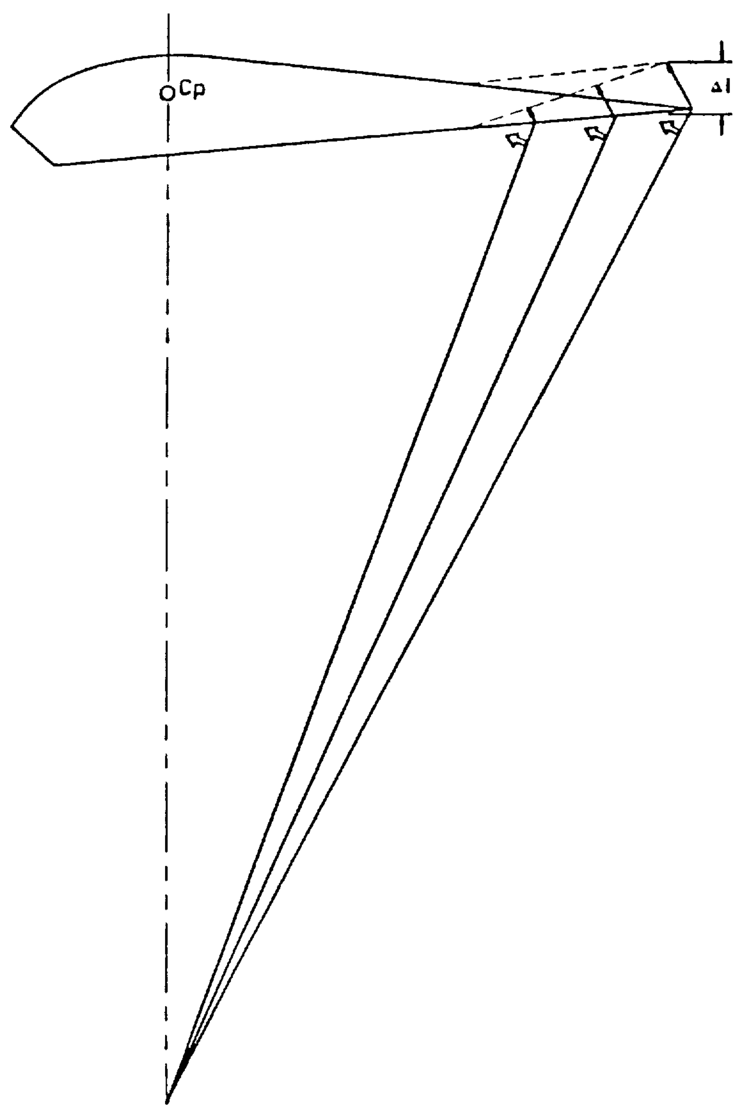

FIGURE 5.5-2, CHORDWISE FORESHORTENING

Prior to Run 5, the suspension lines were rerigged to try and compensate for this. To make the small parafoil similar to the large one, an equivalent/proportional change in rigging was used throughout the time the small parafoil was being tested.

Chordwise foreshortening is a function of suspension line load, line attach angle, rigging and rigidity of the parafoil.

Line Load is dependent on q and S.

> q can be selected the same for comparing data and can therefore be considered equal.
>
> S is four times as large for the larger parafoil. Therefore line load would be four times as great.

Rigging was as near identical as could be achieved.

Rigidity of the parafoil is a function of the stiffness of the fabric and the difference in pressure DEL P across the boundaries of the cells.

Assuming no or identical flow separation (which is hard to determine in this situation) the DEL P would be the same.

The parafoil fabric was the same density for both parafoils. Therefore the smaller one was proportionally more stiff. This would lead us to believe that the smaller parafoil should be relatively more rigid. But this was hard to verify by observation of cell shape as will be discussed later.

Therefore, with four times the line load and a linear scale of two, it can be assumed that the relative chordwise foreshortening would be twice as great in the larger parafoil as in the smaller one.

5.5.1.3 Trailing Edge Configuration

In order to ease fabrication of the parafoils, the gore between the parafoil cells was terminated forward of the trailing edge. Therefore there was no attachment between the upper and lower surfaces of the parafoil near the trailing edge. The result was a parafoil which looked like it had a tube running along the trailing edge in the spanwise direction (Figure 5.5-3). In effect, it did.

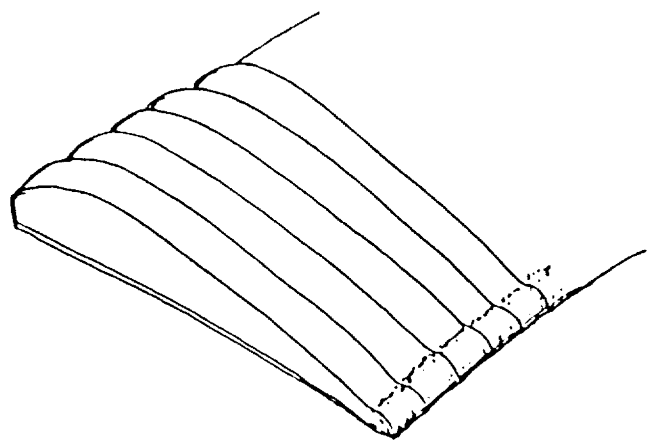

FIGURE 5.5-3, TRAILING EDGE CONFIGURATION

Ignoring the problem of configurational integrity, the concern settles on whether the two different size parafoils had equivalent configurations.

This trailing edge configuration anomaly is dependent on the gore length/attachment and the differential pressure across the fabric.

The gore length/attachment was modeled identically.

Assuming all other factors are the same (which seems to be a poor assumption, but one without an alternative since we do not have pressure data), the pressure differential will be the same, therefore the trailing edge configurations can be considered to be correctly scaled from one model to the other.

5.5.1.4 Trailing Edge Deflection

Parafoils are designed such that local loads are opposed by tension on the individual suspension lines. Under great load the lines are pulled taut. Under light loads, other factors such as line drag can become significant. Near the trailing edge the load distribution goes to near zero. This provides little tension on the trailing edge suspension lines. As could be observed during the test, there was considerably more drag produced bow in the trailing edge lines than in those lines closer to the leading edge. The result of this was that the trailing edge of the parafoil was deflected downward, enough to be noticeable even with the curve up caused by the chordwise foreshortening (Figure 5.5-4). The trailing edge deflection is a function of local parafoil load on the line and of aerodynamic drag acting on the line.

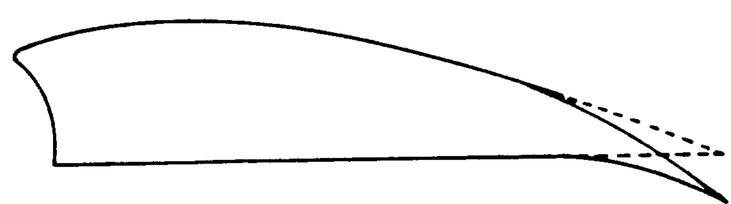

FIGURE 5.5-4, TRAILING EDGE DEFLECTION

As discussed previously, the distributed load is four times as great for the larger parafoil as it is for the smaller one.

The line drag is a function of line diameter, line length and q.

Choosing data for comparison at equal q eliminates q as a consideration.

The line lengths are linearly scaled between the two parafoils although a larger percentage of the length may be exposed to the flow in the test set up of the larger parafoil.

Line diameter is identical for the two sizes of parafoil, which means the line drag would be relatively twice as large for the half linear scale smaller parafoil as it would be for the larger parafoil.

5.5.1.5 Flow Angle

In order to keep flow from impinging on the Parafoil Attitude Control System (PACS) and other attachment hardware, and therefore causing erroneous measurements by the primary balance, a six foot high flow deflector was positioned upstream of the PACS (Figure 5.5-5). This was of little concern with the large parafoil which when being tested was positioned somewhat above the center line of the 80 foot tall test section. With the small parafoil however, there was some concern that the flow deflector could be causing a change in local flow angle and therefore a different and erroneous angle of attack. The test data seem to support this theory. The suspension lines of the smaller (half linear scale) parafoil were half the length of those of the larger parafoil. The effect of this is hard to determine.

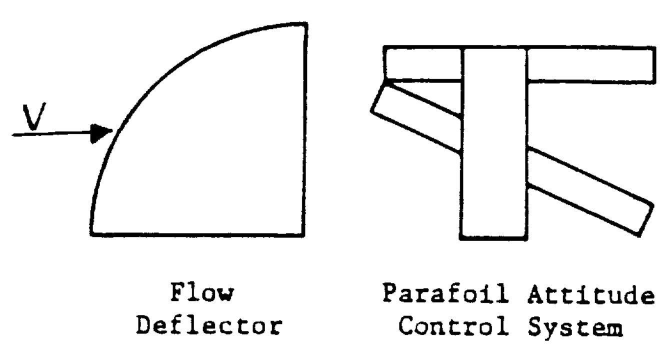

FIGURE 5.5-5, HARDWARE TEST ARRANGEMENT

5.5.1.6 Cell Shape

When a parafoil is in flight the pressure at the open leading edge is at or near the total pressure of the system. Since there are no other air passages, total pressure acts over the entire interior of the parafoil. Since virtually none of the external surfaces are at that high of a pressure, the pressure differential from the outside to the inside is always positive and this causes the parafoil to take its' intended shape. The greater the differential the more "round" the surface of either the top or the bottom of each cell (Figure 5.5-6). Different cell shapes might cause different flow over the parafoil and therefore create different loads. Cell shape is a function of fabric stiffness, and the relationship between pressure differential and spanwise tension.

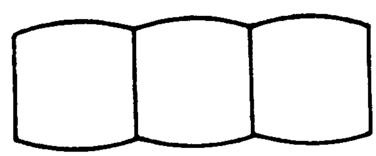

FIGURE 5.5-6, PARAFOIL CELL SHAPE

The fabric weights (stiffness) are the same for both size parafoils, therefore the smaller parafoil is relatively twice as thick and stiff as is the larger one.

At identical q's, the interior pressures will be the same. Assuming the configuration is the same (which again may be a poor assumption), the external pressures will also be the same. Therefore the pressure differentials across the parafoil fabric will be relatively the same.

The spanwise tension is dependent on q, the wing area (S), wing span (b), and distributed pressures.

q can be chosen to be identical.

S and b are linearly scaled between the two different size parafoils.

Again assuming similar configurations, the pressure distribution should be similar.

The spanwise tension should therefore be properly scaled.

Therefore the only difference in cell shape would be caused by the fabric which should have little or no affect.

5.5.1.7 Spanwise Shape/Length

The spanwise shape of the parafoil is defined by the suspension line length and attach location (Figure 5.5-7). This was properly scaled. Shape can also be affected by any spanwise foreshortening. Spanwise foreshortening would be a direct result of changes of shape in all the individual cells. As was discussed above, it is not believed that cell shape was different between the two sizes of parafoil.

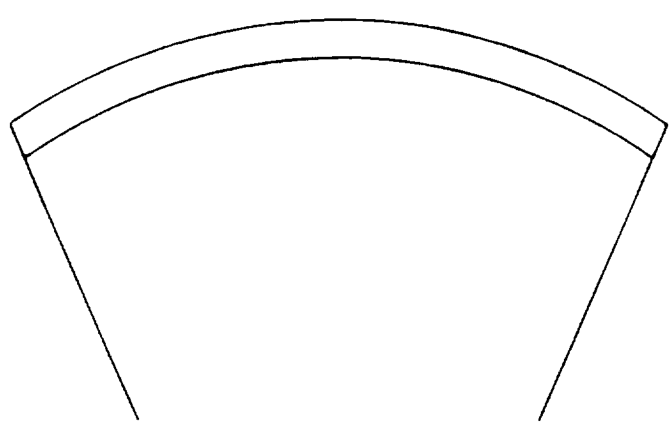

FIGURE 5.5-7, PARAFOIL SPANWISE SHAPE

5.5.2 Summary

The nose shape distortion was relatively twice as great for the large parafoil as it was for the small one. The chordwise foreshortening was also relatively twice as great for the large parafoil. The trailing edge deflection was relatively only half as great for the large parafoil as it was for the small parafoil. Recorded attitudes give cause to believe that the small parafoil was in local flow which was not parallel to the test section floor due to the effects of the flow deflector. Table 5.5-8 gives a summary of parafoil scaling effects.

5.5.3 Conclusion

The trailing edge deflection problem has the least effect due to the small loads in that area. The leading edge shape and chordwise foreshortening, however, are in critical areas and as can be seen in photographs and videos of the test, had significant distortions. Even ignoring potential problems resulting from flow angularity when testing the small parafoil, there were enough differences in configuration between the large (20' x 60') and the small (10' x 30') parafoils to preclude a proper evaluation of the effects of scaling.

5.5.4 Recommendations

Data from tests of the larger parafoil should be used in simulations of the full scale ARS parafoils. This is because they are closer to the correct size and also they are not affected by any potential flow angularity problems.

Future models of full scale flight articles should be designed so that distortions will be representative of distortions of the fullscale configuration, taking into account differences in load, fabric stiffness, line stretch, etc.

Parametric tests should be conducted and should use models in some kind of boilerplate configuration.

TABLE 5.5-8, SUMMARY OF PARAFOIL SCALING EFFECTS

EFFECT	SCALING FACTOR	
	Large (20' x 60' Model)	Small (10' x 30' Model)
Leading Edge Distribution	4 times small	1
Chordwise Foreshortening	2 times small	1
Trailing Edge Configuration	No effect	No effect
Trailing Edge Deflection	1	2 times large
Flow Angle	Indeterminant	Indeterminant
Cell Shape	Little effect	Little effect
Spanwise Shape	No effect	No effect

5.6 Sample Results

The information contained in this section is selected examples of the wind tunnel test reduced data. Due to the large quantity of data taken explanations can not be provided for every run, therefore selected examples have been provided to give a overview of the complete results.

The Appendices contain the complete set of results.

5.6.1 Longitudinal Aerodynamics

The aerodynamic data taken during this test was obtained by tether testing techniques to simulate a free flight environment. The data in this report is presented with no correction factors applied to C_L or C_D due to wall interference. Computations were done using a 3-D panel code which is a potential flow simulation of the aerodynamics. The lift correction for the 20' x 60' wing is approximately 7% for C_{Lmax} in flare.

The 20'x 60' parafoil was tested using tether testing techniques where the parafoil was allowed to fly in the wind tunnel. The angle of attack was adjusted by changing the parafoils rigging angle and establishing a new stable trim point. The longitudinal aerodynamic coefficients are an average value taken over a finite period of time. Figure 6.5-1 shows the longitudinal aerodynamic coefficients C_L, C_D and C_M as a function of angle of attack (α) for various dynamic pressures.

The airfoil distortion associated with increasing dynamic pressure caused a decreased lift coefficient and increased drag coefficient.

The angle of attack at which the parafoil stalled was directly related to the dyamic pressure. The parafoil would stall at lower angles of attack with increasing dynamic pressure. This effect can be related with airfoil distortion associated with increasing dynamic pressure. The effects of the parafoil distortion can be seen graphically from the L/D versus angle of attack plots (Figure 6.5-2). The L/D decreases with increasing dynamic pressure and the curves tend to shift to the left with the increasing dynamic pressure. The L/D_{max} can be calculated from the drag polar (Figure 5.6-3). The L/D_{max} of 2.7 is less than the L/D_{max} of 3 that was predicted. An equation for the drag can be obtained from the plot of C_D versus C_L^2 as in Figure 5.6-4. The parasite drag increases for increasing dynamic pressure while the induced drag remains almost constant.

5.6.2 Flare Aerodynamics

The flare maneuver was accomplished by symmetrically deflecting the trailing edge of the parafoil at a constant angle of attack. Figure 5.6-5 shows how the control force varies with deflection, dynamic pressure and angle of attack. From Figure 5.6-6, it can be seen that both C_L and C_D increase with deflection. The L/D decreased when the wing is flying at high angles of attack; and

L/D increased with deflection at low angles of attack, showing that the flare can be optimized when initiated at low angles of attack.

5.6.3 Load Cell Data

The distributed load across the span of the parafoil was measured by five load cells located along the quarter chord and half the span of the wing. The data points were mirror imaged and a third order curve fit used to determine the spanwise load distribution (Figure 5.6-7). The spanwise load distribution shows how the load increases with increasing dynamic pressure.

The chordwise load distribution was measured by placing twelve load cells along a center span keel. A third order curve fit was used to plot the chordwise load distribution (Figure 5.6-8). The chordwise load distribution can be used to calculate the localized center of pressure location by integrating the load distribution curve and iterating until Xcp is found as in the following equations:

$$\text{Load} = \int_{0}^{c} f(x)dx$$

$$\text{Load}/2 = \int_{0}^{Xcp} f(x)dx$$

Once the center of pressure is found, the lift and drag can be transferred to the quarter chord location and the moment about the quarter chord calculated. Figure 5.6-9 shows plots of Xcp and C_M quarter chord versus angle of attack.

5.6.4 Lateral Aerodynamics

Lateral aerodynamic data was acquired for two different assymetrical control deflections. Figure 5.6-10 shows how the control force is a function of deflection for airfoil local distortion and trailing edge deflection. It can be seen from this graph that the control force required is approximately equal for both methods. Figure 5.6-11 shows the yawing moment and rolling moment for right side control line deflections. The airfoil local distortion has very little yawing moment and a large rolling moment in the positive right direction. The trailing edge deflection causes the parafoil to yaw in the positive direction and roll in a negative or left direction. This is known as the adverse rolling tendency and is usually associated with large parafoils.

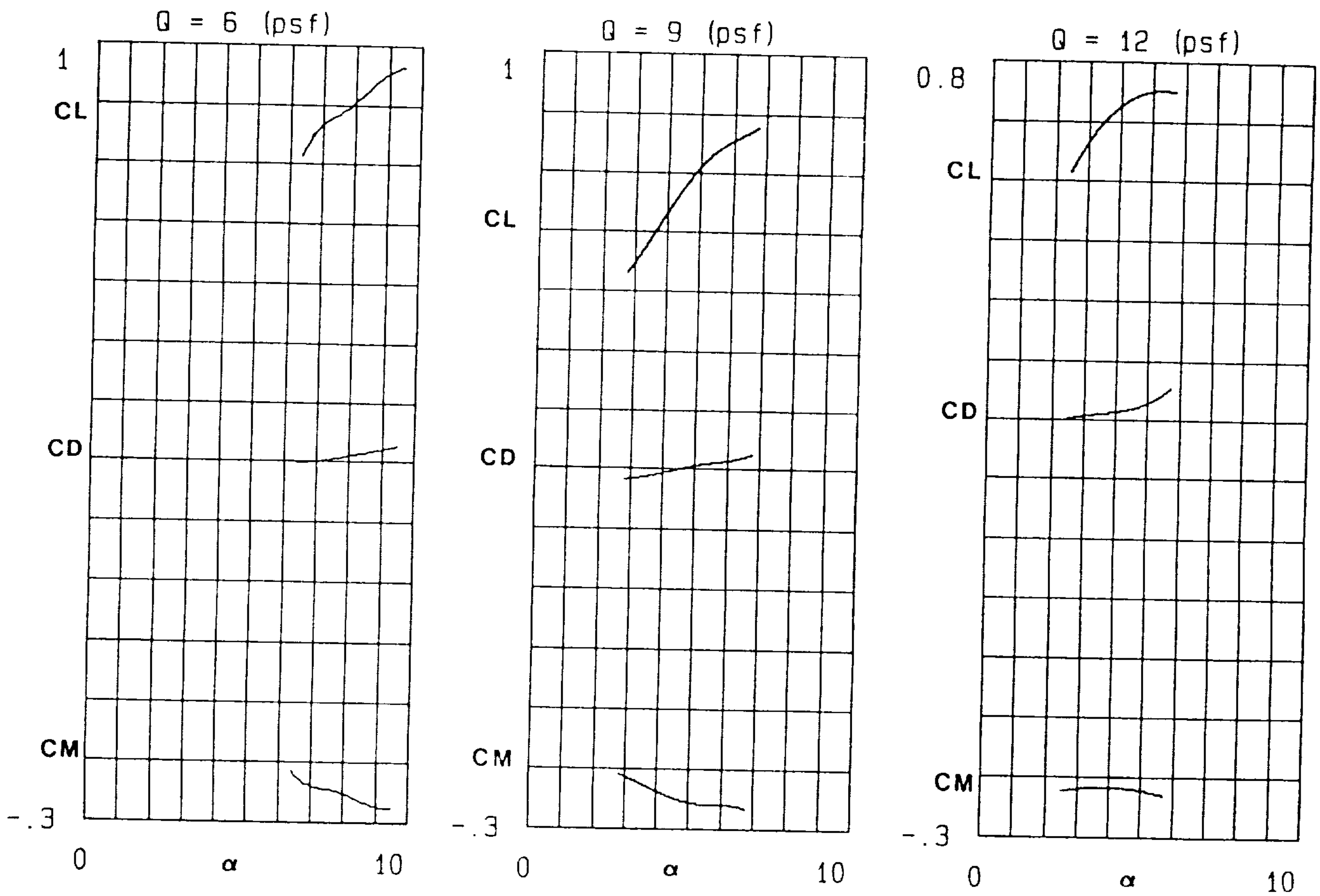

FIGURE 5.6-1, C_L, C_D, AND C_M AS FUNCTIONS OF ALPHA (α) FOR VARIOUS WING LOADINGS

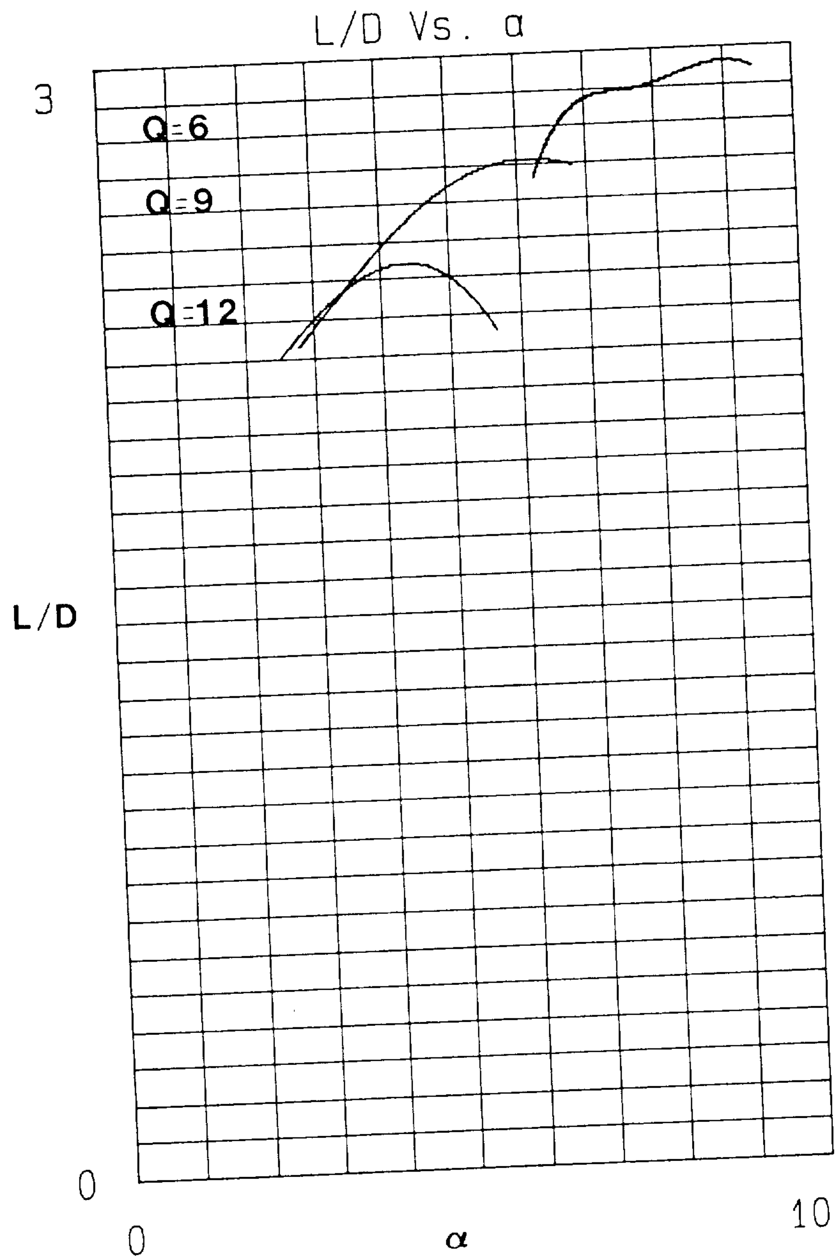

FIGURE 5.6-2, LIFT-DRAG RATIO (L/D) DECREASE WITH INCREASING DYNAMIC PRESSURE

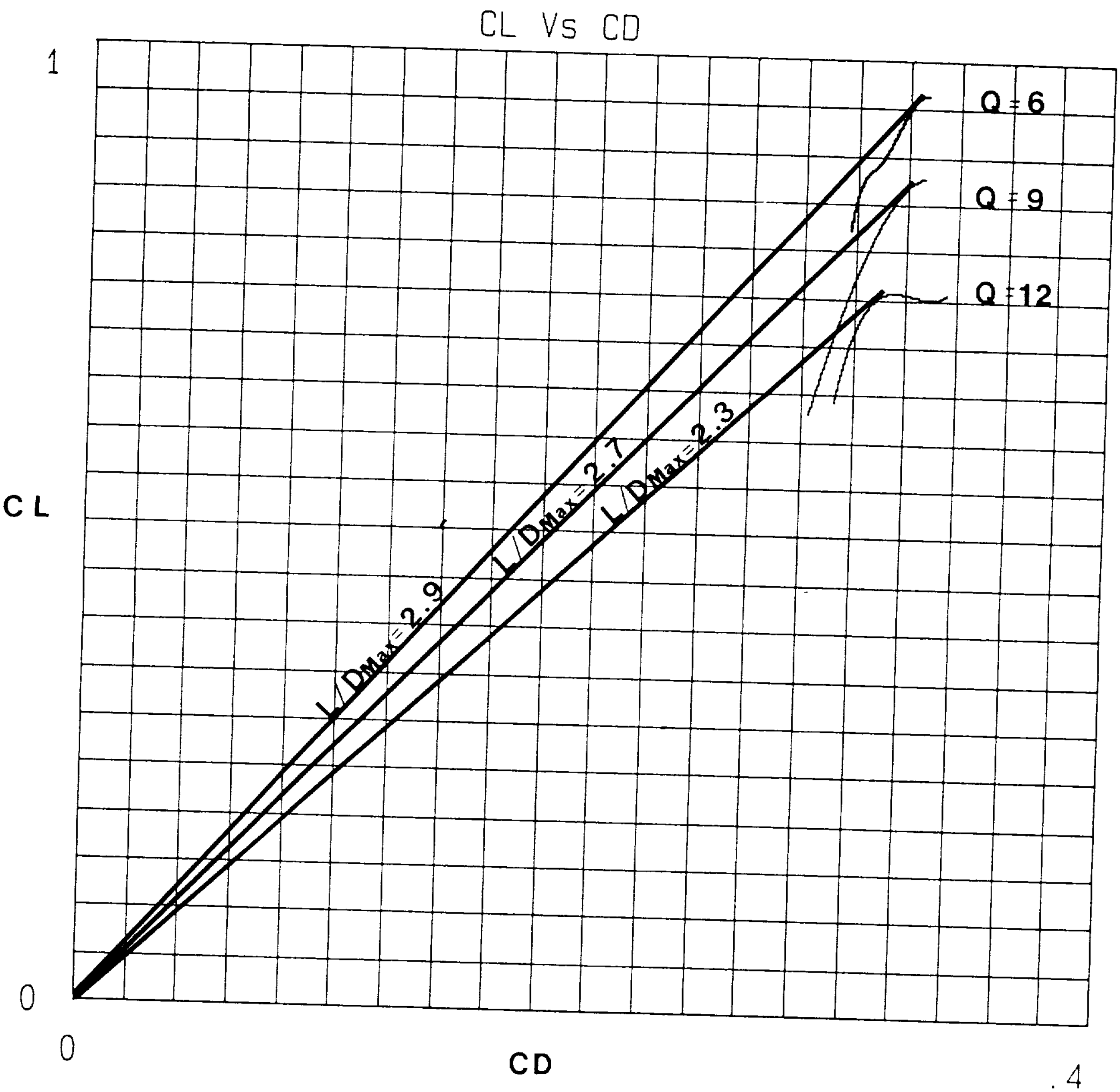

FIGURE 5.6-3, LIFT-DRAG RATIO (L/D) MAXIMUM FROM PLOTS OF C_L VS. C_D

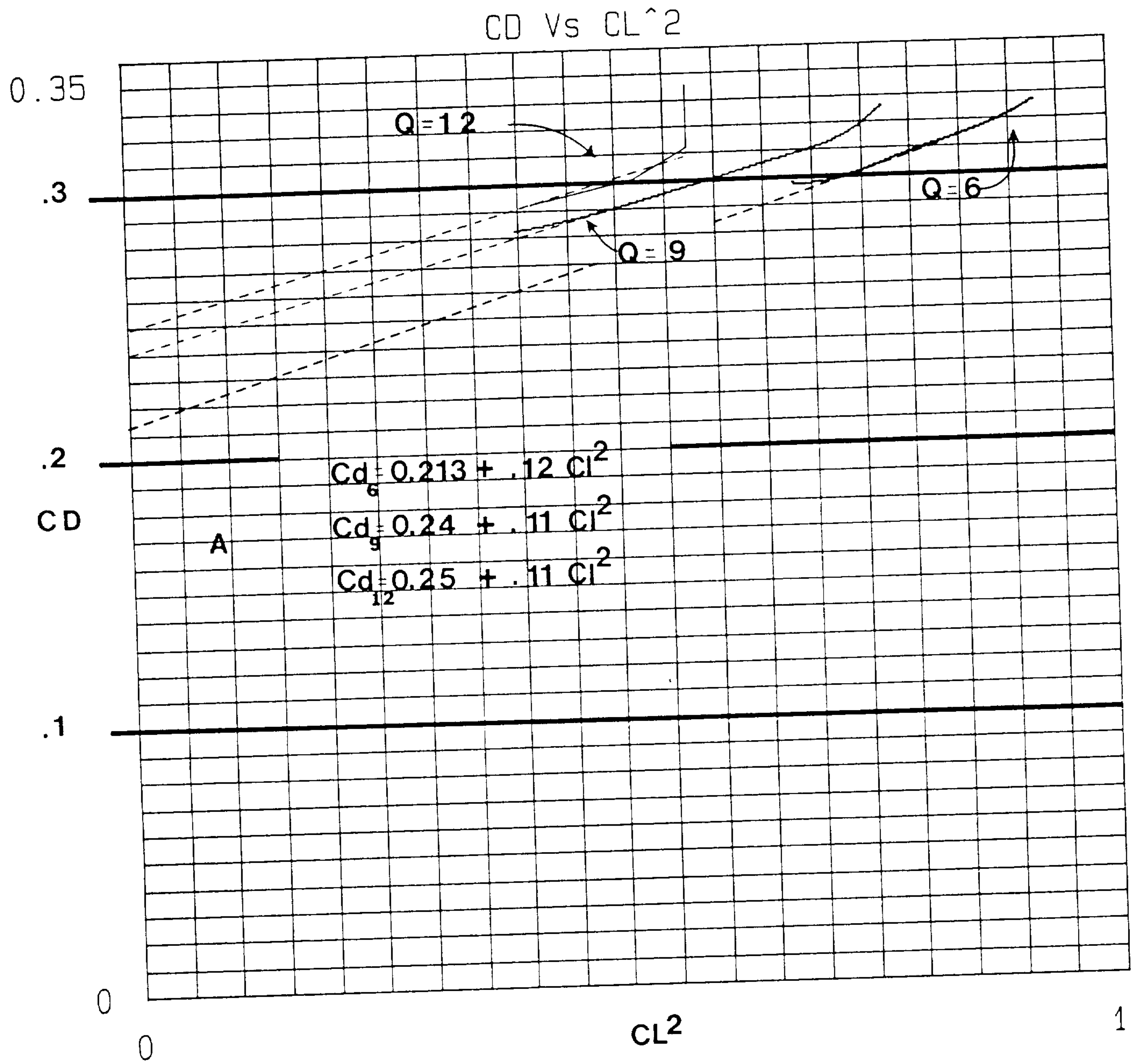

FIGURE 5.6-4, C_D VS C_L^2

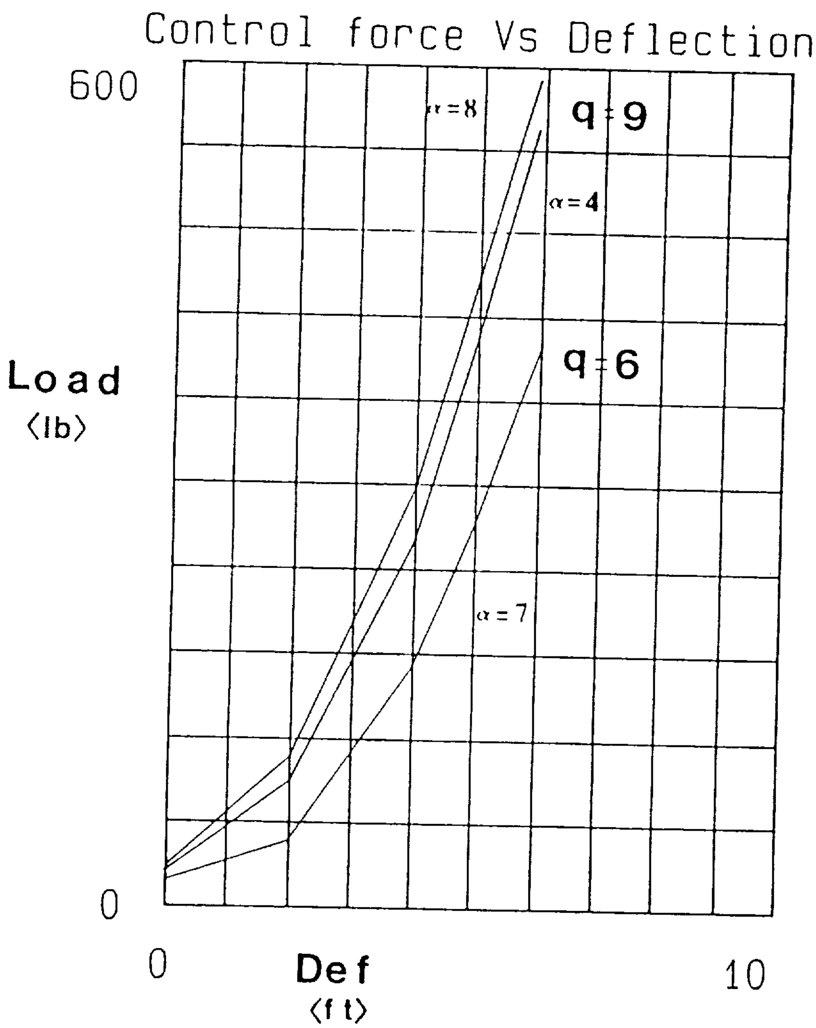

FIGURE 5.6-5, CONTROL FORCE VS. DEFLECTION FOR FLARE MANEUVER

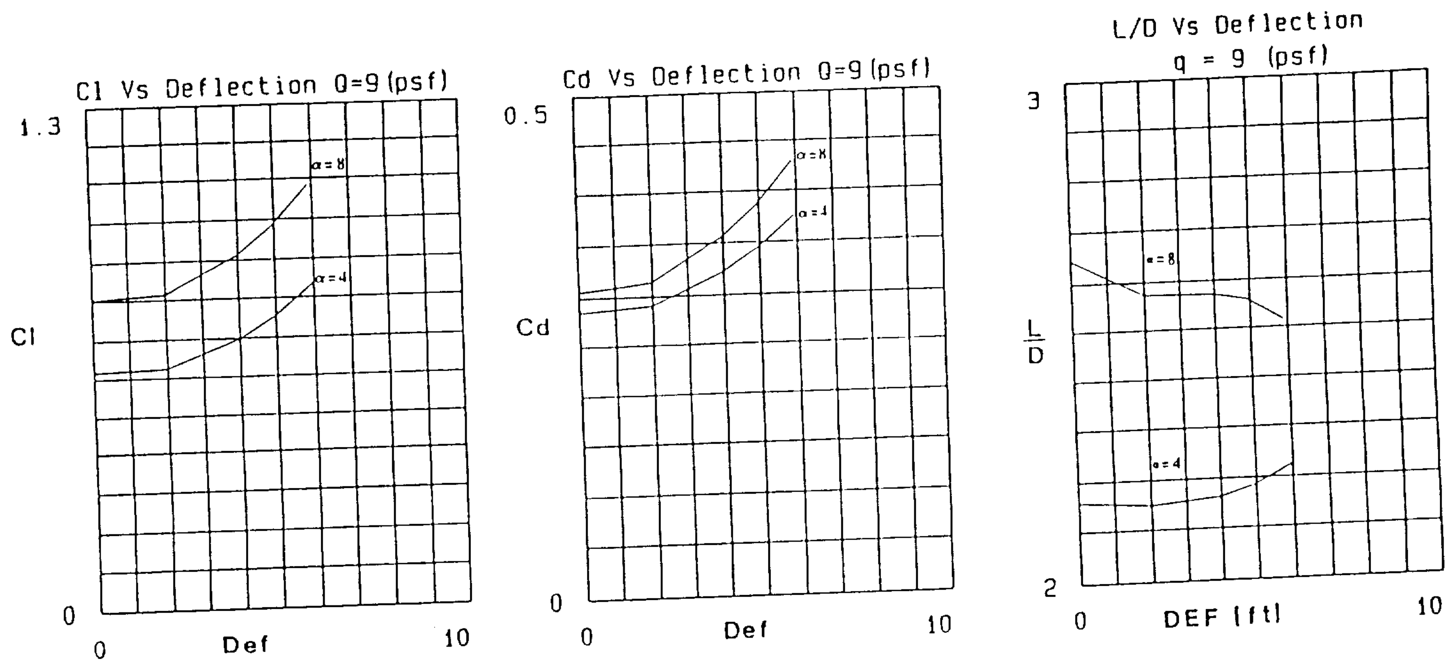

FIGURE 5.6-6, VARIATIONS IN C_L, C_D, AND L/D WITH DIFFERENT DEFLECTIONS AND DYNAMIC PRESSURES

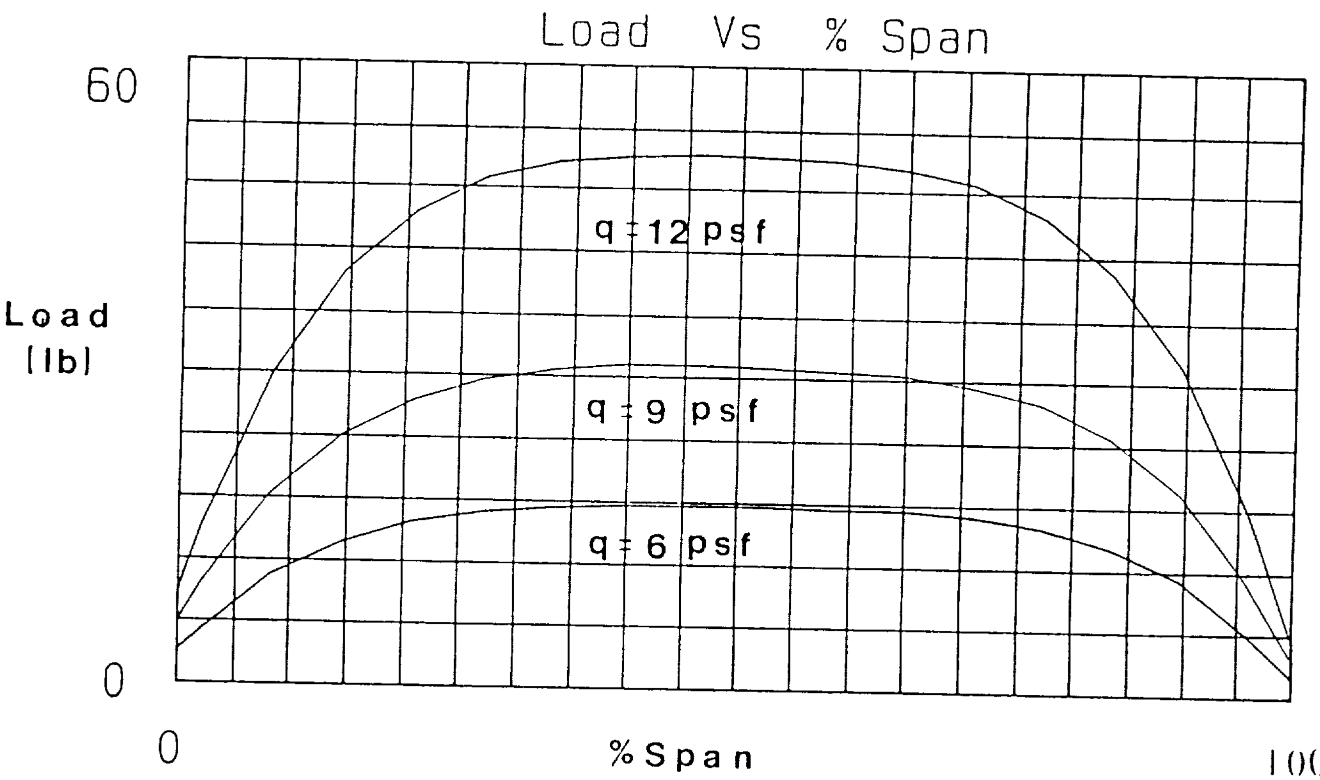

FIGURE 5.6-7, SPANWISE LOAD DISTRIBUTION AT VARIOUS WING LOADINGS

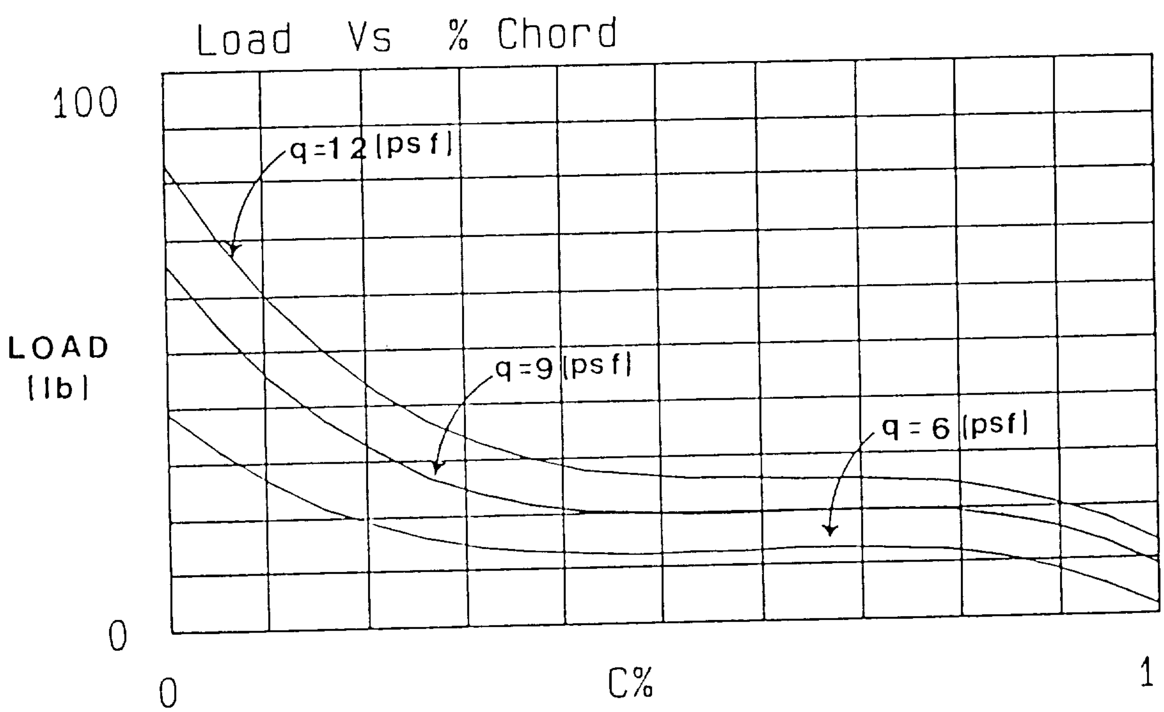

FIGURE 5.6-8, CHORDWISE LOAD DISTRIBUTION AT VARIOUS WING LOADINGS

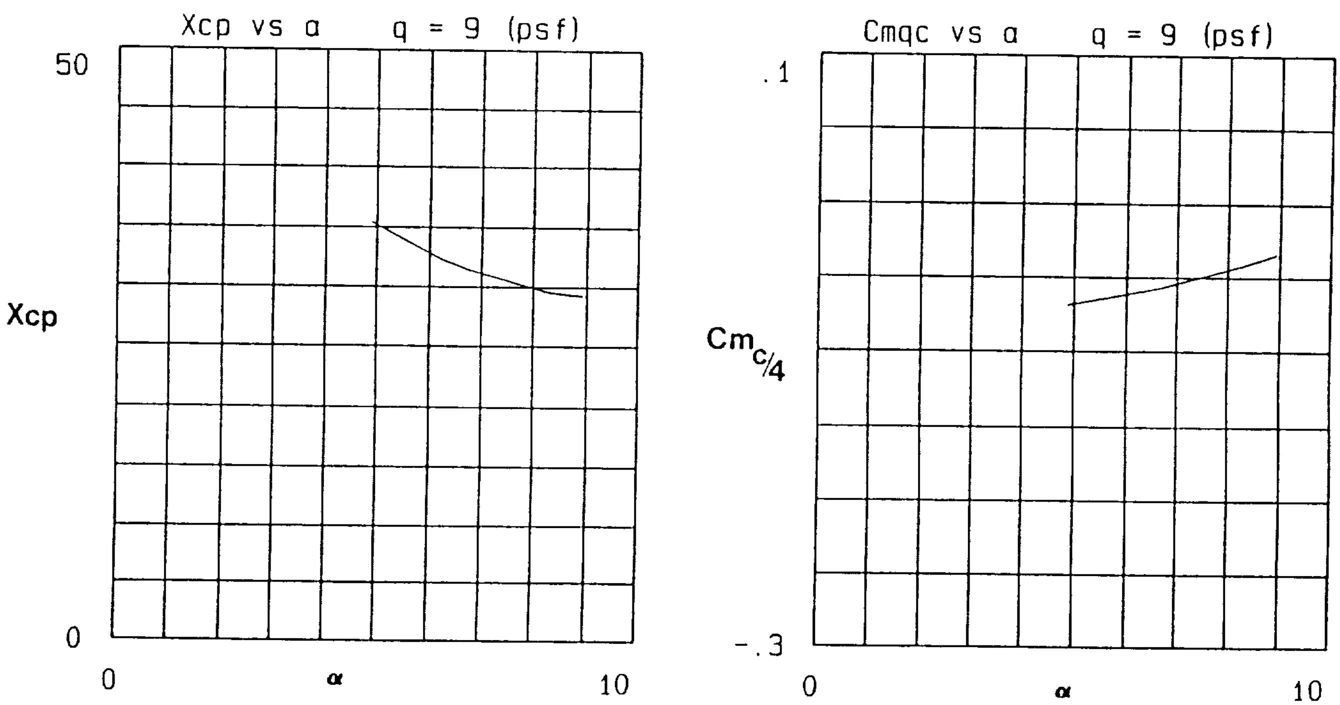

FIGURE 5.6-9, XCP AND CM VS. ANGLE OF ATTACK (α)

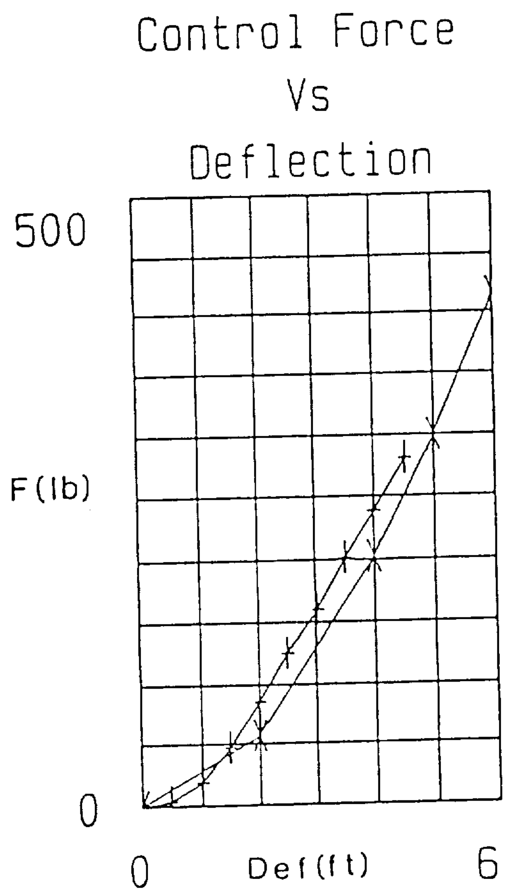

FIGURE 5.6-10, CONTROL VS. DEFLECTIONS FOR TWO CONTROL METHODS

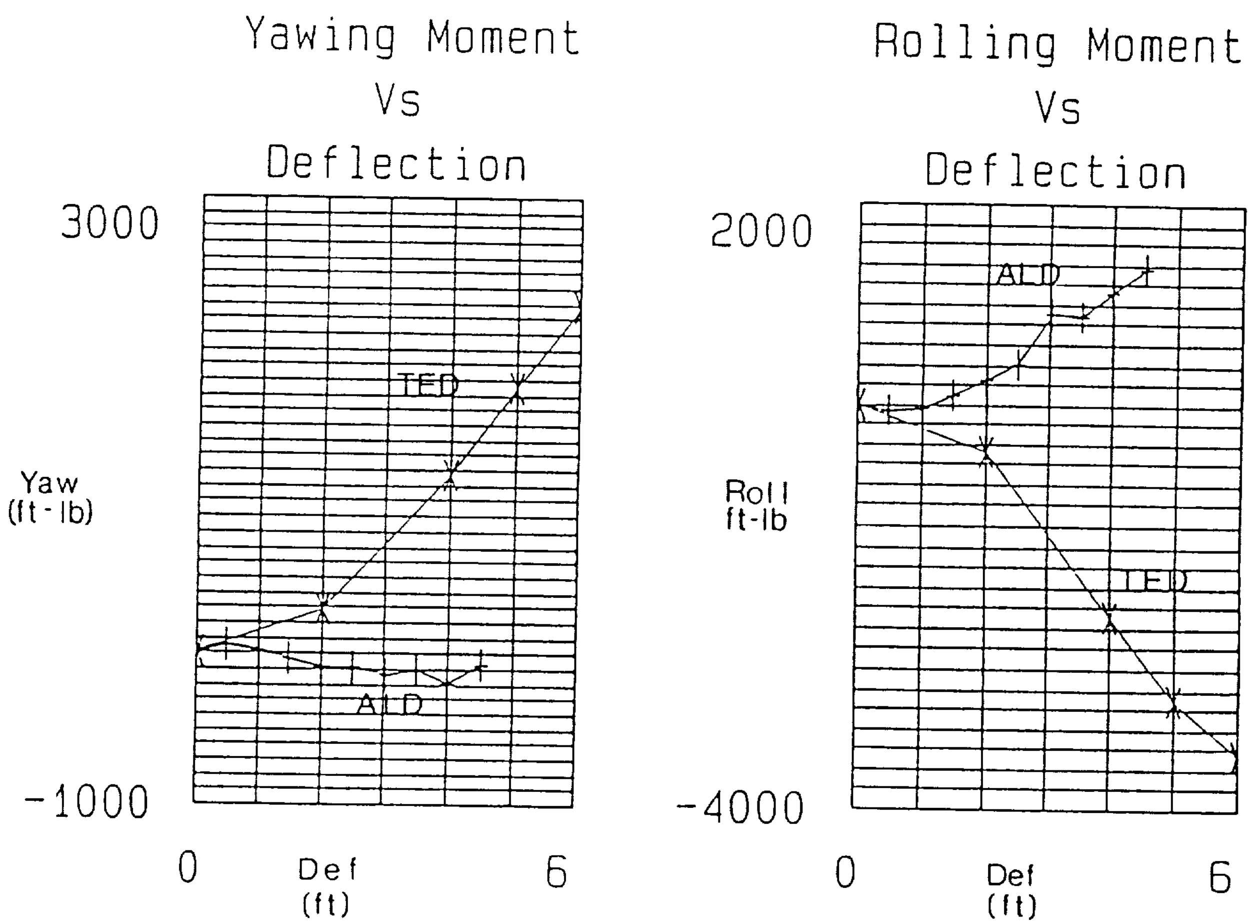

FIGURE 5.6-11, YAWING AND ROLLING MOMENT DATA VS. CONTROL LINE DEFLECTION

6.0 Conclusions and Recommendations

The success of the ARS Phase 2 wind tunnel test exceeded previous expectations. Although scaling effects could not be evaluated aerodynamic data was obtained to support airdrop testing and full-scale development of the advanced recovery system.

Interface hardware, instrumentation and testing procedures have been validated. Structural, operational and safety issues have been addressed.

The major conclusion of phase two testing was that wind tunnel testing of large scale parafoils is practical and useful. Additional testing should be implemented to expand a high glide parafoil data base.

7.0 References

1. Anderson, John D., Jr.: "Fundamentals of Aerodynamics," McGraw-Hill Book Company, New York, 1984.

2. Hoerner, Sighard F.: "Fluid-Dynamic Drag," Publ. by the author (P.O. Box 342, Brick Town, New Jersey 08723), 1965.

3. Rae, William H., Jr.; Pope, Alan: "Low-Speed Wind Tunnel Testing," John Wiley & Son, New York, 1984.

4. Nicolaides, John D.: Parafoil Wind Tunnel Test, AFFDL TR-70-146, 1971.

5. Ware, George M.; Hassel, James L., Fr.: Wind-Tunnel Investigation of Ram-Air-Inflated All-Flexible Wings of Aspect Ratios 1.0 to 3.0, NASA TM SX-1923, 1969.

6. Pioneer Aerospace Corporation: "Preliminary Analysis of Parafoil Attitude Control (PAC) Model", ARS-WP-09, 1989.

7. Pioneer Aerospace Corporation: "Advanced Recovery System Parachute/ Parafoil Stress and Design Loads Analysis", ARS-WP-10, Rev. A, 1989.

NASA
National Aeronautics and Space Administration

Report Documentation Page

1. Report No.	2. Government Accession No.	3. Recipient's Catalog No.
NASA CR-177563		

4. Title and Subtitle	5. Report Date
Advanced Recovery Systems Wind Tunnel Test Report	August 1990
	6. Performing Organization Code
7. Author(s)	8. Performing Organization Report No.
R. H. Geiger and W. K. Wailes	A-90259
	10. Work Unit No.
	906-65-43
9. Performing Organization Name and Address	11. Contract or Grant No.
Pioneer Aerospace Corporation 250 East Drive, Suite G Melbourne, FL 32904	NAS8-36631
	13. Type of Report and Period Covered
12. Sponsoring Agency Name and Address	Contractor Report
National Aeronautics and Space Administration Washington, DC 20546-0001	14. Sponsoring Agency Code

15. Supplementary Notes

Point of Contact: James C. Ross, Ames Research Center, MS 247-2, Moffett Field, CA 94035-1000
(415)604-6722 or FTS 464-6722

16. Abstract

Pioneer Aerospace Corporation (PAC) conducted parafoil wind tunnel testing in the NASA-Ames 80 by 120 test section of the National Full-Scale Aerodynamic Complex, Moffett Field, CA. The investigation was conducted to determine the aerodynamic characteristics of two (2) scale ram air wings in support of air drop testing and full scale development of Advanced Recovery Systems for the Next Generation Space Transportation System.

Two models were tested during this investigation. The primary test article, a 1/9 geometric scale model with wing area of 1200 square feet and secondary test article, a 1/36 geometric scale model with wing area of 300 square feet, both which had an aspect ratio of 3. The test results show that both models were statically stable about a model reference point at angles of attack from 2 to 10 degrees. The maximum lift-drag ratio varied between 2.9 and 2.4 for increasing wing loading.

17. Key Words (Suggested by Author(s))	18. Distribution Statement
Parafoil Ram-air-inflated wing Parachute	Unclassified–Unlimited Subject Category–02

19. Security Classif. (of this report)	20. Security Classif. (of this page)	21. No. of Pages	22. Price
Unclassfied	Unclassified	103	A06

NASA FORM 1626 OCT 86

For sale by the National Technical Information Service, Springfield, Virginia 22161